KARSZTFEJLŐDÉS IV.
Szombathely, 2000. pp. 7-30.

THE MAIN TYPES OF KARREN DEVELOPMENT OF LIMESTONE SURFACES WITHOUT SOIL COVERING

MÁRTON VERESS
„Berzsenyi Dániel" College, Department of Geography
9700 Szombathely, Károlyi G. tér 4.

Abstract: Mostly based on examples studied in the Austrian Totes Gebirge limestone surfaces without soil covering can be identified into categories regarding where the karren development took place, what is the position and shape of the developed karstic surface. Sub-types of karren, variation of karren and processes of solution within these are differentiated in the karren types. Forms originated by solution are categorized and suggestions are offered for the nomenclature of hitherto unspecified processes and forms.

1. Introduction

The morphological specification of karren has been already completed (*MONROE, W-WATSON, H.,* 1972, *BÖGLI, A.* 1976, *FORD D. C.-WILLIAMS, P. W.* 1989, *BALÁZS, D.* 1990). The latest surveys analyze the factors that influence karstification. *MOTTERSHEAD, D. N.* (1996) analyzed the relation between certain karst forms and gradient of slope, *GLEW, J. R.-FORD, D. C.* (1980) between the length of rillen and gradient of slope. *CROWTHER, J.* (1996) analyzed the roughness of karren forms.

The specification of the phenomena of karstification and the genetic explanation of the forms can happen with the consideration of the kind of geometrical shapes generated on the interface of the solvent and the dissolved rock surface. (*VERESS, M.-PÉNTEK, K.* 1992, *VERESS, M.-PÉNTEK, K.* 1994). In this paper with respect to this principle those solution processes are classified - mostly using Totes Gebirge, Dachstein and Julians Alps examples - that are responsible for the development of karren types and their constituent morphological elements. The basis of the classification is the location (on the ground surface or in the rock) extension and position of the interface of the solvent and the dissolved rock (the location of the solution). Within the classification suggestions will be offered for the extension of the nomenclature of the karren. There have been attempts for classification observing this principle (*VERESS M.* 1995), but then only the types of solution and the processes of solution were specified. The types of solution (sub-types in this paper) were not classified into the karren types.

Karren development may occur on surfaces with or without soil covering. In this paper three types karren development, the surface-, the vertical- and the subsurface karren development will be specified and their forms analyzed.

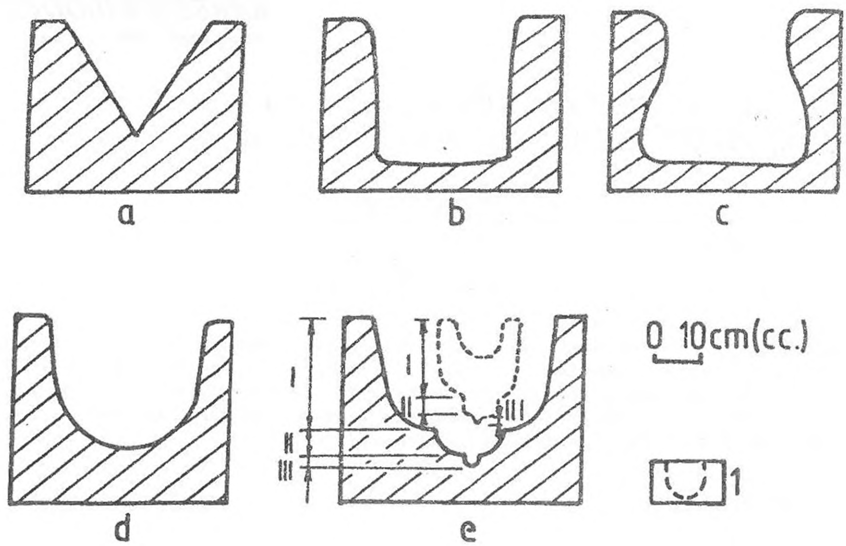

Fig 1: Various cross sections of simple (a-d) and composite (e) troughs
Legend: I, II, III trough types, 1: older troughs

2. Surface Karren Development

The surface karren development occurs on the rock surface.

2.1. Surface solution

Compared to lateral solution vertical solution is relatively small. It occurs primarily on bedding plane surfaces. It results in the increasing roughness of the surface, edges, crests, rises, cones, towers and occasionally blocks of debris are left behind.

It may occur that steps develop resulting from selective solution. The fronts of the steps retreat more or less parallel to themselves.

Trittkarren surfaces are possibly the results of surface solution where the solution is differently effective on the various points of the surface. Observations hint that the heel prints may be responsible for other karren forms (fluting, solution pans.)

2.2 Linear Solution on the Surface

The solution occurs in a strip or line considerably in the vertical direction as well.

Linear solution may be the cause of the development of slope-karren that are composed of various measure long depressions, troughs (rills, runnels, major runnels) that are more or less parallel, various in density.

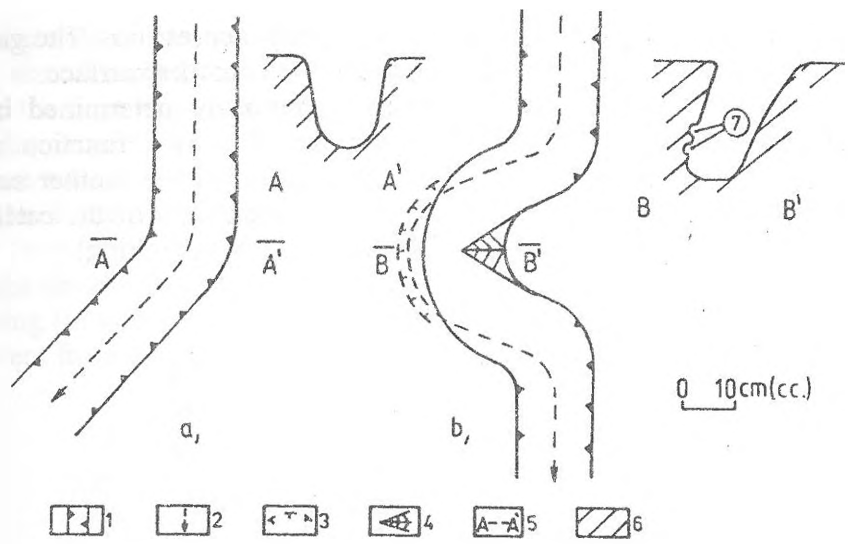

Fig. 2: False meander (a) and true meander (b)
Legend: 1. vertical trough side, 2. streamline, 3. the edge of concave trough-side, 4. the moderately sloping side of the trough (skirt), 5. cross section, 6. bedrock, 7. scour grooves.

2.2.1. Linear, Straight Solution on the Surface.

The strip of solution is straight, the solvent flowing on the slope forms runnels. The runnels are specified by their dimensions. The small ones are the "rillen" (*BÖGLI, A.* 1976) rain flutes (esőbarázda, *VERESS, M.* 1992), the more sizable ones rinnens (*BÖGLI, A.* 1976), runnels (*WHITE, W. B.* 1988), flutes (barázda *BALÁZS, D.* 1990) and solution channels (oldódási csatorna *VERESS M.* 1992). *FORD, D. C.-WILLIAMS, P. W.* (1989) separate small sized microrills (developed by solution effect of capillary water) and solution channels. The letter ones are the rillens and different types of runnels. According to *WHITE, W. B.* (1988) rills (ribbenkarren) develop on slopes where sheet flow, rinnens (rinnenkarren) on slopes, where channel flow takes place. Rillen develop on steep slopes, when sheets of water separate into ribbons, and there will be a jump from laminar flow to turbulent flow because of disruption of boundary layer's continuity (*TRUNDGILL, S.* 1985). According to *KUNAVER, J.* (1984) rinnenkarren occured between about 1650-1700 metres height above the sea level.

Rinnen develop on slopes of low angle without soil covering when the flow is banded (*WHITE, W. B.* 1988). They can also develop on surfaces covered with soil (*FORD, D. C.-WILLIAMS, P. W.* 1989.)

Troughs can be simple and composite as for their cross section *(Fig. 1)*. Both simple and composite troughs can be major troughs. These letter are solitary big (width and depth exceeding one meter) depressions. The gradient of the bottom of the major troughs is less that of the mother surface.

The shape of the simple troughs is probably determined by the quantity of the solvent as a function of time. This is a function of the discharge of the solvent (a function of the gradient of the mother surface) and a function of recharge (a function of the morphology of the catchment area, the thickness of the snow covering, the intensity of melting).

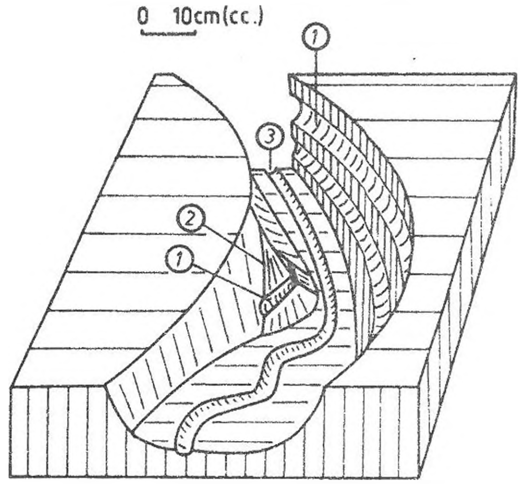

Fig. 3: The slip of a bend (after a photo)
Legend: 1. scour groove, 2. skirt, 3. type III trough

In active periods due to the gradual decreasing of the solvent solution is spread over a decreasing strip. A V-shaped trough develops. The trough will be V-shaped if solvent is recharged laterally. In these cases rounded inter-trough edges, rises, crests develop. It may occur that troughs develop on the crest between the troughs (crest-trough).

At constant discharges for longer periods the development of wide bottomed, vertical walled troughs can be expected. It is supposed that at quickly decreasing discharges half-circle or U-shaped (concave walled) troughs develop. Overhanging walled downwards widening troughs develop if the flow of water in the trough is steadily stabilized.

The described simple troughs can be easily said from the composite ones (*Fig. 1, Photo 1*) that are called ineinandergeschachtelten forms by *LECHNER, J.* (1953).

A sharp decrease of the discharge of the solvent and the stabilization of the smaller discharge results that a smaller (type II) trough develops in the original (type I) trough followed by an even smaller one (type III). Though this classification has a meaning only in the case of a composite development of the troughs, the individual troughs can be differentiated by their size. The depth and width of the type I troughs is some decimeters, while the type III is only several centimeters. The dimensions of the type II troughs range between types I and III. Such type II trough containing type III size trough may occur that did not develop on the bottoms of type I troughs. It may occur that type III troughs develop on the bottom of type I ones (even more than one can occur in the same trough) or that type III troughs develop elsewhere than in the bottom of a bigger trough. The rate of growing (in width and/or deepening) of the carrier trough can be identical or different from that of the inner trough.

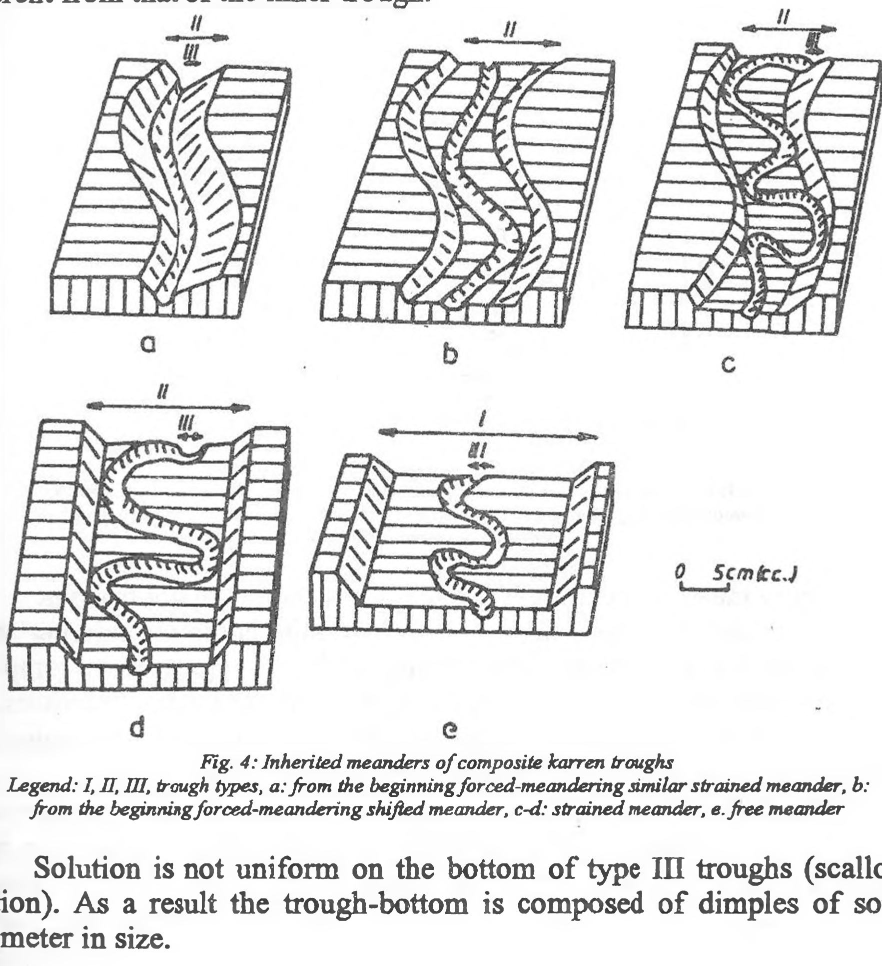

Fig. 4: Inherited meanders of composite karren troughs
Legend: I, II, III, trough types, a: from the beginning forced-meandering similar strained meander, b: from the beginning forced-meandering shifted meander, c-d: strained meander, e. free meander

Solution is not uniform on the bottom of type III troughs (scallopy solution). As a result the trough-bottom is composed of dimples of some centimeter in size.

2.2.2 Meandering Linear Solution, and Origin of Meanders

The strip of solution is not straight but of changing direction.
The meander-karren was first described by *BÖGLI, A.* (1976).

The troughs can be bending due to solution that is not following a straight line. The bending can be false meandering or true meandering. Troughs of false meandering are of symmetric cross section at any point. The troughs of true meandering have asymmetric cross sections in bends. (*Fig. 2*). At the concave side of the meander its wall is overhanging often with side channels (meander scour grooves). At the convex side the trough slope is less than at other parts (skirt) (*Fig. 3*)

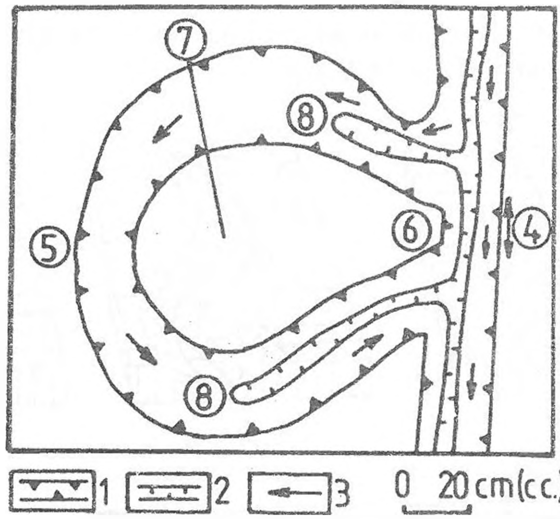

Fig 5: The beheading of a bend (after a photograph)
Legend: 1: type I trough, 2: type III trough, 3: direction of the fall of the trough-bottom, 4: location of beheading, 5: karren trough oxbow, 6: karren trough neck 7: karren trough inselberg. 8: retreating troughs

Truly meandering troughs are the flutes and the major troughs.

The smaller is the trough the more definite is the meandering and it develops for longer sections. Meandering is mostly increased in composite karren troughs types II and III (the length of the meanders increases, the wavelength decreases. It can be observed that downwards to the bottom the measure of the meandering increases (*FRIDTJOF, B.* 1954).

Both in the case of the false and true meanders inheritied meanders develop. In inheriting it is understood that the meandering of the inner trough is originally staked out by the master trough. Type II and III troughs developing in the false-meandering troughs can forced-meandering. Forced-meandering can be specified as a property of the inner troughs following the bends of the false- or true meanders. Similar (the inner trough is parallel with the master trough) or shifted (the inner trough is not parallel with the master trough) meanders can develop in the inner troughs. The troughs that are truly meandering may be strained (*Picture 1*) or free (*Fig. 4, Picture 2*).

In the first case the meanders reach to the walls of the master trough, in the letter case they don't. Type III troughs produce the most varied meandering in their whole length or in sections. Upstream or downstream (recharge from solution pans or discharge to pits) of the strained or free meandering sections of the type III troughs (*Fig 4/e*) the gradient of the slope significantly changes.

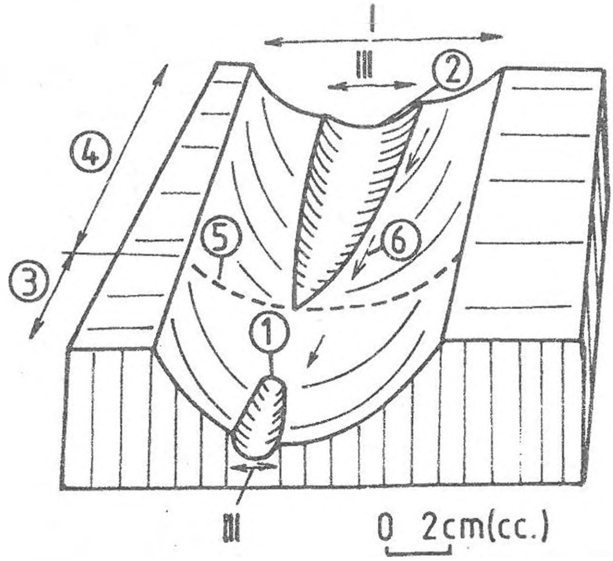

Fig. 6: Development of a watershed and catchment differentiation in young regressive troughs
Legend: type I, III troughs, 1: trough retreating to slope direction, 2: trough retreating against slope direction, 3: catchment area of trough retreating to slope direction, 4: catchment area of trough retreating against slope direction, 5: watershed (divide), 6: direction of the fall of the trough-bottom

2.2.3. The Beheading of a Bend

In well developed bends the karren-trough isle and the karren-trough neck can be differentiated. The beheading of the bend may occur and karren-trough oxbow is resulted that surrounds a karren inselberg (*Fig. 5*). The beheading is probably promoted by cavity development at the neck (neck karren-cavity) and the spilling of the solvent at this point (neck channel).

2.2.4. Trough Regression

The linear solution occurs even more upstream from the actual trough-end, thus the troughs retreat. The deepening that accompanies the retreating is considerable especially in sections of big gradient (regressive karren canyons). An accented roughening, the pectinated karren develops at the regression of the trough edges and initial troughs (*Picture 3*). (Semipits too develop besides troughs.)

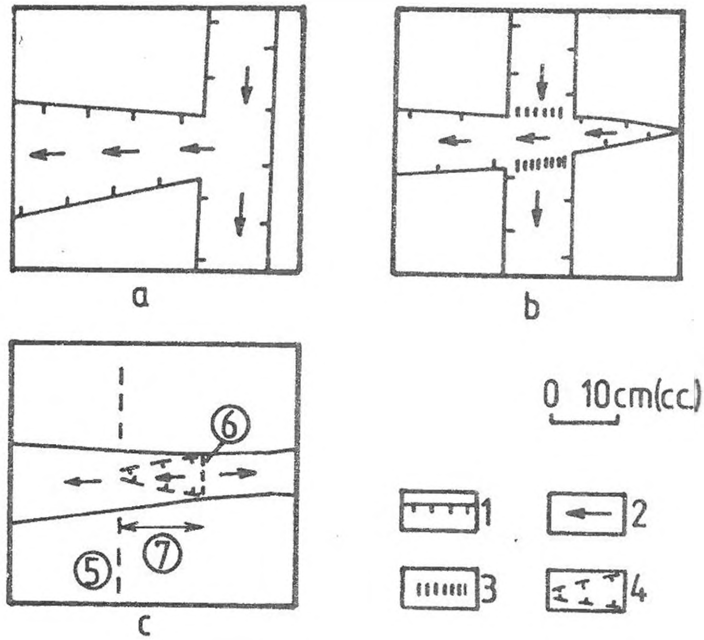

Fig 7: Trough beheadings by regression (after photos)
Legend: a: trough beheading by the contact of the trough-end and the trough-rim, b: trough beheading by trough crossing, c: trough beheading by the contact of trough-ends, 1: trough-edge, 2: slope of the trough-bottom, 3: step, 4: vanished trough-edge, 5: vanished watershed, 6: present watershed, 7. obsequent trough section.

It is frequent that at regressive type II troughs the crests thin out and finally hole through (crest karren natural bridge) (*Picture 4*).

The retreating of the type III troughs that are frequent on the bottoms of type I troughs are often accompanied by bifurcations (*Fig. 10*). Very often the branching off troughs are at right angles at each other rather than acute angle.

The retreating of the troughs is usually slope directed but it can also occur on horizontal surfaces or even against the slope (*Fig. 6*).

It occurs frequently at type II and even more at type III troughs that one trough is perpendicular to the other. The retreating trough-end can decapitate the other trough (*Fig. 7/a*). It can occur that the retreating trough not only decapitate but cross the other (trough crossing *Fig. 7/b*).

The retreating of a karren trough to the other may develop a trough bottom watershed (*Fig. 7/c*). In case one of the cuts more intensively than the other, that digests the bottom of the other in part and the slope of it will be opposite (obsequent karren trough section). A trough-ruin results if not only the upper but the lower end of the trough is decapitated as well (*Fig. 8*). Self beheading occurs when the quickly retreating tributary troughs decapitate the main trough (*Fig. 9*).

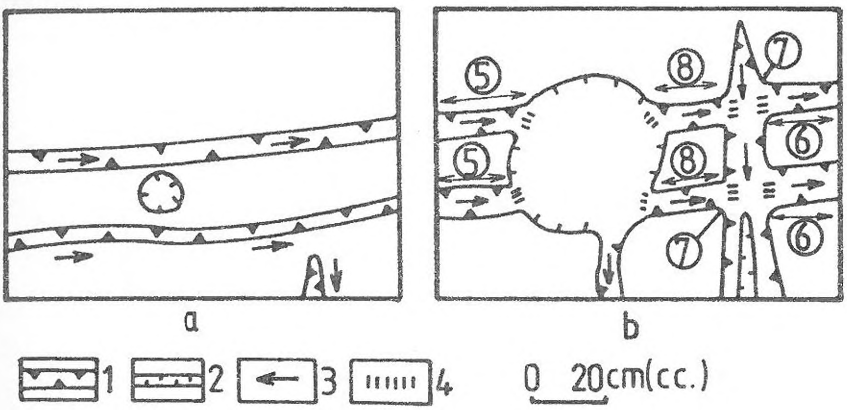

Fig. 8: Beheading by solution pan and trough-crossing (after sketch and photo)
Legend: a: before beheading, b: beheading and trough-crossing, 1: edge of type I trough, 2: edge of type III trough, 3: slope of the trough-bottom, 4: step, 5: trough beheading at the lower section, 6 : trough beheading at the upper section, 7: trough-crossing, 8: trough-ruin

It may occur that a type III trough developing diagonally retreats from one of the type I troughs decapitates the other one. The beheading can be simple or composite. A simple beheading occurs when a type III trough has not yet developed within the type I trough (*Fig. 10/a*). In this case the type III trough branches off downstream in the bottom of a type I trough and retreats in the opposite direction. A composite beheading occurs when a type III regressive trough develops in the type I trough for the duration of the beheading (*Fig. 10/b*). In this case not only the type I trough is decapitated but the type III trough too. The waters upstream of the place of beheading are discharged by the decapitating type III trough (the water that does not spill over) while waters downstream are not. It shall be noted that the waters in the downstream section may discharge into the type III trough in an increasing ratio. (Because the type III trough that causes the beheading commences to retreat in opposite direction to the section under beheading in the type III trough.)

2.2.5 *Karren Terraces and Their Development*

Karren terraces are slightly sloping trough-bottom remnants (sloping inwards and downstream) in the insides of composite wide bottomed troughs, that gradually smooth into the side slope of the trough while they continue with sharp rims in the steep side of the lower positioned trough. Though terraces are not only known in troughs. *BAUER, F.* (1953) describes terraces in the solution pans of the Dachstein Mts.

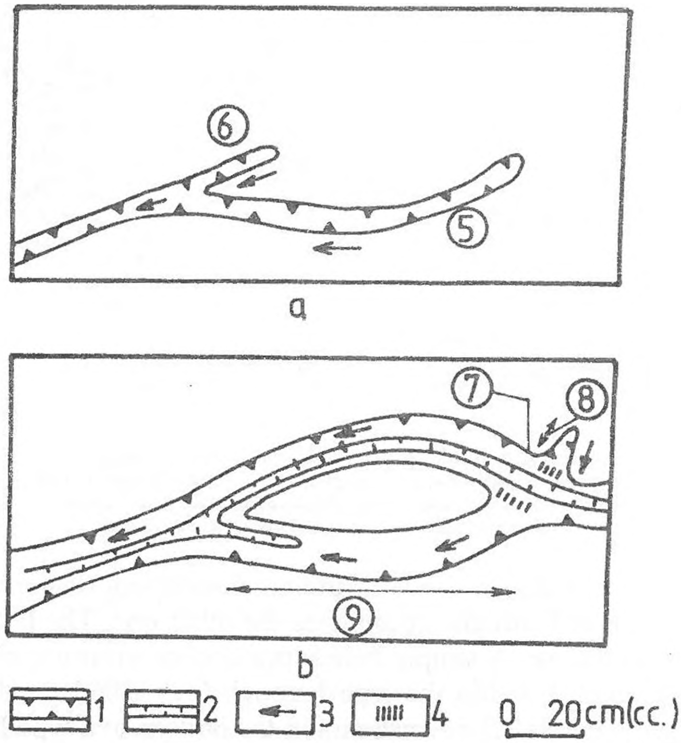

***Fig. 9:** Self beheading with trough crossing*
Legend: a: before beheading, b: after beheading, 1: type I trough, 2: type III trough, 3: slope of the trough-bottom, 4: step, 5: main trough, 6: side trough, 7: location of beheading (trough crossing), 8: hanging trough, 9: remnant of trough

These forms develop when the development of bigger, older troughs stop or slow down (e.g. the quantity of the solvent decreases or the trough grows too large), the growing of the younger trough (or troughs) digests the bottom of the older trough (or troughs, *Fig. 11*). A similar process takes place when the intensity of the discharge of the solvent occurs. In this case an inner trough develops that retreats from the point of beheading. This may be caused by the piracy (see later) of a pit developing in the trough-bottom

(*Fig. 12*). Possibly both phenomena have a role in the development of terraces.

Due to the subsequent solution of the trough-bottom the terraces usually do not make continuous surfaces (terrace remnants). It may happen that a terrace appears only at one side of the trough (odd terraces). They can be completely destroyed, in this case in the meeting of differently sloping sides of the trough edges can be observed. Even these edges discontinue (edge remnants) probably caused by lateral recharge of solvent.

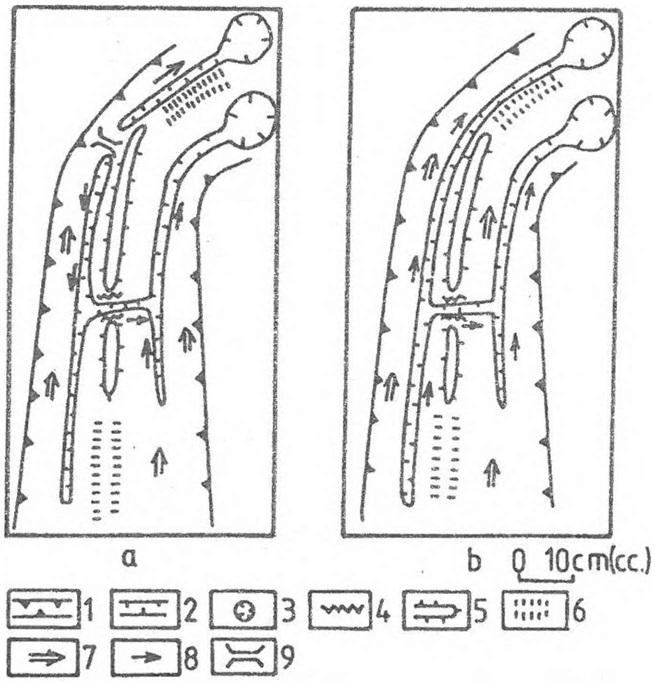

***Fig. 10:** Simple(a) and composite beheading (after sketch and photo)*
***Legend:** 1: edge of type I trough, 2: edge of type III trough, 3: pit, 4: diagonal canyon, 5: inter-trough crest, 6: rise between the troughs, 7: slope of the type I trough, 8: slope of the type III trough, 9: trough-bottom watershed*

The corrosion terraces show genetic relationship to river terraces or mostly to glacial terraces.

2.3 Spot Solution

Vertical solution is relatively substantial compared to lateral solution. Small area surface solution produces solution pots. The morphology of the solution pots is probably determined by the recharge and discharge of the solvent. If recharge suddenly increases the solution pot will be cut open. The discharge trough of the solution pot on its sharp edge is canyon-like (cut open karren canyon). It may happen that it's not the water that spills from the solution pot that develops the karren-trough but a regressing trough reaches up to the pot.

When the solution results a solution pot in the inside of a karren trough, trough-bottom solution pot is resulted. These are small size forms their development barred by the size of the trough. Trough-end solution pots and hanging solution pots are connected with karren troughs. These letter are large diameter and small depth pots. Their existence is a condition for the development of large trough systems. Hanging solution pots line up at the sides of the troughs discharged by trough tributaries (mostly characteristic type III troughs).

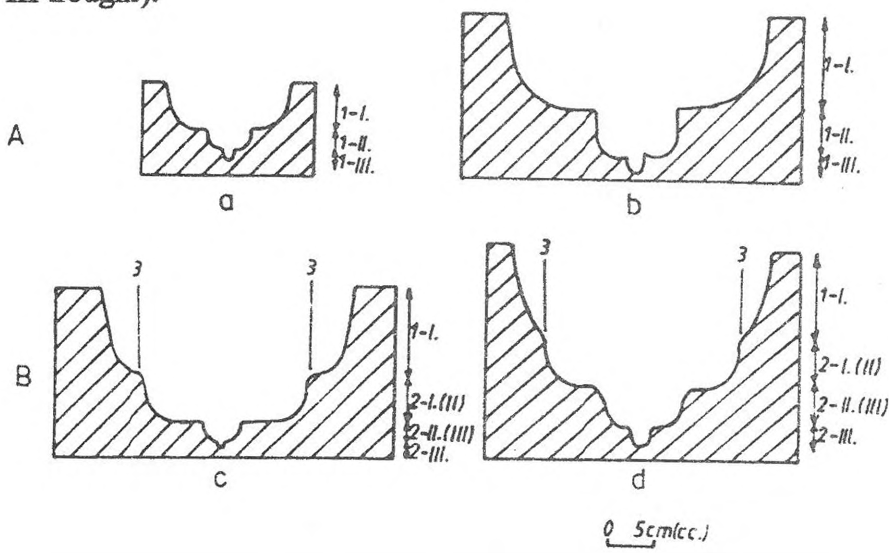

Fig. 11: Development of (a) terrace-less composite trough (b) and terraced (c, d) troughs
Legend: A: the rate of growth of various troughs is similar, B: the master trough does not grow but the discharge decreases (c), or it grows but the discharge remains the same (d), 1: trough that developed before the growth (before terrace development) of the master trough, 2. trough developing after the growing of the master trough (in the period of terrace development) or trough changing to type II from type I, or to type II from type III. (the Roman numeral in the parenthesis indicates the type of the trough before terrace development), 3: terrace

The developing solution pot digests or bisects the karren troughs of the previous ground surface (trough beheading by solution pots). In this case the trough sections at the upper edge of the solution pot will recharge the pot while the others at the other side become inactive (hanging trough). The opposite may also happen, a growing karren trough can reach the edge of a solution pot and opens it up (solution pot made by beheading). In this case the pond in the solution pot is discharged to the beheading trough at low water and through the higher positioned trough as well in high water (*Picture 11*).

It may occur that two discharging troughs develop and one of them deepens at a bigger rate than the other. The one developing at lower rate becomes gradually inactive and becomes a hanging trough.

The temporary pond that develops in the solution pot is of varying size. At low water new, secondary solution pot(s) may develop at its bottom (composite solution pot). At the bottom of the composite solution pot terraces develop (*Picture 5*).

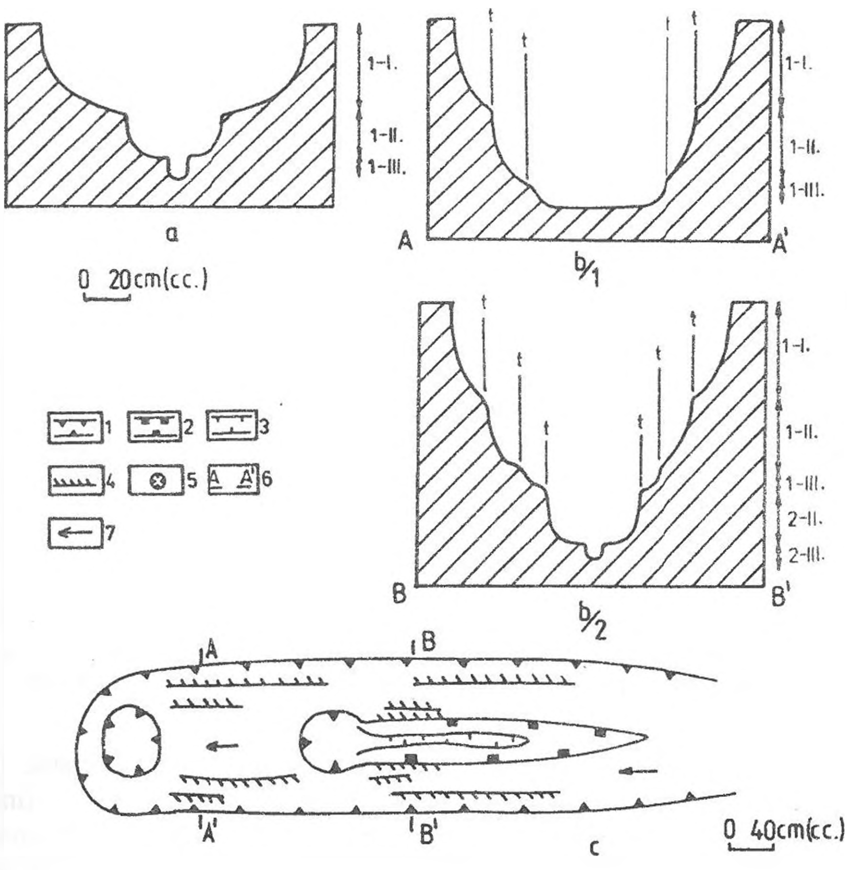

Fig 12: Terrace development in the case of piracy (after survey, sketch and photo)
Legend: a: stage of development before piracy, b: stage of development after piracy, b/1: inactive trough section after the second location of beheading, b/2: active trough section after the second location of beheading, c: plan, I, II, III trough types on the cross sections. 1: edge of the 1-I trough, 2: edge of the 2-II trough, 3: edge of the 2-III trough, 4: terrace, terrace remnant, 5: pit, 6: location of section on the plan, 7: slope of the trough-bottom.

3. Vertical Karren Development

In the course of vertical karren development solution takes effect from the surface towards the inside of the rock along fractures. The development of network karren (two direction solution), fracture karren (one direction solution) and pits. Pits may develop solitary or in groups (pit karren).

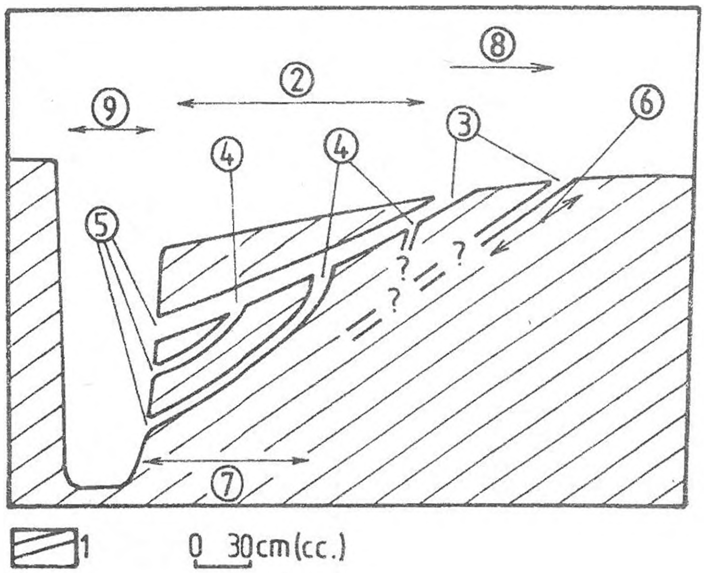

Fig. 13: Karren cavity system (observation)
Legend: 1: bedding plane, 2: through karren trough cavity, 3: karren trough swallet, 4: karren cavity swallet, 5: debouchure, 6: swallet type karren cavity, 7: spring karren trough cavity, 8: retreating of piracy, 9: fissure.

Solitary pits can develop outside (solitary pits) or inside of the troughs (trough-bottom pits). A type of trough-bottom pits (blind pit) develop at places where the troughs are crossed by fractures that have been developed to sizable solution fractures. These pits develop probably blindly (*Picture 6*), they may be filled with soil and vegetation. The other type of trough-bottom pits is of bigger diameter, they are not filled with soil and vegetation, they develop during the beheading of troughs (piracy pits). Trough-end pits (*Picture 6*) occur at the downstream end of the troughs and do not open on the trough-bottom but on the bank (they have their edge on the same elevation where the trough does). Their morphology is similar to that of the solitary pits (arched, concave side slopes that are dissected by half-pits and solution runnels). Solitary pits show a transition towards the karstic meso-forms, the shafts.

4. Cavity- and Cave Development

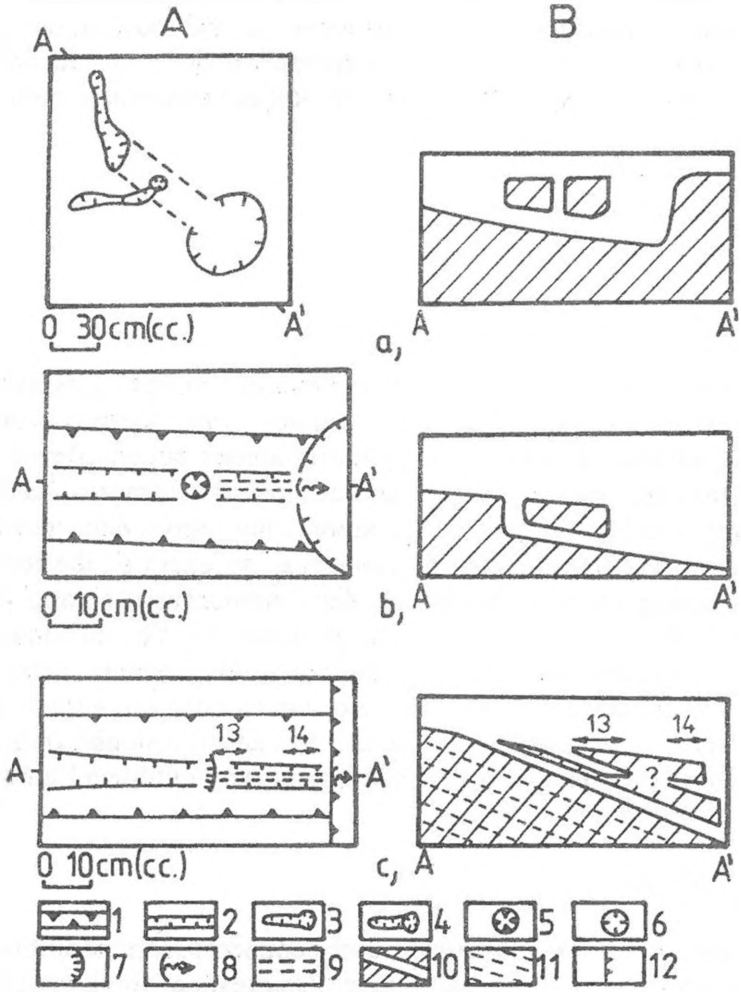

Fig. 14: Types of piracy (vertical beheading, after photos and sketches)
a: development of blind karren trough and secondary swallet when the karren trough is of the same age with the cavity, the development of the pit occurred after the cavity development; b: beheading of a type III trough by a pit. The development of the karren trough cavity occurred after the development of the trough; c: the beheading of a type III trough by a karren trough swallet cavity along a bedding plane.
Legend: A: plan, B: profile, 1: type I trough, 2: type III trough, 3: blind karren trough with karren cavity, 4: blind karren trough with pit, 5: karren trough swallet (pit), 6: solution pot, 7: karren trough swallet. 8: karren trough debouchure cavity, 9: cavity (plan), 10: cavity (profile), 11: bedding planes, 12: fracture, 13: swallet cavity, 14: debouchure cavity

Cavity development occurs along fractures or bedding planes. Subsurface solution can occur independently of the surface solution or in dependence with it. In the letter case a piracy (vertical beheading) occurs simultaneously with cavity development. Piracy is typical in epigene karstic valleys (*JAKUCS, L.* 1971, *HEVESI, A.* 1978). This phenomenon develops on the trough-bottoms too. Observations show that the location of the piracy is not invariable as in the case of the epigene valleys. The location of the beheading shifts to the upstream end of the trough (retreating of the location of piracy).

Cavities may develop:

— between karren depressions,

— under karren troughs.

4.1 Types of Karren Cavities

These cavities may be swallets (sinkhole), springs (resurgence) and through cavities (*Picture 7, Fig. 13*). Swallet type karren cavities may originate in solution pots (*Picture 8*) and in karren troughs. Spring cavities may open into pits, karren troughs, solution pots and fissures. Karren caves below karren troughs (karren trough cavity) may show delta development. Delta development starts in swallet cavities as an effect of the retreating of piracy. To spring cavities developing delta debouchures belong in various elevations in the sides of the fissures (*Picture 9*). The debouchures one below the other develop when spelean beheading occurs (karren cavity swallet). This process probably does not occur only in cavities under the karren troughs. It is possible that under the karren troughs (where cavity development occurs parallel to the bedding planes) multilevel karren trough cavity systems develop.

4.2 Types of Piracy

It may occur that the karren cavity connects such a solution pot and trough that are located on the same level. Upstream of the karren cavity the trough has no continuation (blind karren trough). The karren cavity is connected with the surface by a pit. The origin of this pit is subsequent solution in whole or in part or by cave in (collapse pit). The trough leading to this type of pit (blind karren trough with pit) developed by regression after the development of the pit (*Fig. 14/a*).

In case the karren troughs are beheaded (karren trough piracy) the trough can continue after the point of beheading (*Fig. 14/b, Picture 7*). The karren trough swallets develop at these points (pits by morphology). Karren trough swallet cavity may develop at the point of the beheading e.g. if the solution occurs along a bedding plane, pitless swallet or through cavity develops (*Fig. 14/c*).

5. Merging Karren forms

The merging of karren forms can happen by solution or cave in. Merging by solution can happen between surface forms, or between surface and subsurface forms. In the letter case the merging may be promoted by cave in.

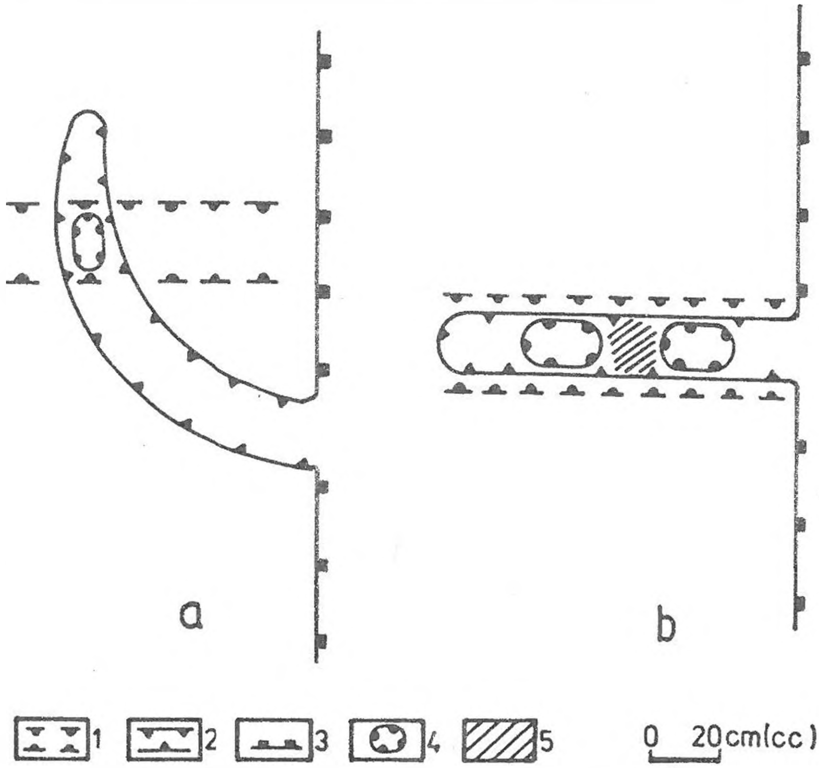

Fig. 15: Circular (a) and elongated (b) windows on karren cavity roofs
Legend: 1: karren cavity, 2: type I trough, 3: solution fissure, 4: karren window, 5: karren bridge

5.1 Merging by Solution Between Surface Forms

Existing various karren forms may merge by lateral solution growth. It can occur between

- pit and pit (*Picture 10*),
- heel print and heel print,
- solution pot and solution pot (*Picture 5*),
- karren trough and karren trough.

The merging of similar surface forms (pit and pit, heel print and heel print, solution pot and solution pot) produces pit, heel print and solution pot uvalas (*Picture 11*). The merging of similar or different forms may result remnants (e.g. pit remnants or half-pits).

As a result of solution merging various forms, thin crests, edges, cones remain of the original surface. Some residual parts of the surface may retain the original elevation (karren inselberg).

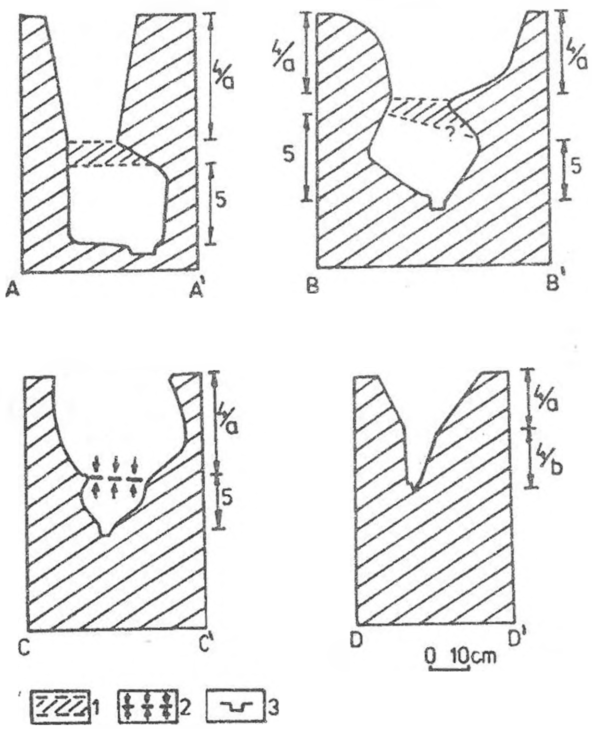

Fig 16: Characteristic cross sections of opened-up karren trough in various stages of development (survey)
Legend: 1: roof destroyed by cave in, 2: roof destroyed by the merging of trough and karren cavity, 3: type III trough, 4a: upper trough section developed by surface solution independently from piracy, 4b: lower trough section intensively developing due to beheading. 5: trough section developed by subsurface solution.
Comment: in the A-A' and B-B' cross sections the opening up happened by the cave in of the roof of the karren trough cavity; solution merging at C-C' section; piracy occurred between the C-C' and D-D' sections.

Different karren forms can merge during their solution growth. Most frequently combine troughs with heel prints, troughs with solution pots (*Picture 12*), pits with solution pots.

5.2 Merging by cave in

This process results the merging of a trough and the trough cavity below it (the opening up of the cavity). The karren cavity positioned below the troughs lose their roofs partly due to solution (that occurs from below upwards and from the surface downwards merging the karren trough and the karren trough cavity) partly to cave in. At the beginning of the process karren bridges and karren windows develop. The windows are circular if the karren trough traverses the karren cavity, elongated if the karren trough develops above the karren cavity in its whole length (*Fig. 15*). Troughs of characteristic cross section develop to the sink point of the earlier cavities (opened-up karren trough). This type is narrowing downwards then it is almost circular at the bottom. Remnants of the roof occur in the trough-sides (*Fig. 16, Picture 13*).

REFERENCES

BALÁZS, D. (1980): Karrformák-karregyüttesek - Karszt és Barlang II. sz. pp. 117-126.

BAUER, F. (1953): Verkastung und Bodenschwund im Dachsteingebiet - Mitteilungen der Höhlenkomission 1. f. p. 53-56.

BÖGLI, A. (1976): Die Wichtigsten Karrenformen der Kalkalpen - In: Karst Processes and Relevant Landforms. ISU Comission on Karst Denudation. Ljubljana pp. 141-149.

FRIDTJOF, B. (1954): Verkarstung und Bodenschwund im Dachsteingebiet- Mitteilungen der Höhlenkomission 1. p. 53-56.

FORD, D. C.-WILLIAMS, P. W. (1989): Karst Geomorphology and Hydrology, Unwin Hyman, London

HEVESI, A. (1978): A Bükk szerkezet- és felszínfejlődése - Földr. Ért. p. 169-203.

JAKUCS, L. (1971): A karsztok morfogenetikája - Akadémiai Kiadó, Bp.

JAKUCS, L. (1980): A karszt biológiai produktum - Földr. Közl. 28., 4. pp. 331-344.

KUNAVER, J. (1984): The high mountains karst in the Slovene Alps- Geographica Yugoslavia 1983. Savez geografskih drustova Jugoslavije, Ljubljana p. 15-22.

LECHNER, J. (1953): Neue Formen des Hochgebirgskarstes im Totes Gebirge - Mitteilungen der Höhlenkomission, pp. 47-49.

MONROE, W.-WATSON, H. (1972): A Glossary of Karst Terminology - US Geological Survey, Washington

TRUDGILL, S. (1985): Limestone Geomorphology - Longman, London and New York

VERESS M. (1992): A karsztosodás mikroformái a karrok - Természet Világa 3. pp. 129-131.

VERESS M. (1995): Karros folyamatok és formák rendszerezése Totes Gebirge-i példák alapján - Karsztfejlõdés I. (Totes Gebirge karrjai) Pauz Kiadó, Szombathely p. 7-30.

VERESS, M.-PÉNTEK, K. (1992): Physical and Chemical Aspects of Hydrodynamics of Some Karstic Process. - New Perspectives in Hungarian Geography, Studies in Geography in Hungary 27, Akadémia Kiadó, Bp. pp. 91-104.

VERESS, M.-PÉNTEK, K. (1994): Néhány karsztos folyamat leírása fizikai-kémiai hidrodinamika alapján - Berzsenyi Dániel Tanárképzõ Fõisk. Tud. Közl. IX. Természettudományok 4. pp. 145-172.

WHITE, W. B. (1988): Geomorphology and Hydrology of Karst Terrains - Oxford University Press, Oxford

List of pictures:

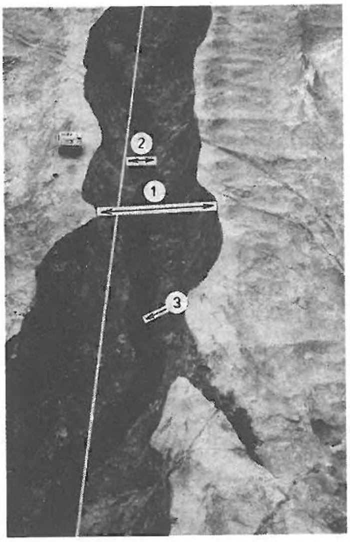

1. | 3.
4.
2. | 5.

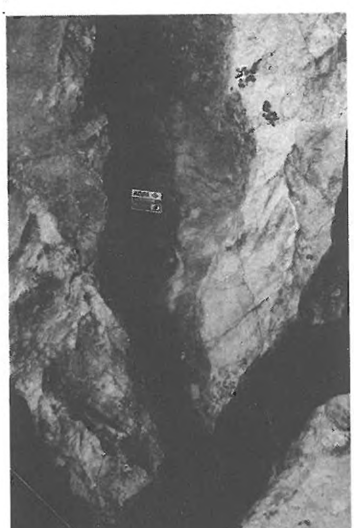

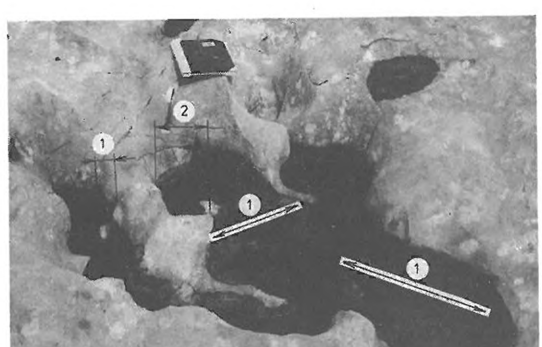

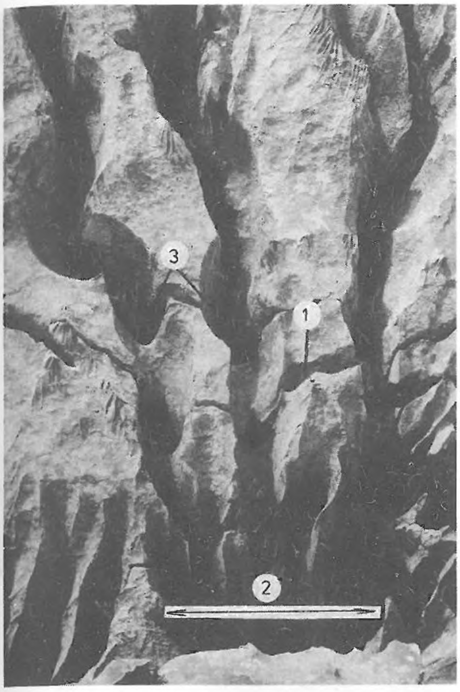

6.

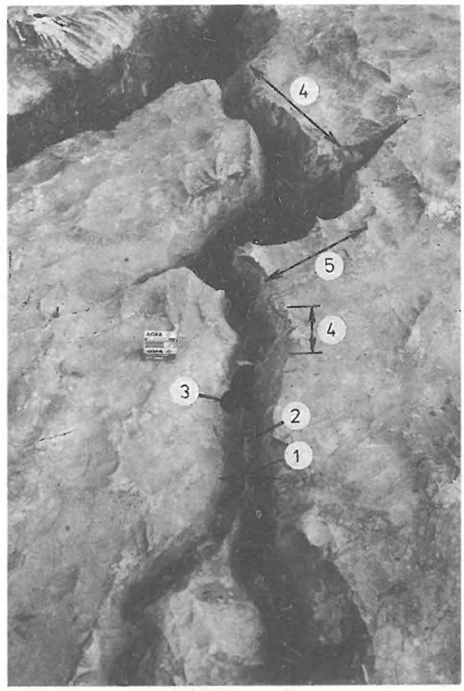

7.

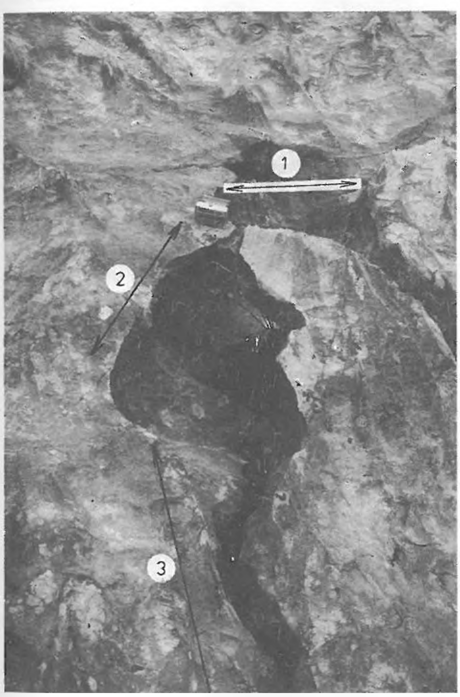

8.

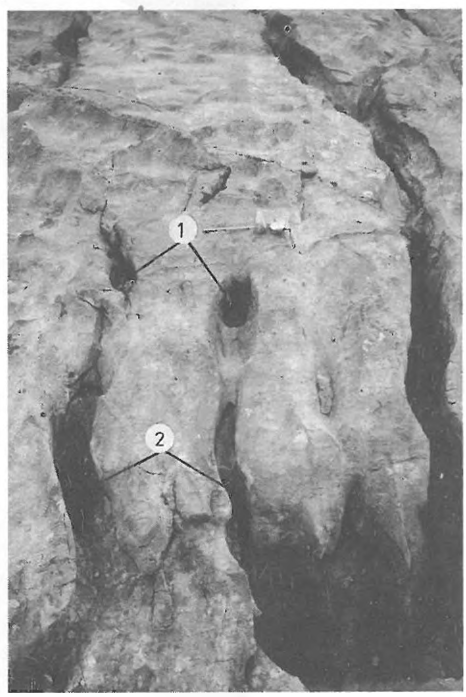

9.

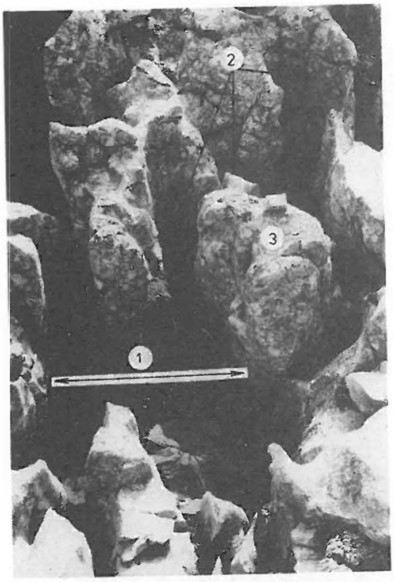

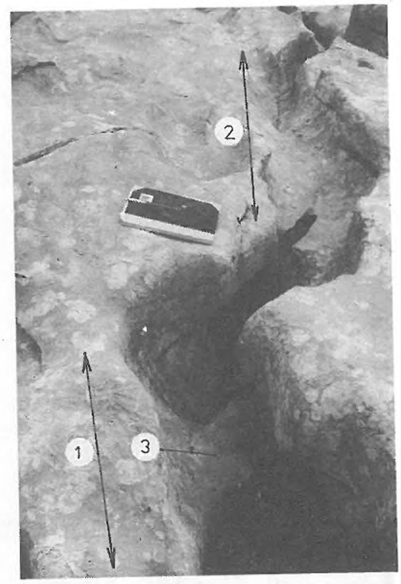

10. | 13.

11.

12.

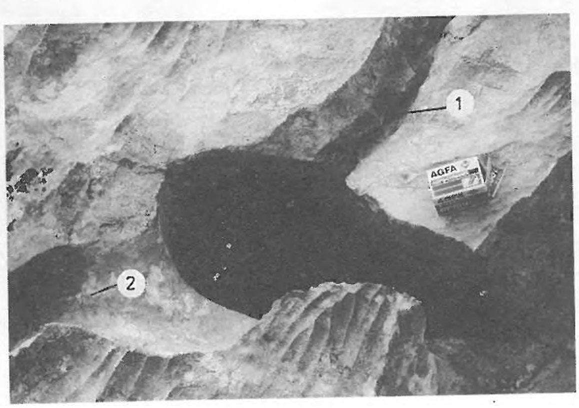

KARSZTFEJLŐDÉS IV.
Szombathely, 2000. pp. 31-40.

THE HISTORY OF THE DEVELOPMENT OF A KARREN TROUGH BASED ON ITS TERRACES

MÁRTON VERESS
„Berzsenyi Dániel" College, Department of Geography
9700 Szombathely, Károlyi G. tér 4.

Abstract: A major karren trough in the Totes Gebirge (Austria) is being studied. Applying the theories of piracy (vertical beheading) and the origin of terraces the genetics of the various forms in the trough are classified and their development is sketched. The processes recognized in the trough offer facts for a better understanding of karren development.

1. Introduction

The area where the studied karren trough is located is situated in the Totes Gebirge mountains (Austria, the Salzburg Alps) at the bottom of a valley of glacial origin close to the Wiesenlacke Lake (*Fig. 1*). The ground surface that was formed rough by the glacier is now developing the karstic way. The mostly bedding plane surfaces are individual karren units that are separated by steps. These meso-karst units (*SZABÓ, L.* 1995) develop into more or less closed karst forms that *LECHNER, S.* (1953) refers to as half dolines (halbdolinen).

The karren trough - that is a major trough - in study developed on such a bedding plane surface dipping to south-east (*Fig. 2, Picture 1*). The trough is NW-SE directed, 6 m long, 0.8 m wide at its lower end and approximately 1.6 m at the upper end. It is deeper than 1.0 m at the lower end and this depth gradually falls under 0.5 m at the upper end. It forks at its upper end. Karren forms are absent in its immediate vicinity of several meters.

A detailed (scale 1:20) contour map was prepared of the trough. The interior forms (inner troughs, terraces and pits) are showed on the contour map of the trough.

Piracy with swallet development is typical in epigene karstic valleys (*JAKUCS, L.* 1968, 1971, *HEVESI, A.* 1978, 1984). According to *JAKUCS, L.* (1971) piracy occurs when the sediments covering the karst are not excessively impermeable while *HEVESI, A.* (1984) says it occurs in case the karstic water level is deeper than two meters under the limestone surface and the system of voids of solution origin is adequately developed. Due to the retreating of the sink points (*JAKUCS, L.* 1971) new swallets develop the earlier ones becoming sinkhole-dolines (*JAKUCS, L.* 1968, *HEVESI, A.* 1980).

Many observations prove that piracy occurs in the troughs of karren surfaces. During piracy pits or karren trough cavities develop (*VERESS, M.* 1995).

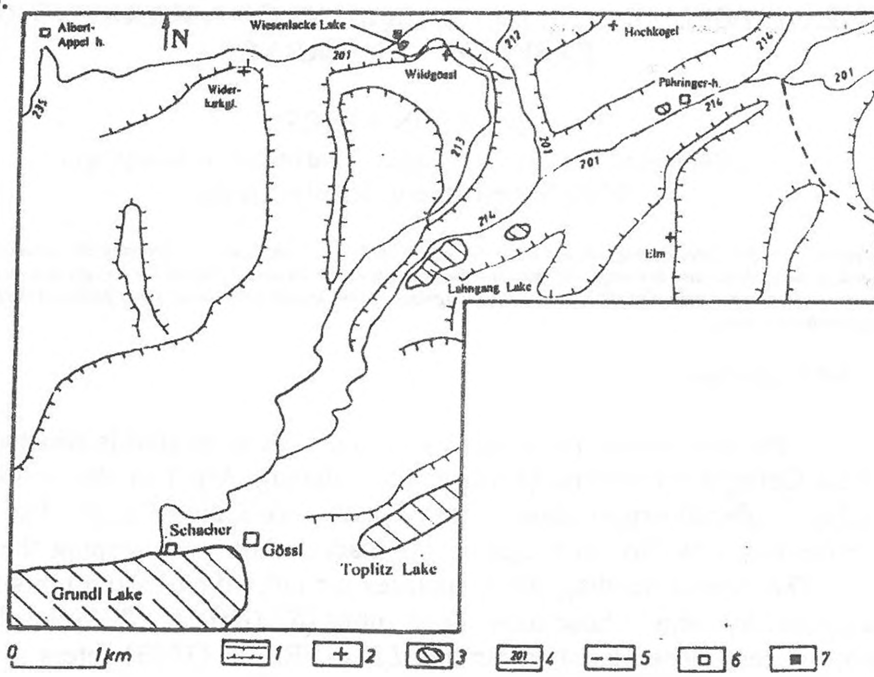

Fig 1: The study site in the mountains
Legend: 1: glacial valley, 2: summit, 3: lake, 4: hiker's track, 5: ski track, 6: hiker's hut, 7: study area.

Due to the above listed reasons piracy points could not develop in the trough bottoms because lacking a covering rock a lithographic interface is absent an active karstic aquifer and karst water table does not develop.

It is suggested that the piracy is due to the change of flow conditions of the solvent. The saturation of the solvent can be expected in the relatively deeply flowing solvent in the trough bottom if the flow is turbulent. In the case of laminar flow after an adequately short distance the stream reaching the point of sinking can remain unsaturated as only the volume of the solvent close to the rock surface is saturated. This can result the development of pits. At certain points the flow of the solvent can turn to laminar from turbulent if the gradient drops considerably (the velocity of the flow drops). The drop of the gradient of major troughs is a natural phenomenon as major troughs are definitely characterized by small bottom gradients.

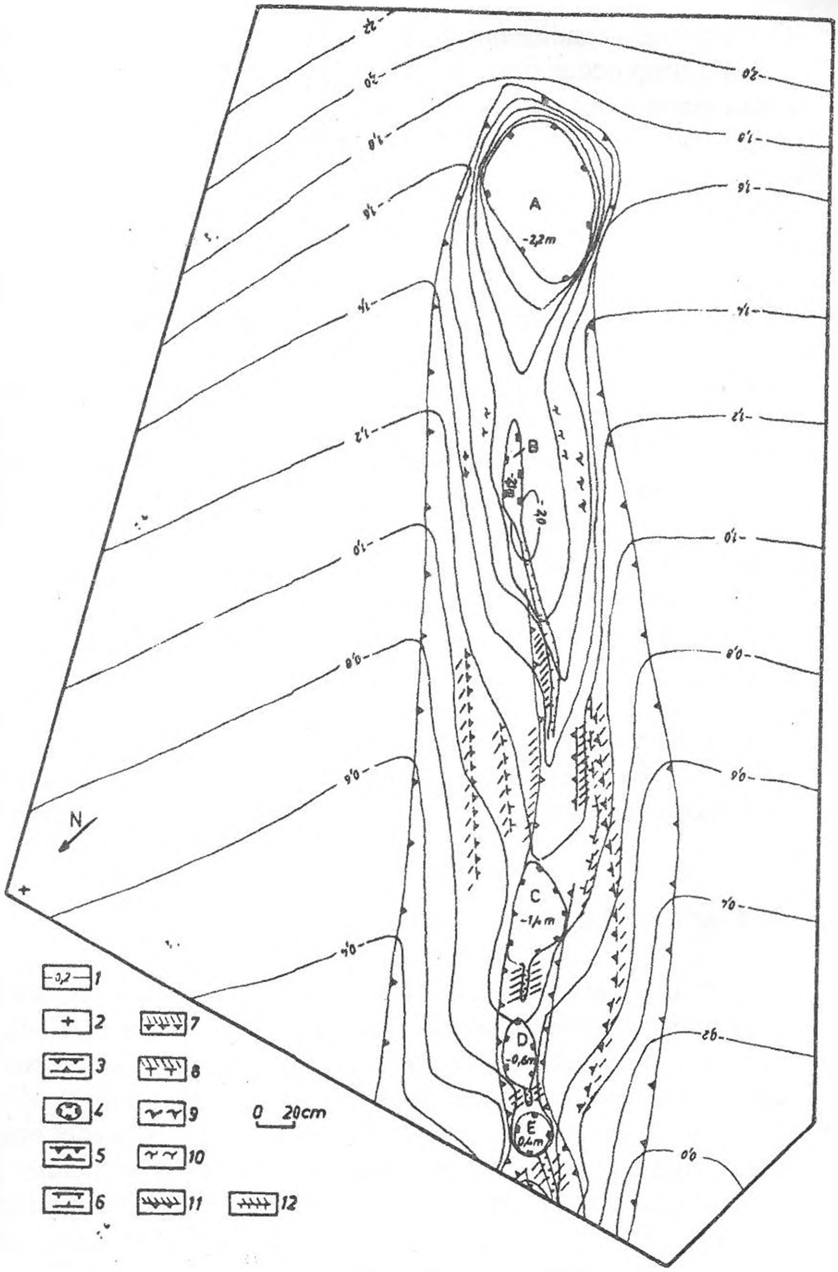

Fig 2: Contour- and morphological survey of the major trough
Legend: 1: arbitrary local contours, 2: position of the surveyor, 3: rim of the major trough, 4: pit, 5: type II trough of pit B, 6: type III troughs, 7-8: remnants of terraces of various elevation, 9-10: edges (remnants of terraces) of various elevation, 11: terrace, 12: terrace in development

The gradient conditions of the trough in study indicates that the decrease of the drop occur from the downstream parts of the trough towards the upstream parts. This attracts the extension of the laminar flow to the upper trough-end that can result the retreating of piracy (development of new pits).

Existing pits can promote the development of new pits. According to *WILLIAMS, P. W.* (1985) to pits - as to locations of minimal pressure - the water stored in the rock will collect. Supposedly the existing pits of a trough enhance the vertical movement of the water that promotes the development of further pits.

Karren terraces can develop in the troughs when the development of type II and type III troughs is quicker than that of the lateral development of the master trough. This way due to the widening of the inner trough only narrow strips of the master trough bottom remain. The initial condition of this phenomenon is a wide trough bottom. The development of trough bottom remains (terrace) can be due to the listed causes:

- The master trough loses its catchment area thus only that much solvent can flow in the trough steadily that allows only the development of type II and III troughs.
- The master trough can grow to such size that the solvent from the original catchment area fills it only partially.
- Piracy occurs in the trough bottom. Starting at the point of piracy further trough(s) develop that digest the bottom of the master trough in part during their regression.

2. The Morphology of a Major Trough

The pits in the master trough in study (henceforth trough) are typical piracy (water drainage) trough bottom pits. In the case of the B, C, D, E pits the piracy is proved by their development in the bottom or at the end of the inner trough. The drainage of water is proved by the development of type III troughs retreating from the pits. Possibly the A pit or its predecessor may have been a trough-end pit. This letter has lost its activity as neither type II nor type III troughs are connected to it. (The A pit could be specified as a trough bottom pit if the it were developed in the bottom of an inner trough or if the inner trough continued beyond the pit).

The retreating of the locations of the piracy occurred as the size of the pits decreases upwards from the lower trough end.

Two types of troughs can be specified in the bottom of the major trough (main trough). One of these types is represented by a type II trough that is the older regressive trough of the B pit (henceforth the type II trough of pit B). To the other category type III troughs belong. The type II occupies a considerable part of the bottom of the master trough but is partially damaged and separated to parts by the C, D, E pits. Type III troughs are forms retreating from the B, C, D, E in the bottom of the type II troughs.

Remains of terraces can be identified between the B and C pits on two levels. (The upper No. 1 terrace stretches to pit E on the south side of the trough.) The remnants of the terraces are a couple of centimeters wide. (The remnant of the trough bottom at the north slope of the trough - the lower N° 2 terrace - exceeds 10 centimeters.)

Terrace No. 1 is the remnant of the trough bottom (major trough), terrace No. 2 is the remnant of the type II trough leading to pit A. Even the remnants of the terraces are now missing on the trough sides between the pits A and B. Only the remnants of edges can be identified in the same two levels.

In essence the terraces were wholly digested between pits A and B. In this phenomenon the development of pit B might have had a role or the recharge of solvent to the trough from its rims. Subsequent trough(s) could not develop from pit A as the catchment of this pit became too small after the development of pit B.

It can be stated with much certainty that the described remnants of terraces and edges are the remnants of these two terraces because 2-2 straight lines can be fitted to the edges of these two remnants on both sides of the trough. The troughs responsible for these terraces can not be observed beyond the lower end of the major trough and the straight lines fitted to the upper terrace remnants and edges touch pit A. The described fact hint that the terraces and the troughs that are responsible for them developed above and after the development of pit A. This proves as well that the development of pit A started after the development of the trough. In this case the major trough gradually changed to be a blind karren trough after its development (similarly to the blind valleys of karst areas).

The development of a type II trough resulted the development of a new terrace or is presently resulting it. This is terrace No. 3 that is the remnant of the type III trough leading to pit A. It is visible that because of the missing older terraces it develops only locally because there is no chance for this because of the ending of the above mentioned trough it can not develop between pits A and B. The changing of the terrace to a remnant can be observed on the south side of the trough in the section between pits B and C. This can be explained by the widening of the type II side of pit B reaching the type III side of pit A in a short section.

The development of a No. 4 terrace is in progress from the bottom of the type II trough of pit B at those places where type III troughs have developed.

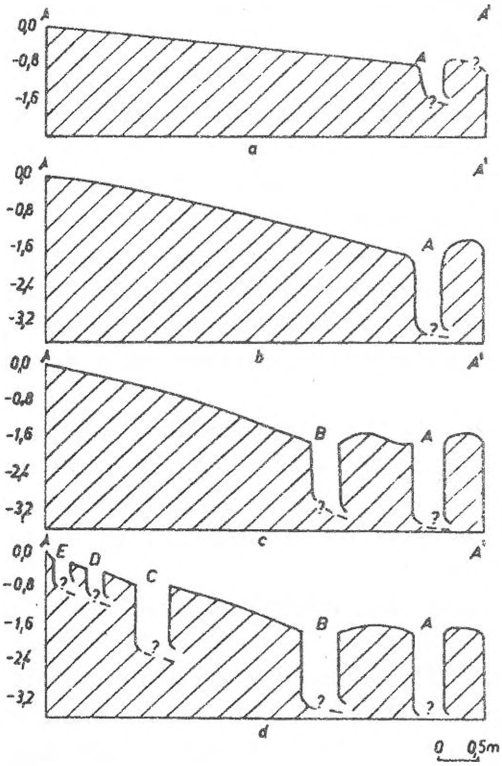

Fig 3: The history of the karren trough in profile

3. The History of Development of a Trough

The trough develops, then its A pit does (*Figures 3a, 4a*). Supposedly no surface drainage of the trough developed. The retreating and widening of the type II trough digesting most of the bottom of the major trough resulted the development of terrace No. 1. With the development of the type III trough of pit A the development of the No. 2 terrace begins. Then pit B develops followed by its type II trough (*Figures 3b, 4b*).

The widening of this type II trough digests the bottom of the type III trough belonging to pit A and results the No. 3 terrace. The development of a new trough (type III trough) commences from pit B. The change of terraces No. 1 and 2 to remnants occurs with the change of remnants to mere edges at certain sections (*Figures 3c, 4c*).

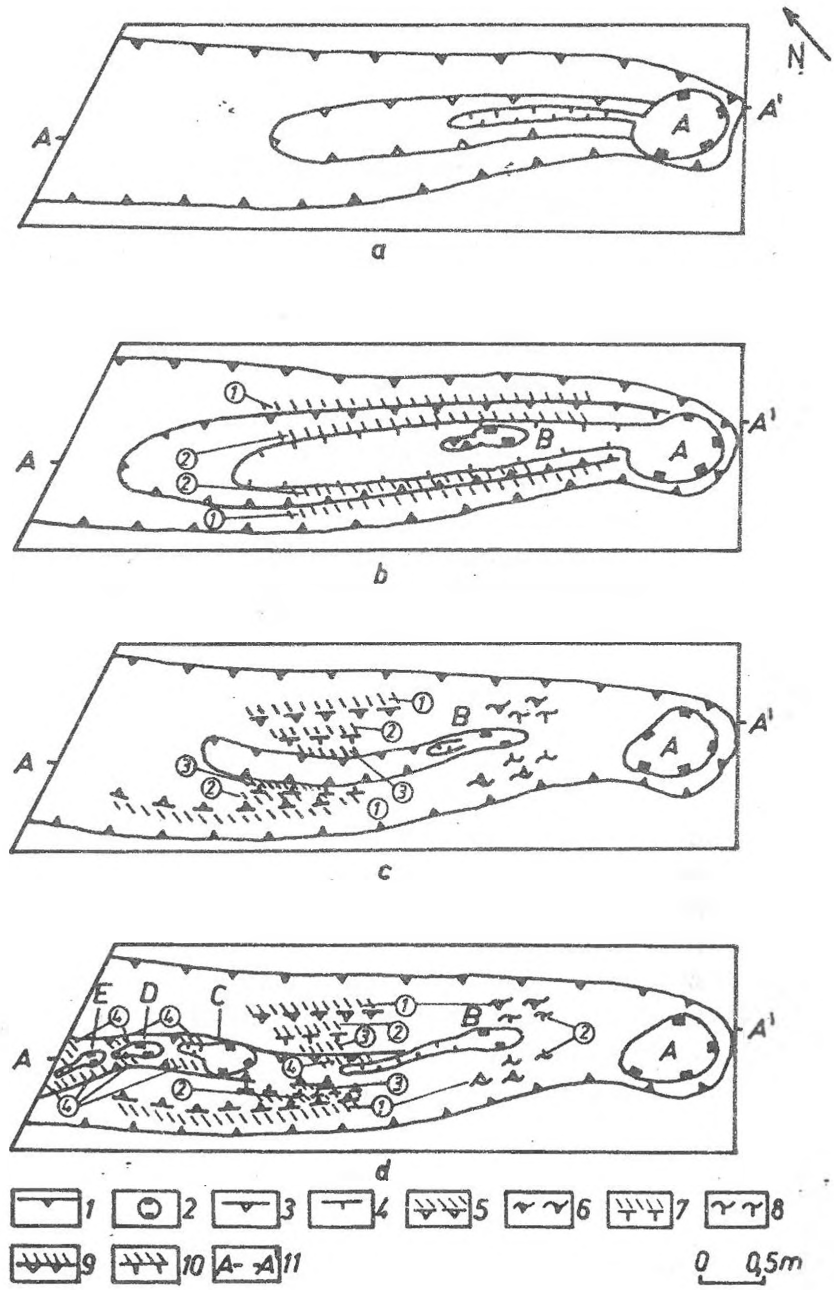

Fig 4: The history of the karren trough in plan
Legend: 1: rim of the major trough, 2: pit, 3: type II trough of pit B, 4: rims of type III troughs, 5: No. 1 terrace and residual terrace (remnant of the major trough bottom), 6: edge (remnant of No. 1 terrace), 7: No. 2 terrace and residual terrace (remnant of type II trough bottom of pit A), 8: edge (remnant of No. 2 terrace), 9: No. 3 terrace and residual terrace (remnant of type III trough bottom of pit A), 10: developing No. 4 terrace (remnant of type II trough bottom of pit B), 11: location of section

Following this during beheadings first pit C then further pits develop (D, E) in the type II trough of pit B. (The development of the No. 3 terrace probably stops because it gets no solvent or only a little after the development of the rest of the pits.) The type III troughs of the C, D, E pits develop (*Figures 3d, 4d*). The development of type III troughs means the development of a new No. 4 terrace from the bottom of the type II trough of pit B. This letter is not uniform even at the beginning because it is originated in the widening of four type III troughs that were separated by pits. Possibly the time of their development is different too: the type III trough at pit B is the oldest while it is the youngest in the type III trough at pit E.

It occurs that the development of terraces can be fitted without contradictions if the causes are explained by piracy.

Resulted by the uniform (surface) solution of the side slopes the rims of the trough are rounded, the terraces are separated to remnants and then transform to edges. The dissolution of the trough sides is most considerable at the lower part of the trough. This may be connected with the fact that due to the slope of the sides the lower part of the trough receives more solvent than the rest of it.

It is expected that the laterally recharging solvent does not widen the trough significantly. This seems to be supported by the fact that the distance of the rims of the oldest terrace remnants and edges to the trough rims is nearly equal but the trough sides are more steep here than in the upper part of the trough. Here the dissolution of the trough sides appears as the digestion of the irregularities (terraces) and the lower part of the trough sides. The upper section of the trough is wider and the side slopes are less steep. Possibly here the upper part of the slopes is dissolved. This is hinted at by the better condition of the No. 1 terrace than it is in the lower section. (This is only possible if the bordering surface is dissolved in a greater degree than in the neighborhood of the lower section of the trough. This hints that the slope of the host ground surface is becoming ever less steep because of surface solution.)

Results

By the recognition of morphological properties and the explanation of their origin the history of development of a certain karren form can be sketched. It occurs that these forms in the case of karren troughs it is the terraces and pits.

- The position of the pits, their eventual discontinuity or missing the development by solution of the side slopes of the master trough can be deducted (slope retreating).

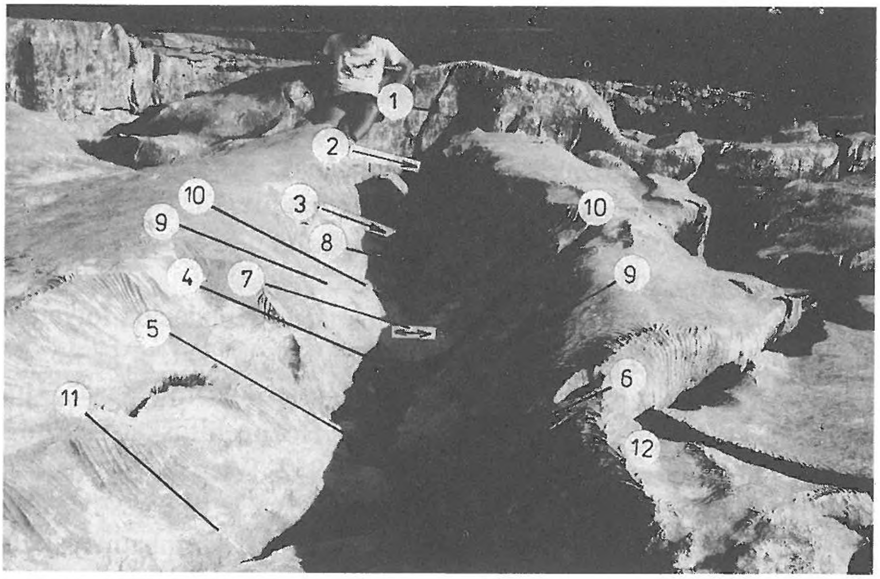

1.

Picture 1: Picture of the karren trough as seen from the north (vegetation at the Wiesenlacke Lake in the background)
Legend: 1: end of closed trough, 2: pit A, 3: pit B, 4: pit C, 5: pit D, 6: pit E, 7: type II trough of pit B, 8: type III trough of pit B, 9: No. 1 residual terrace, 10: No. 2 residual terrace, 11: the left hand tributary of the trough, 12: the right hand tributary of the trough

- The karren trough presented as an example developed as the result of a number of solution processes. The developing small- or part-forms generate new processes making the development of further forms possible.
- The development of a particular major trough is the result of self enhancing processes in case the initial conditions had been advantageous. The trough developing on a bedding plane terrain attract the solvent from its vicinity. Thus the development of other troughs stops or does not even commence, this resulting in the further development of the existing trough at an increasing pace.
- Two ways of the partition of bedding plane terrain is possible by troughs. It can be done by many troughs or by a single or several major troughs. In the letter case the developing trough extends its catchment area to an ever increasing area and an ever more complex development occurs in its interior.

REFERENCES

HEVESI, A. (1980): Adatok a Bükk hegység negyedidőszaki ősföldrajzi képéhez - Földtani Közl. 110 3-4. f. p. 540-550.

HEVESI, A. (1984): Karsztformák kormeghatározásával és mészkőhegységeinek új harmadidőszaki-jégkori arculatának megrajzolásában játszott szerepükről a Bükk hegység példáján - Földrajzi. Ért. 33. 1-2. f. p. 25-56.

HEVESI A. (1978): A Bükk szerkezet- és felszínfejlődésének vázlata Földr. Ért. 27. 2. f. p. 169-203.

JAKUCS L. (1968): Szempontok a karsztos tájak denudációs folyamatainak és morfogenetikájának értelmezéséhez - Földr. Ért. 17. 1. f. p. 17-46.

JAKUCS L. (1971): A karsztok morfogenetikája - Akadémia Kiadó, Bp.

LECHNER, J. (1953): Neue Formen des Hochgebirgskarstes im Totes Gebirge - Mitteilugen der Höhlenkomission, 1952. Wien p. 47-49.

SZABÓ L. (1995): Karrvályú rendszerek térképezése a Totes-hegységben - Karsztfejlődés I. (Totes Gebirge karrjai) Pauz Kiadó, Szombathely, p. 61-70.

VERESS M. (1995): Karros folyamatok és formák rendszerezése Totes-Gebirge-i példák alapján - Karsztfejlődés I. (Totes Gebirge karrjai) Pauz Kiadó, Szombathely, p. 7-30.

WILLIAMS, P. W. (1983): The Role of the Subcutaneous Zone in Karst Hydrology - J. Hidrol. 61. p. 45-67.

KARSZTFEJLŐDÉS IV.
Szombathely, 2000. pp. 41-76.

THE MORPHOGENETICS OF THE KARREN MEANDER AND ITS MAIN TYPES

MÁRTON VERESS
„Berzsenyi Dániel" College, Department of Geography
9700 Szombathely, Károlyi G. tér 4.

Abstract: Applying observations taken in a couple of karren terrain in the Totes Gebirge (Austria) the forms of karren meanders and their development were studied and karren meander types were specified. In the knowledge of the conditions of development of the meander types not only the types of karren troughs can be specified but the development of specific karren troughs can be explained too.

The properties of the bends (arc-length, meander wavelength, state of development and slip-down intensity) of four karren troughs were studied in order to know the laws of meander development and to know the factors that influence slipping. Data hint at the slipping depending on the gradient while to the lateral swing of the channel line that determines the development and rate of development of the bend the gradient has little and indirect effect.

I. Introduction

Scientists studying karren development specify a special meandering (bending) type of karren troughs (*FRIDJOF, B.* 1954, *BÖGLI, A.* 1976, *BALÁZS, D.* 1990). According to the observations meandering can be characteristic to simple or composite troughs or even to rillen (*DUNKERLEY, D. L.*, 1979). This statement is well documented and represented by surveys illustrating karren forms (*SZUNYOGH G.-LAKOTÁR K.-SZIGETI I.* 1998, *VERESS M.-BARNA J.* 1998, *BARNA J.* 1998). *VERESS M.* (1995) specifies meanders as true meanders when the channel line bent before the development of the karren trough or false meanders when the channel line started to bend only after the trough had developed. In composite troughs according to the position to one another of type I and III troughs forced-, similar-, slipped-, confined-, and free meanders were specified. (Though the author describes the slipping of the bend but at the specification of the meanders the lateral shifting of the channel line has not been considered.) The listed meanders can either be false or true meanders. The type of the meander can be identified only considering if a *slip of bends* occur after the entrenchment of the master trough or not.

During the swinging of the channel line channel bends (meanders) develop. The lateral extension of the meander can be measured by the width of the meander zone (the area enveloped by the enveloping curves of the outer fringes of the meander arcs), its size with the wavelength of the meander (the shortest distance between two neighboring points of inflection or along the axis of the channel), the arc of the meander with the length of the meander (the distance between the points of inflection measured on the channel line) (*BALOGH, K.* 1991, *BORSY, Z.* 1992). Because during the development of karren troughs entrenchment occurs in the first place the development of karren troughs is not identical with the lateral development of middle course type water courses but with the bend development of rivers of forced meandering. In the valleys of rivers of forced meandering meander slippage occurs (*PÉCSI, M.* 1975).

For the study of meander slippage observations were made in the Totes Gebirge at the No. 201 hiking trail to the Widerkar Peak and at the No. 230 trail to the Gr. Scheibling Peak. Meandering troughs were surveyed in the letter location.

II. Bend (Meander) slippage and its forms

1. The Swinging of the Channel Line

Solvent flowing on carbonate ground surface can progress straight or bending (*Fig. 1*). Any particular point of the channel line can be positioned in the central line of the flowing solvent or anywhere else.

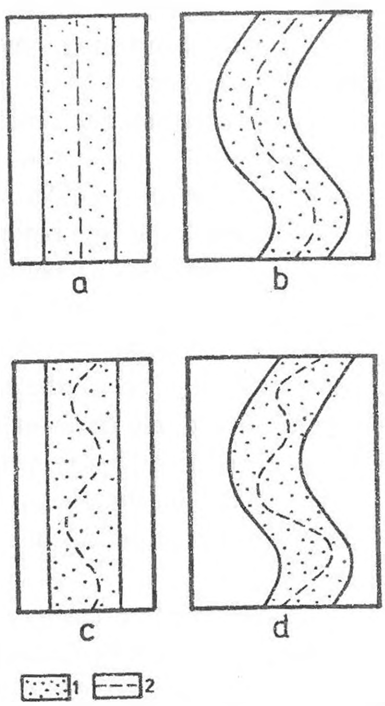

Figure 1: Channel lines showing no swinging (a), false swinging (b) and true swinging (c, d)
Legend: 1. solvent, 2. channel line

If it is positioned on the central line but the solvent is bending, false swinging occurs (*Fig. 1b*) because the lining of the edge of the flow and its channel line is the same. If the channel line does not follow the central line, true swinging occurs (*Figures 1c, d*). The swinging of the channel line can be temporary (functional) and steady.

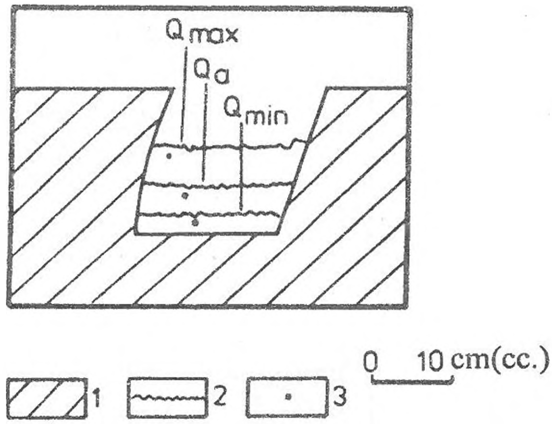

Figure 2: Channel lines of asymmetrical trough at various flow rates
Legend: 1. karren development on the rock, 2. water level, 3. channel line, Q_{min} low water level, Q_a medium water level, Q_{max} high water level

Functional swinging of the channel line is caused by the changing discharge of the solvent in the trough (*Fig. 2*). To higher discharge higher flow velocity belongs that increases the length of the channel line. Functional swinging can occur either at false or true swinging.

During steady channel line swinging slippage occurs. This letter is not restricted to one single function. The causes of steady channel line swinging can be as follows:

a/ In case of channel line swinging caused by external effect the channel line is not positioned there where it should during normal flow. The swinging does not occur because of the flow of the solvent but because water particles moving along the channel line hit obstacles. Swinging can be caused by the below listed causes:

- false meander in the trough (*Fig 3a*) or the bending of the flow,
- asymmetric trough (*Fig 3b*),
- flow from tributary trough (*Fig 3c*),
- trough-side (*Fig 3d*),
- unevenness of the surface (crack, calcite filling, eventually existing karren forms).

In false meanders due to the inertia of the flow the channel line can not precisely follow the changes of direction of the trough. The channel line section

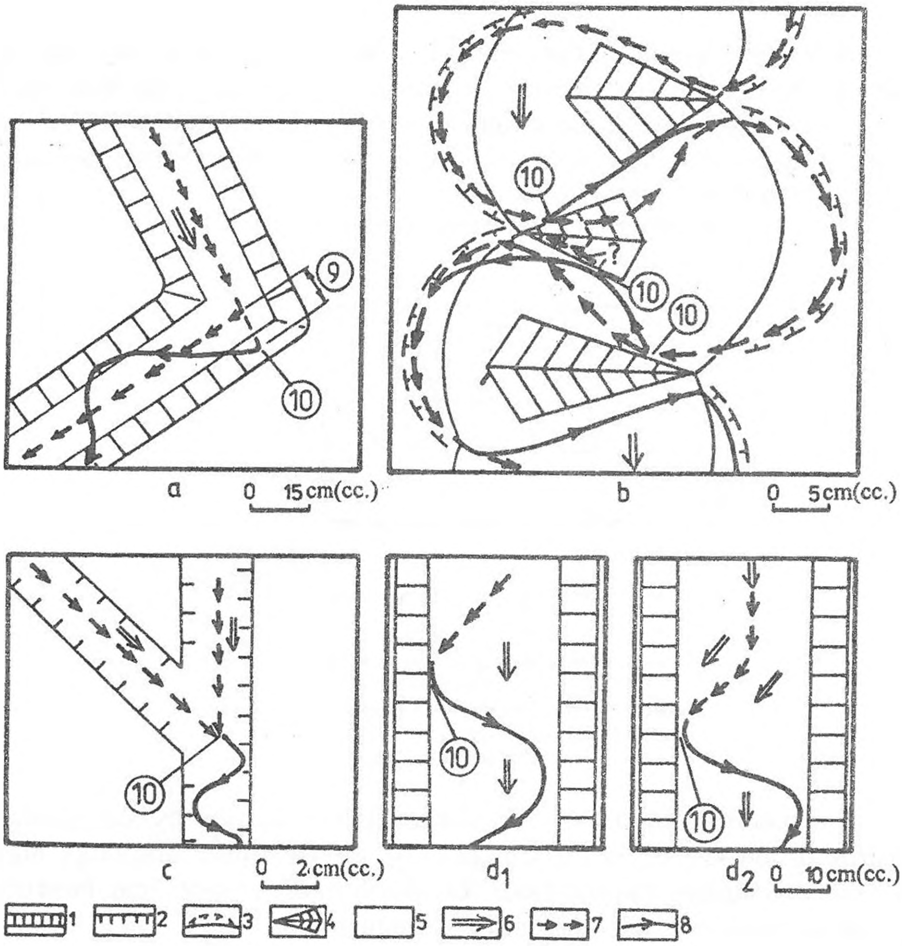

Figure 3: Swinging of channel line caused by external causes
Legend: 1. gently sloping trough side, 2. vertical trough side (type III trough), 3. overhanging trough side, 4. skirt, 5. trough bottom, 6. slope of trough bottom, 7. channel line, 8. swinging of channel line caused by external causes, 9. lengthening of channel line caused by flow inertia, 10. location of obstacle hit by the channel line, a. false meander, b. asymmetric trough, c. flowing water from tributary trough, d. there is an angle between channel line and trough side (d_1 the channel line has already swung, d_2 the channel line is swung by the slope of the trough bottom)

of the upstream trough section elongates towards the downstream rim of the trough and hits the side of the trough.

On ground surface without troughs the channel line of increasing flow can not follow the bending of the solvent. The series of functional swings can lead to the development of skirts. As a conclusion the steady swing of the channel line can occur if the laterally ever elongating skirt reaches the channel line at the entrenching trough bottom.

In the case of a symmetric trough the collision is caused by different influence. In such troughs arcing niches (overhangs) vary with variously shaped convex trough wall sections (skirts). Consequently water particles that move along a channel line parallel with the arced section arrive to a section with a different arc where the channel line will not be parallel with the new arced section will collide with the trough wall.

The role of the skirt and trough sides in the deviation of the channel line is secondary. They can only cause swinging if it had occurred caused by some other effect. It shall be noted that the channel line can hit the trough side even if its swinging had not yet occurred. E.g. in a case when the trough bottom is of such gradient that the solvent does not run parallel with the trough side but at an angle with it (*Fig. 3d₂*).

The swinging of the channel line if it is caused by external forces will subside if the forces cease to act. The channel line "smoothes out", the subsequent meanders of the trough become ever smaller, the meander zone decreases. The local swings of the channel line make the meanders themselves of local development. It may occur that an individual swing causes a series of swings as the swinging channel line hits one and the other trough side. Finally it can be mentioned that self generation is frequent. This shall be understood that caused by some form (e.g. skirt) the channel line swings this causing the further growth of this form that influences the magnitude of the swinging.

b/ Channel line swing due to inherent causes is generated by the flow of the solvent. It can develop on homogenous, smooth rock surface where the movement of water particles is not hindered by any obstacle. (The cause of development is unknown, it can be caused by the saturation of the solvent.) The bending of the solvent can occur even before the development of the trough.

2. The Slippage

Dissolution is more intensive where the flow velocity of the solvent is higher. At higher velocity the transportation of the Ca^{++} ions and this way the adequate difference of concentration is maintained between rock and solvent. Thus the dissolution of the trough bottom is of the biggest magnitude at the neighborhood of the water level (laminar flow) or at the water level (turbulent flow) and in the letter case at the channel line.

While at the swinging of a functional channel line its position changes only in plane, at slippage it changes in space, because in the letter case due to the entrenching of the trough in the course of the channel line swing it gets ever deeper too. This process is irreversible. The cause of this is that the development symmetric trough form, the development of which can be linked with the swinging of the channel line "preserves" (bigger swings than the functional channel line swinging are not allowed by the trough sides) the lining of the channel line in a certain time. (It shall be noted that the functional shift of the channel line does not wholly happen in a plane because the water level changes in the function of the flow rate.)

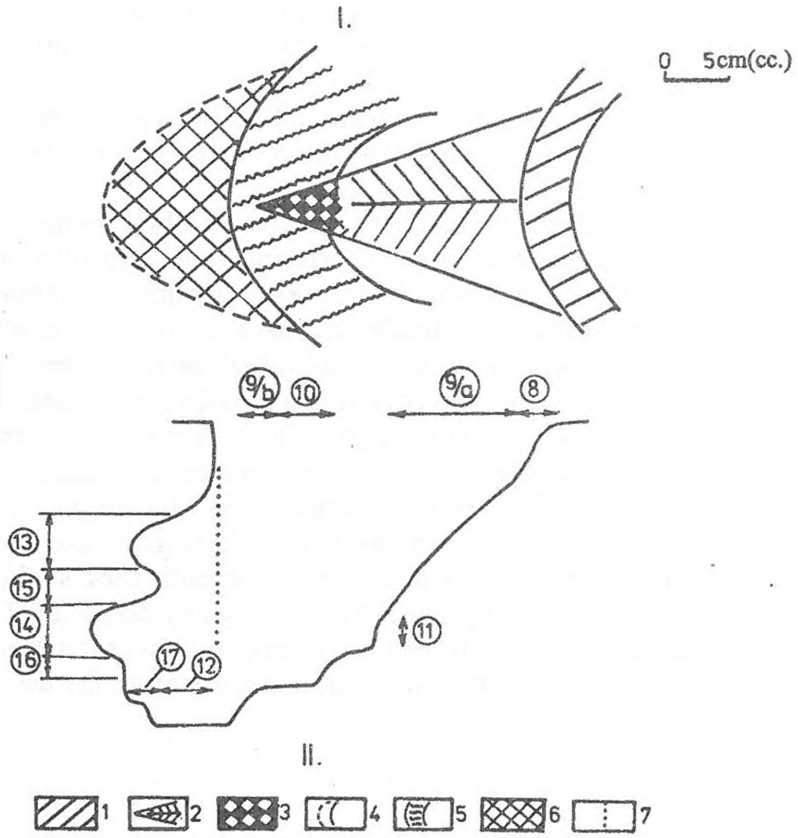

Figure 4: Morphological forms of a karren meander
Legend: I. plan, II. cross-section on the plan: 1. gently sloping trough side, 2. skirt, 3. skirt terrace, 4. overhanging side wall, 5. trough bottom, 6. meander terrace on the concave side, on the cross-section: 7. projection of the rim of the overhanging wall, 8. convex trough side, 9a. skirt remnant at the top, 9b. skirt remnant at the bottom, 10. meander terrace (on skirt), 11. skirt terrace groove, 12. meander terrace (on overhanging wall), 13. asymmetric terrace groove, 14. symmetric terrace groove, 15. crest between terrace grooves, 16. eroded crest between terrace grooves, 17. terrace groove remnant

Linked to the development of the trough the original channel line, the channel line at the initial slippage and the present channel line can be specified. The original channel line characterizes the flow of the solvent until the true swinging occurs. A channel line at the initial slippage on the ground surface - thus at the beginning of the entrenchment - is an already swinging channel line. This channel line is documented by the rim of the trough. The present channel line is the one that can be traced at the plane of the present trough bottom.

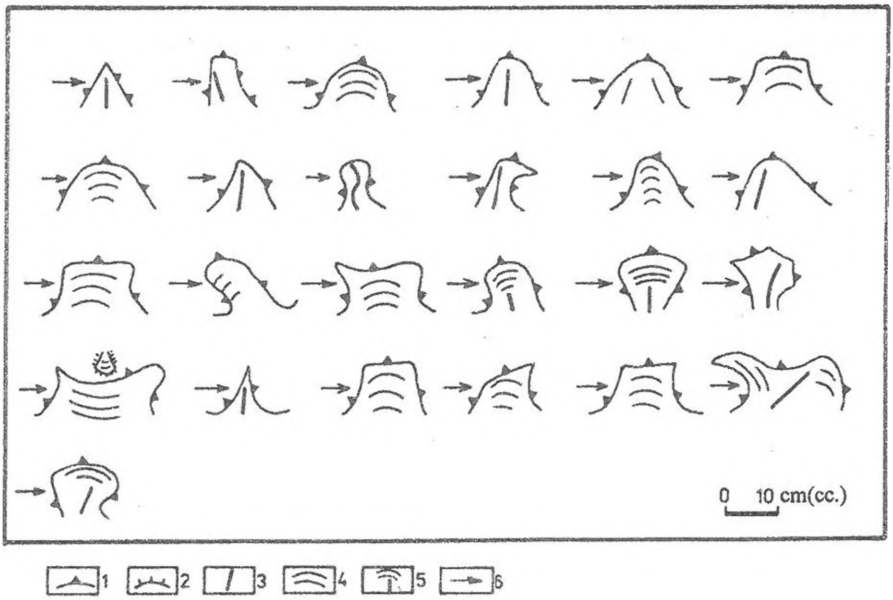

Figure 5: Skirt forms in ground-plan (on observation)
Legend: skirt of type I trough, 2. skirt of type III trough, 3. skirt ending in edge (half pyramid), 4. round (half cone) skirt, 5. skirt ending in edge at top and rounded at bottom, 6. direction of flow

The difference of the initial and original channel line is the channel line swing before the development of the trough, while the initial difference of the present channel line and the slippage is the swinging at trough development, the slippage. The total swing of the channel line can be measured on the perpendicular drawn to the tangent at any point of the trough rim and with the sum of the horizontal projections of the channel line swing prior to trough development. (It can be noted that caused by the slippage two kinds of bed zones can be specified. The original one that can be traced at the trough rims and the present one that is at the level of the trough bottom.)

In such trough bottoms where the channel line is positioned in the middle of the trough at all times (false swing may only occur), the dissolution and entrenchment is the biggest in this location. Resulting from this symmetric troughs develop in the bends (false meander, *Picture 1*).

If the channel line is not positioned in the middle of the trough (true swing) the trough does not entrench most intensively in the middle of the bottom. In these cases troughs of asymmetric cross section develop (true meander). As channel line swinging may occur at false swinging as well (functional channel line swinging) the trough can assume an asymmetric cross section. In a plan view the concave side of the trough becomes overhanging the convex side of it becomes sloping (*Fig. 4*). Skirts develop in these letter locations, skirts that are of various form in plan view (*Fig. 5*) mostly of convex rimmed, widening down from the top, sloping trough sides in profile (*Picture 2*).

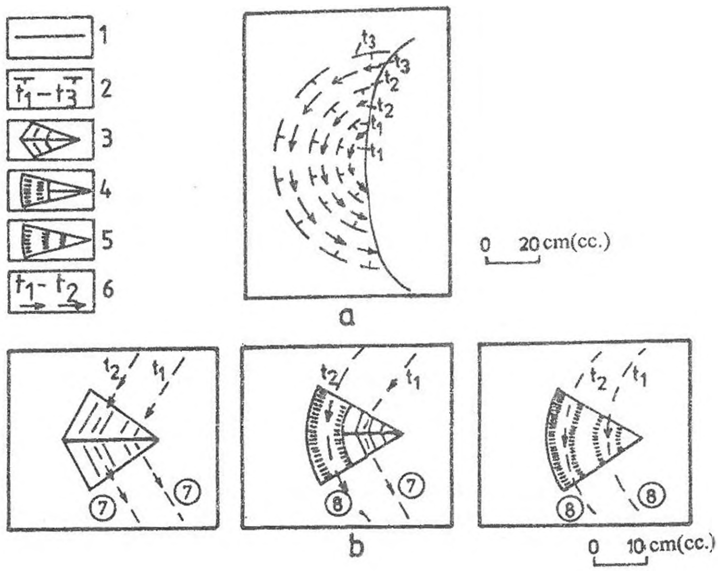

Figure 6: Connection of channel line slippage with development of the overhanging wall (a) and different skirt shapes (b)
Legend: 1. upper edge of overhanging side wall, 2. lower edge of overhanging side wall at actual trough bottom, 3. half pyramid shaped skirt, 4. half cone shaped skirt at top above, half cone shaped skirt at bottom, 5. half cone shaped skirt, 6. channel line at actual trough bottom, 7. broken channel line, 8. arced channel line

3. The Morphogenetics of the True Meander

3a. The Morphology of the Overhanging Wall and the Skirt

Overhanging wall parts can develop in such trough sections too where the upper trough rims are straight. This hints that the swung channel line touches the trough rim only in a point (or in a short section) at the beginning of the entrenchment. (There where the upper trough rim is of arced lining itself it is possible that the channel line followed the rim in a longer section at the beginning of the slippage.) At the same time it is characteristic to the three dimensional development of the overhanging wall that the length of the overhanging wall increases towards the present trough bottom. This can be explained by the steady slippage of the channel line. That is, in this case an ever longer section of the channel line adheres to the trough side resulting that lateral solution becomes more intensive at ever longer sections developing overhanging walls (*Fig. 6a*).

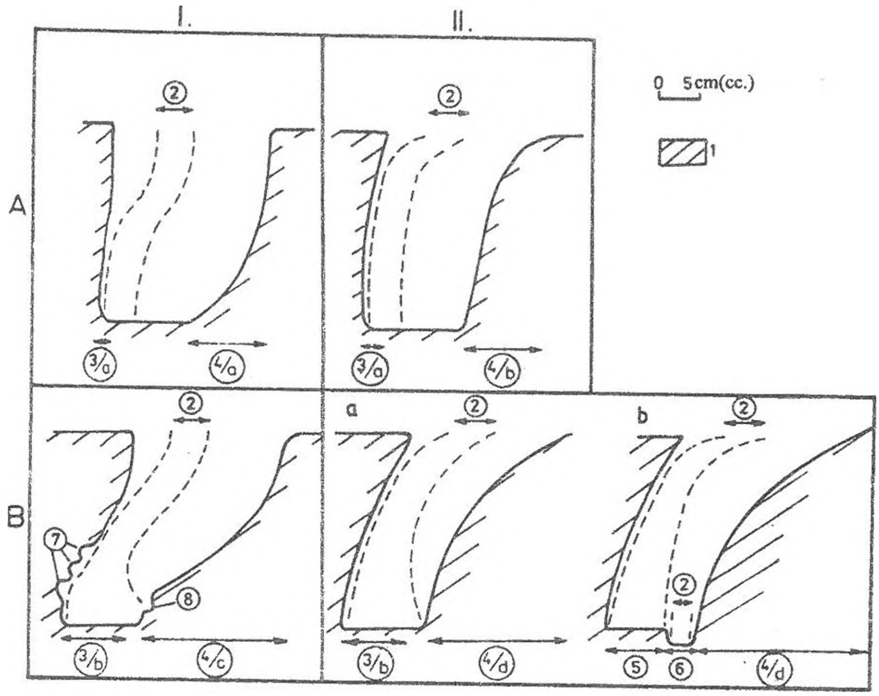

Figure 7: Morphogenetic specification of asymmetric meanders
Legend: A. small size slippage, B. large size slippage, I. initially slow slippage, II. initially quick slippage, 1. fresh rock, 2. change of the channel line zone between maximum and minimum flow rate (the measure of swinging increases during the progress of time in BI. And BII. cases, due to the asymmetric form of the trough), 3. concave side and terraces, 3a. narrow meander terrace, 3b. wide meander terrace, 4. skirt, 4a. small cross section, concave skirt, half cone at top and half pyramid at the bottom, 4b. small cross section, convex skirt, half pyramid at the top and rather a half cone at the bottom, 4c. large section concave half pyramid skirt, 4d. large section convex skirt large half pyramid at the top but rather half cone at the bottom, 5. hanging terrace, 6. type III trough, 7. terrace groove, 8. skirt terrace groove

Skirts develop at locations where the actual channel line is positioned further on from the half width of the actual trough bottom, because here the solution is less intensive as it is at the opposite wall of the trough. According to slippage the surface of the skirt is mostly cut off. A certain trough section can develop bends with or without skirts. The area bordered by the bend can shift gradually to the surface of the skirt but it may develop a sharp border with it.

Because of the different development of the channel line skirts of varying forms develop (*Figures 5, 6*). If the change of direction of the channel line is sharp, the skirt protrudes from the trough side as a half-pyramid. If it is rounded the skirt will be a rounded half-cone. If it becomes ever more arced during entrenchment the upper part of the skirt will be half-pyramid, the lower part half-cone shaped.

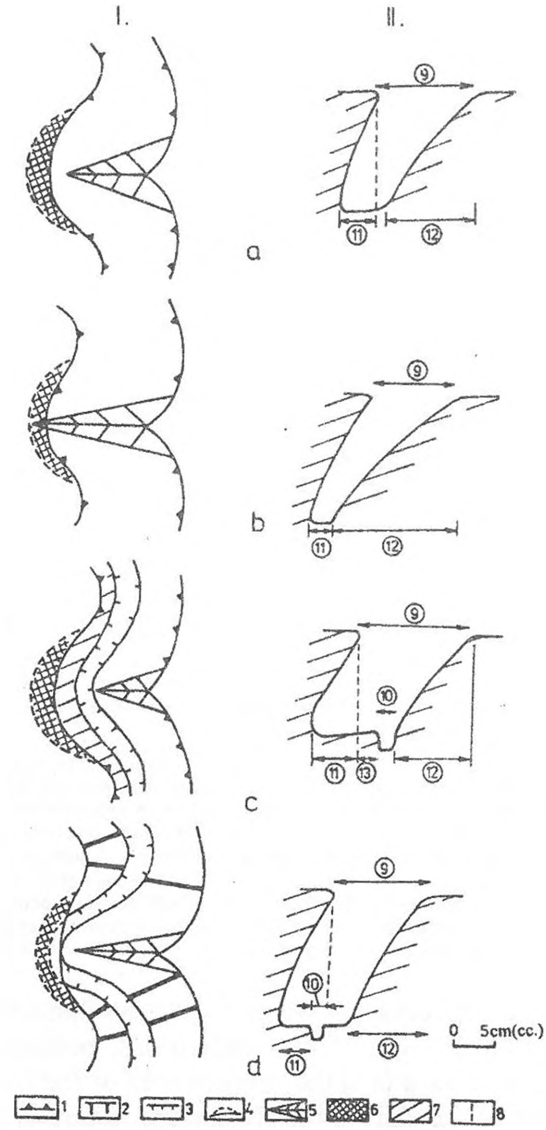

Figure 8: Meander terrace types
Legend: a. full terrace, b. damaged terrace, c. composite terrace, d. hanging terrace, I. ground-plan, II. cross-section on top-view (sections near the skirts), 1. edge of type I vertical side trough, 2. gently sloping side of type I trough, 3. edge of type III trough, 4. overhanging side wall, 5. skirt, 6. meander terrace, 7. trough bottom terrace in cross-section, 8. projection of edge of overhanging wall, 9. type I trough, 10. type III trough, 11. meander terrace, 12. skirt, 13. trough bottom terrace

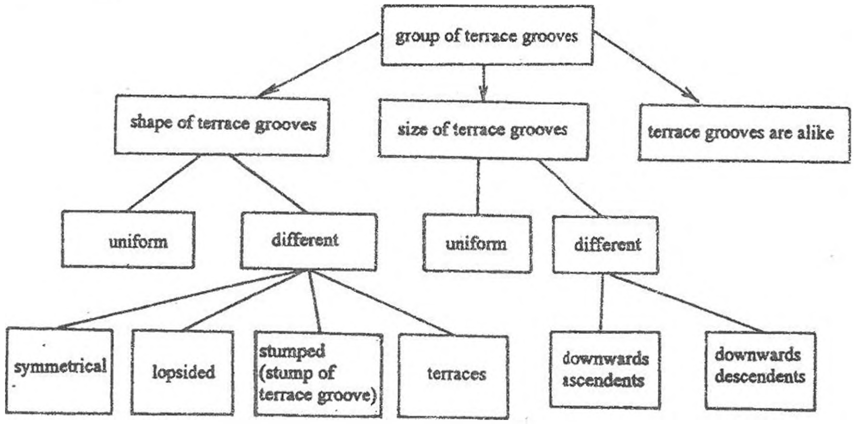

Figure 9: Variations of the observed terraces in asymmetric trough sides

The shape of the skirt is not only developed by the geometry of the channel line but by the measure of the slippage too. At quick entrenchment and big channel line swing or when the functional swing is small the skirts will be half pyramids while at slow entrenchment and small channel line swing and at big functional swing, half-cone shaped skirt develop. That is, in the first case the channel line is positioned farther in the letter cases nearer to the skirt. If the two processes are consequent at the same skirt it will be half-pyramid shaped at the top and half-cone shaped at the bottom.

The morphology of the bend is shaped by the measure and pace of the slippage of the channel line. If the entrenchment is quick or if in the course of one function the flow rate does not or only slightly changes, only small slippage will belong to a unit entrenchment (*Fig. 7.A*). In this case the skirt is short in profile. If the measure of the swing gradually increases the section of the skirt will be concave (the point of inflection closer to the trough bottom) but if the swing is considerable at the beginning of the entrenchment and than it gradually decreases, a convex skirt develops (the point of inflection closer to the trough-rim). The opposite side of the trough is less overhanging or vertical.

To slower entrenchment bigger bend slippage may belong, the section of the skirt will be long (*Fig. 7.B*). The opposite side of the trough is overhanging. It may occur in this case too that the section of the skirt is concave (the measure of the swing gradually increases) or convex (the measure of the swing decreases during the slippage).

The slippage can be gradual or intermittent. At gradual slippage the flow rate does not vary or not much, the channel line does not shift during the same function. The surface of the skirt and the opposite overhanging walls are smooth.

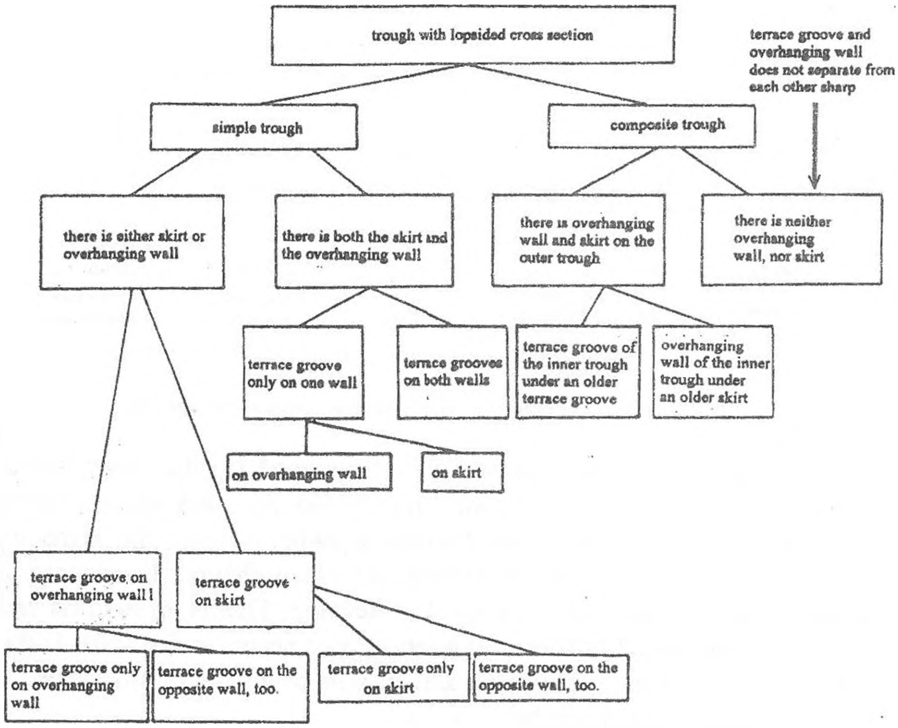

Figure 10: Terraces and terrace groups observed on features of asymmetric troughs

The skirts are often damaged. Active developing skirts can be damaged by the flow in the trough bottom. This can happen longitudinally (lopsided skirt) or laterally at right angle to the skirt. In the letter case a bend-beheading occurs. The remnant of the skirt turns into an inselberg. Older inactive skirts are damaged by frost (damaged skirt).

3b. Meander Terraces

True meanders can be terraced or without terraces.

Meander terraces can be well differentiated from karren terraces (*VERESS, M.* 1995). The letter can be traced continually on the trough bottoms at considerable length while the other can be found only locally in the meanders (*Picture 3*). The meander terraces are such plane surfaces of small extension that can be located in the concave side of the bend or in the skirts of the convex side (*Figures 4, 8*). Terraces can be located at the trough bottoms (trough bottom meander terraces) or above the bottom in the trough sides (hanging terraces). The trough bottom terraces can be full terraces (the skirt does not extend beyond the rim of the concave side) incomplete terraces (the skirt extends beyond the rim of the concave side) and composite terraces (the meander terrace transforms to karren terrace).

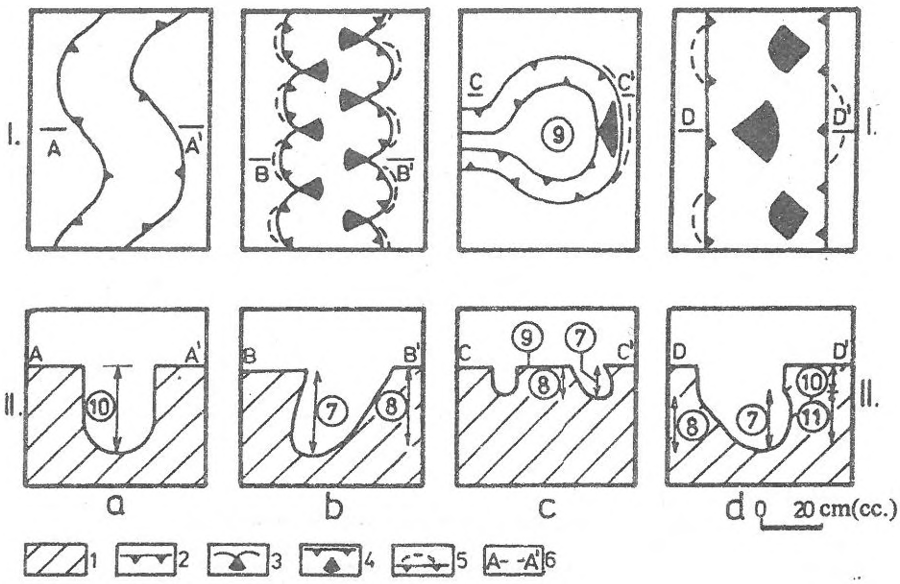

Figure 11: Meander types
Legend: on ground-plan: 1. karren development on the rock, 2. type I trough, 3. skirt starting at the trough rim, 4. skirt on the lower part of the trough side, 5. overhanging wall, 6. place of section, on cross-section: 7. overhanging side wall, 8. skirt, 9. recess, 10. symmetric cross-section trough and part of trough, 11. asymmetric cross-section trough, a. false meander, b. meander remnant, c. loop meander, d. developing meander, I. vertical-view, II. side view.

While the development of karren terraces can be explained by the development of inner troughs (the remnants of the older trough bed make the terrace), the development of the meander terraces of the concave side are due to the slippage. The slippage is not enough as an explanation for the development of these forms. The following hint at this:
- the niche (overhanging wall) is not located opposite to the skirt,
- the plan view of the skirt and the shape and size of the terraces are not identical,
- terraces don't always develop in the true meander at the concave trough side,
- terraces can develop on skirts.

The terraces of the concave trough side develop if the channel line stays at this side for extended periods of time (not only at maximal discharge). The following causes may have a role in this phenomenon:

- Due to the trough morphology resulted by the slippage (the developing skirts have a decisive role in this respect) the channel line will be such as in the maximal discharge for ever extending periods of time.

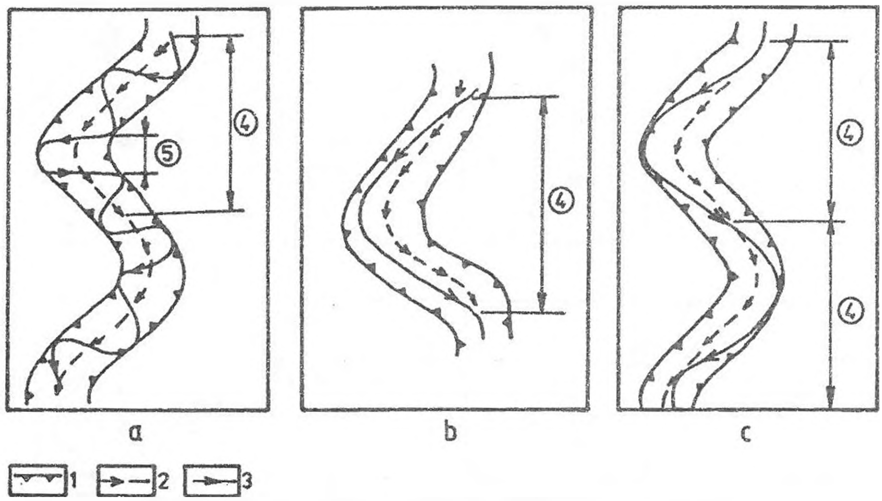

Figure 12: Channel line wave-lengths of different meander types

Legend: a. on falsely meandering trough with meander remnants, b. false meandering on trough with loop meander with simple direction change, c. false meandering on trough with loop meander with double direction change, 1. solvent, or the edge of developing trough, 2. original channel line, 3. swung channel line, 4. wave-length of original channel line, 5. wave-length of swung channel line

- During entrenchment the trough narrows. Therefore the filling of the trough will be higher even at smaller discharges. This results that the channel line will adhere to the concave trough side.
- During entrenchment some troughs are recharged by more water. This results durably higher water level resulting the described situation.

Skirt terraces possibly develop when the lining of the channel line completely changes in a part of the trough. This is made possible by the change of the morphology of the trough.

Hanging terraces may develop if the lining of the channel line changes (it does not reach the concave trough side even at maximal discharge). In this case an inner trough develops at the edge of the existing terrace. The terrace gets into hanging position.

Meander terrace-grooves are half channels (on the concave side) or step-like some cm deep and some dm long grooves (on the skirt of the convex side) in the trough sides in the meanders (*Fig. 4*). Sometimes their width may be so large that the whole overhanging of the trough wall will be nothing but one of them (giant groove). The giant grooves can be easily said from the meander terraces as their lower plane is not horizontal but tilted (*Picture 4*). Giant grooves can be observed on the overhanging walls most frequently. They seldom occur singly. Most of the time two or three grooves occur one above the other (*Figures 9, 10*). They characterize not only one bend of a certain trough or section of a trough but don't necessarily occur in each and every bend. It seems that the similarly positioned solitary terrace grooves or the groups of them in subsequent meanders are situated along a plane tilted toward the lower end. Grooves can be so close to each other that the side of the trough is nothing but an inter-groove ridge. (This ridge may be sharp or rounded.) The grooves can be symmetric or asymmetric in cross section. The upper or lower face of the groove may be missing (groove remnant). Regarding the occurrence of terrace grooves they can appear on one or on both sides of asymmetric troughs and in only the main trough or the inner trough or in both in a composite trough (*Figures 9, 10*).

The terrace grooves possibly develop at or near to the level of the

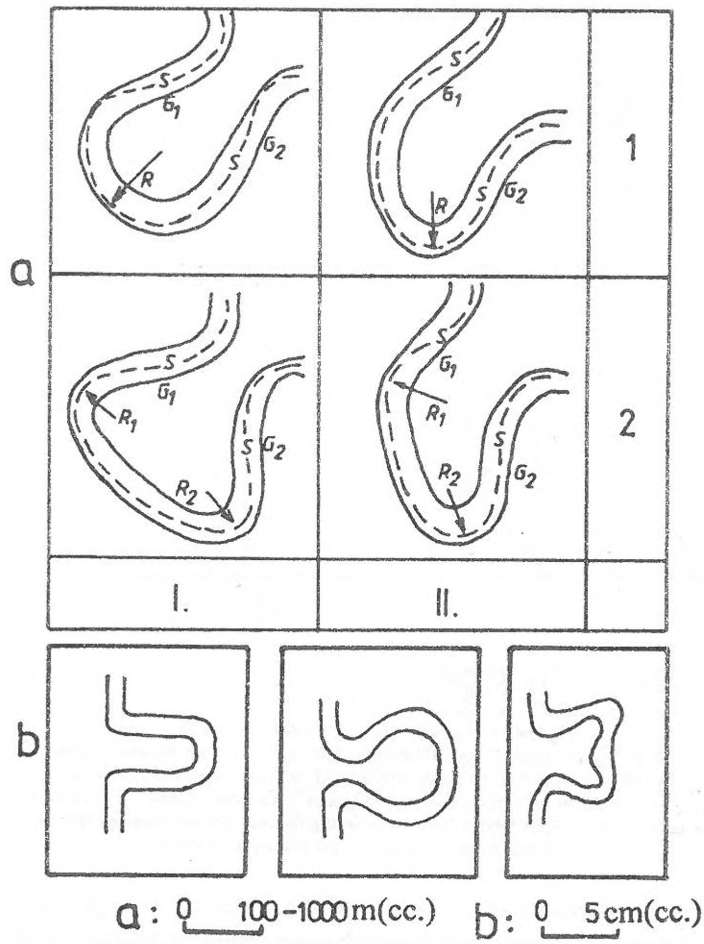

Figure 13: Various river- (a, after Allen) and loop meanders (b)
Legend: G_1, G_2 inflection point, R_1, R_2, R_3 bend radius, S channel line I. symmetric, II. asymmetric, 1. simple, 2. composite

maximal flow (*Fig. 7*). For the development of terrace grooves the lateral solution in one particular level shall persist for an extended period of time. The condition of this occurrence is that the levels of the maximal flows persist to be the at the same level in the trough. (In the case of giant grooves the maximal flow characterizes the trough for a long time than it gradually drops during entrenchment.) The vertical sequence of grooves can be explained by the entrenchment of the trough bottom because the level of the maximal flow drops.

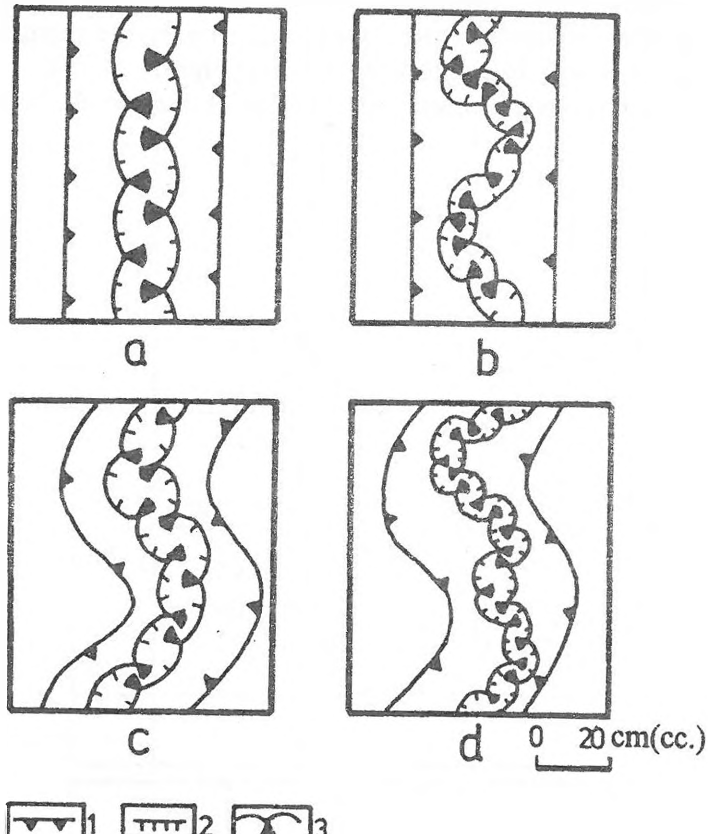

Figure 14: Joined rinnen with meander remains
Legend: 1. type I trough, 2. type III trough, 3. trough edge with meander remnant, with skirt; straight type I trough, straight (a), or falsely meandering strained meander remnant with type III trough (b), falsely meandering type I trough and meander remnant with forced false meandering (c) and slipped meander remnant with forced false meandering, (d) with type III trough..

The development of the terrace grooves near the water level explains the different shapes of them in the overhanging wall and in the skirt. While in the steep or overhanging wall the terrace grooves develop an upper face too, those in the skirt will have only lower faces (the skirt is subdivided into steps of different inclination).It may happen that the inclination of the skirt is not much and it is not divided into terraces at all.

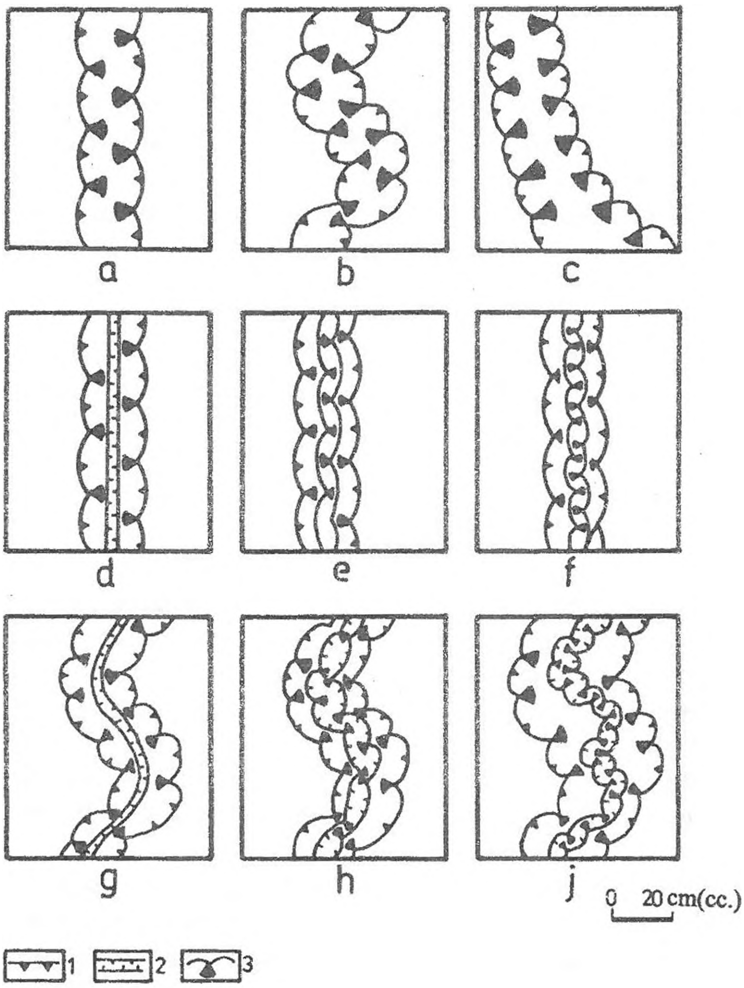

Figure 15: Simple (a, b, c) and composite (d, e, f, g, h, j) troughs with meander remnants Legend: 1. type I trough, 2. type III trough, 3. damaged rimmed trough with skirt, simple troughs: straight (a), with false meander (b), arced (c) composite straight troughs with meander remnants: type I trough with meander remnant, type III trough without meander (d), type III trough with true meander remnants with forced meandering (e), type III trough with truly slipped and forced meander remnants (f) composite false meandering trough: with false meandering type III trough (g), with true meander remnant of forced meandering type III trough (h), with true meander remnant slipped and forced meandering type III trough (j)

The terrace grooves are not of identical height at the two sides. One of the causes of this may be that the solvent surges to the concave side (higher water level) and the other cause may be that the intensity of the solution increases on the skirt when the channel line is near to it. This can happen at decreasing, thus low water level.

III. Meander Types

Karren meanders can be specified in more than one aspects, e.g. by their age or size (*HUTCHINSON, D. W.* 1996). The specification in this paper regards morphogenetic aspects.

Different meanders develop during the development of different karren troughs.

Troughs meander when they are not very frequent or when solitary. If the number of occurrences is large, meandering is less characteristic. There must be a strong relation between the number of troughs and the type of flow of the solvent (it can be a sheet flow or it can be divided to strips). This suggests that the meandering (the swing of the channel line) develops when the solvent flows in strips on the surface. The type of the flow depends on the gradient of the slope as the density of troughs increases with the increasing gradient (*ZENTAI, Z. - HORVÁTH, E. T.* 1995). Thus strip type flow and meandering can be expected on slopes of moderate gradient. The troughs can develop as rainwater runnels or in the regressive way.

The trough (or part of it) will be a rainwater runnel if it entrenches all along its length thus the age of the development is the same at any of its sections. This trough development can occur if the solvent does not move in a sheet flow but in individual strips. The solvent flowing is strips can flow straight down the slope (the direction of the dip of the slope is uniform) on a changing course with false meandering (the direction of the dip of the slope is changing).

In the case of retreating (regressive) troughs the end of the trough shifts in the opposite direction of the slope. Troughs of this type not only entrench but their length increases as well thus their lower sections are younger than the upper ones. The increase of the length occurs because solvent joins the trough-end from surfaces yet free of troughs. As the flow of the water is most intensive parallel to the slope direction, the lengthening of the trough will be opposite to the slope direction. Straight troughs develop if the slope direction is uniform and bending (falsely meandering) troughs develop if the slope direction is changing. The time of the separation to strips of the solvent is earlier than trough development on the same location.

1. False Meander

In false meanders - though the trough is bending - the trough is symmetrical in cross section and neither skirt, nor overhanging wall can not be observed in the bends (*Fig 11a and Picture 1*). This can be explained that the channel line only produced only false swings following the changes of direction of the solvent. This letter followed the changes of direction of the trough. This is possible if the trough develops backwards. (The false meanders are such trough sections that developed along slope parts of different directions.)

In the bends of the false meanders the recess does not separate excessively from the neighborhood (the neck part is missing). In falsely meandering troughs the meander-zone and meander-length is small, the wavelength is long.

2. True Meanders

True meanders develop at the true (factual) swing of the channel line.

2.1. Meander Remnants

The rims of troughs containing meander remnants are arced. Neighboring arcs connecting to each other make characteristic points. The individual points on one rim are located at the half distance of two points on the opposite side. Skirts developed from rim to bottom are located at the points. (The skirts do not continue in such recess parts that are parts of the original ground surface circumvented by the bend.) The side wall is overhanging in the sections between the points (*Fig. 11b, Picture 5*).

The length of the meander arcs of the bend remnants can be very varying compared to the wavelength of the meander regarding that the swing of the channel line can be very varying as well because of the lack of trough walls. The width of the meander zone is relatively small at the same time. This can be explained that the arc of the bends can not increase substantially during entrenchment. The original swing of the channel line is inherited. At the same time the growth of the bends towards their ends is limited by the returning channel line and by the opposite trough rim.

The arced lining of the skirts in the whole extension of each particular trough side but particularly the arced lining of the opposite trough rim proves that the channel line swinging happened on the surface prior to the trough development (channel line swinging prior to trough development). The channel line swings responsible for the development of meander remnants were triggered by internal causes in the case of such troughs that are straight and not inner troughs. The meander remnant morphology suggests the channel line swing of the solvent flowing on the surface that is possible only if the developing trough is not regressive but rainwater runnel type.

It can be observed that the meander remains troughs can not only be of straight lining. As a fact the trough rims don't show dual (composite) arcing. This can be explained only if it is suggested that the solvent causing the uniformly entrenching trough developed false meanders on the surface of varying slope direction. At the same time channel line swing occurred in the falsely meandering solvent. By this effect meander remnants developed on the trough of false meanders. In these cases the wavelength of the bend with meander remnants are always smaller than the wavelength of the false meanders consequently there is a series of bends with meander remnants on a bend of a false meander (*Fig. 12a*).

2.2. Looping meander

The trough turns back on itself in a loop. The slopes and elevation of the recesses surrounded by the loops are identical with that of the original surface. Consequently bend shifting did not occur on the area of the recesses. The trough is asymmetrical, its morphology is similar to that of troughs with meander remnants (*Fig. 11, Picture 6*). The width of the meander zone as well as the length of the meander arc is large, the wavelength of the meander is small or shows a big variety.

Looping meanders develop where the trough changes direction, thus they occur in false meanders (*Fig. 12*). When the difference between the direction of two trough sections is about 90° than the wavelength of the loop will be the same as the wavelength of the false meander. It may occur that the direction of two trough sections are similar (longitudinal trough sections) but these are connected by a transverse section. The transverse section connects to the longitudinal trough sections by false meanders. The wavelength of the two loops is identical with the wavelength of the corresponding false meander. These properties hint that at this meander type the swing of the channel line is caused by the false meandering. Consequently the swing of the channel line can be traced back to an external cause.

If the looping meander is asymmetrical from its rims down means that the channel line swung right at the beginning of the entrenchment of the false meander. In this case the trough development is of the rainwater runnel type.

Looping meanders are most similar to river meanders. These letter can be simple or composite that may have symmetric and asymmetric varieties (*Fig. 13a*). These varieties can be observed at looping meanders as well (*Fig. 13b*).

It is not likely though that looping meanders of varying arcs represent the phases of a development sequence but rather represent the pattern of meandering of the solvent before the development of the trough. Exceptions may be the multiply composite meanders. It is frequently observable here that the multiple composition is caused by the skirt development in the concave arc (counter-skirt). It develops in a way that the swung channel line can not follow the arc of the concave trough wall. It hits the wall at a point and this way a smaller opposite swing occurs. (Caused by this effect the bend becomes one of developing meanders as well.)

The looping meander is a meander type that develops mostly in type III troughs. Especially at locations where the master type I or II trough is wide.

It is possible that the looping meanders develop at the changes of direction of the solvent flow, at functional channel line swings and deviations effected by the developing skirts. According to the above said looping meanders can develop with greater chance at the locations of the direction change of the solvent flow if the change of the quantity of the solvent is the bigger as well as the differences of the parts of the slope are the bigger.

2.3. Developing Meander

The trough rim is straight or if not, the trough is falsely meandering. The upper part of the master trough is symmetric that transforms to an asymmetric trough bottom downwards without a sharp change. The skirts do not develop on the whole side slope of the trough but only at the lower part of it, the overhanging walls don't develop (*Fig. 11d, Picture 7*). There is no recess but if the recess is specified as the area surrounded by the trough rim, it is situated on the skirt.

The described change of the character of the trough cross section indicates that the channel line swing commences at the beginning of the trough entrenchment.

The developing meandering troughs can be either rainwater runnels or retreating ones as the channel line swing is younger than the beginning of the development of the trough. It hints at the regressive origin of troughs of such morphology if the true meanders are missing in the upper stretch them.

Morphological observations indicate - more studies shall be conducted in this respect - that either internal or external causes may contribute to the swing of the channel line.

2.4. Perishing Meander

Asymmetry is restricted to the upper part of the trough. At concave trough rims and above vertical walls giant terrace grooves and hanging terraces develop, skirts of small size develop at the convex side that they gradually merge into the trough sides.

Perishing meanders develop when the channel line does not swing below a certain trough depth. Perishing meanders can be arced rimmed (like the rims of the troughs with meander remnants), or without these. If the trough is arced rimmed, the channel line swing had happened before the commencement of the trough development (rainwater runnel trough development). If the rim of the trough is not arced, the swinging of the channel line occurred during the entrenchment of the trough. In this case the trough can be of either rainwater runnel, or regressive origin. (It hints on regression origin if true meanders are missing in certain parts of the trough.)

The various types of bends occur in the type I, III (*Table 1*) but in type II either.

Table I. Meanders on one of karren ground surface part in Totes Gebirge

	Type I trough		Type III trough	
Sketches of meanders	true meander	false meander	true meander	false meander
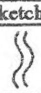 0 5cm(cc.)		+	+	+
 0 5cm(cc.)			+	
 0 5cm(cc.)			+	
 0 5-20cm(cc.)	+	x	+	
 0 5cm(cc.)			+	
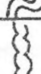 0 5-20cm(cc.)	+	x	+	
 0 5-20cm(cc.)	+			

x special case

IV. The Meandering of Composite Troughs

The meandering of the inner troughs may be false or true. The inner trough contains false forced meanders if its false meanders follow the lining of the false meanders of the master trough. If true meanders develop in the inner trough, true forced meandering develops. True forced meandering can develop either by the false or true meandering of the master trough. Both the false and the true meandering may be similar or shifted forced meandering. In the first case the wavelength and number of bends is identical with that of the master trough (either false- or true meanders), but not in the letter case.

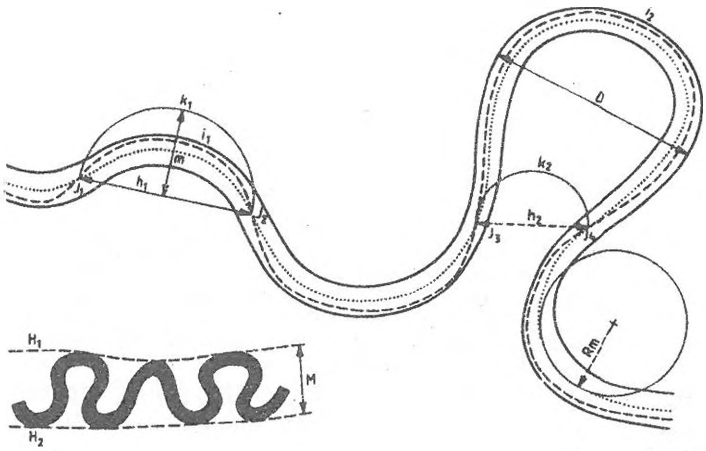

Figure 16a: Main parts of river bends after Z. Borsy (1992)

Legend: J_1-J_4 the inflection points of bends, h_1, h_2 the chords of bends, H_1, H_2 the bounding lines of bends, M the distance of bounding lines of bends (the width of bend), i_1, i_2 the length of the arcs of bends (between the inflection points, along the channel line), k_1, k_2 the circumference of the half circle drawn on the chord of the bend, R_m radius of bend (radius of the circle drawn into the bend), D diameter, m the height of arc measured at right angle to the chord. The middle line of the river is shown with a dotted line, the channel line with dashed line.

If the bending of the inner trough totally differs from that of the master trough (or this is straight) the meandering of the inner trough is false or restricted (*Picture 3*) as well as it can be falsely or truly meandering (*Picture 7*). In the first case the width of the inner meander zone is determined by the bottom width of the master trough, in the letter case the meander zone of the inner trough is less wide than the bottom width of the master trough.

Type I troughs can develop and entrench along their whole length (rainwater runnel type entrenchment) or regressively.

Regressive troughs may be straight or meandering. Straight troughs may be meander-less or with developing meanders. (In the letter case the swing of the channel line commences during the entrenchment.) The falsely meandering troughs may be looping meandering or meander-less as well. Regressive troughs may be simple or composite.

The type II and III troughs in the type I trough of the composite trough are most frequently meander remnants (*Fig. 14a*), or falsely meandering with meander remnants (*Fig. 14b*). In both cases the type III trough is of rainwater runnel origin but in the letter cases it is freely false meandering or restricted true meandering. In a falsely meandering type I trough the type III can be false-meandering or containing meander remnants. The false meandering can be similar forced meandering (*Fig. 14c*) and shifted forced meandering (*Fig. 14d*).

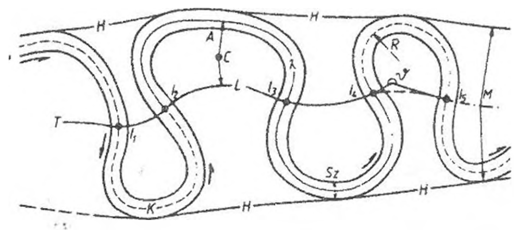

Figure 16b. Main parts of river bends after K. Balogh (1991)
Legend: H the edge of meander zone, $I_1 I_2 I_3$ ... I_5 inflection points, SZ width of the channel, K the middle line of the channel, J the central angle of the meander, T the line of the meander axis, M the width of meander zone, L wave-length of the meander, l length of the meander, C center of river recess, A width of river recess, R radius of the bend

If the channel line had swung before the trough developed, most of the times rainwater runnels develop with meander remnants. The troughs with meander remnants may be straight (*Fig. 15a*), or containing false meanders (*Fig. 15b*) eventually changing their direction (*Fig. 15c*).

The rainwater runnel type troughs may be simple (*Figures 15a, b, c*) or composite (*Figures 15d - j*). In the letter case mostly type III troughs occur in type I troughs. Inside the straight composite troughs the type III troughs are mostly meander-less (*Fig. 15d*) or it may be a morphology made of meander remnants (*Fig. 15e*). *Fig. 15d* shows a case where the type III trough is regressive while in the cases shown *Figures 15e* and *f* it is a gradually entrenching rainwater runnel type development.

The *Figures 15e* and *f* show true forced meandering. That is, the true meanders in the type III trough are determined by the true meanders of the type I trough. On *Fig. 15e* a true and similar type, on *Fig. 15f* a true shifted forced meander is shown.

Type III trough can develop in falsely meandering type III troughs falsely meandering themselves with regression (*Fig. 15g*) or with a morphology made of meander remnants, that is with rainwater runnel type development. In this case both the false- and true meandering may be similar (*Figures 15g, h*) or shifted (*Fig. 15j*) forced meandering.

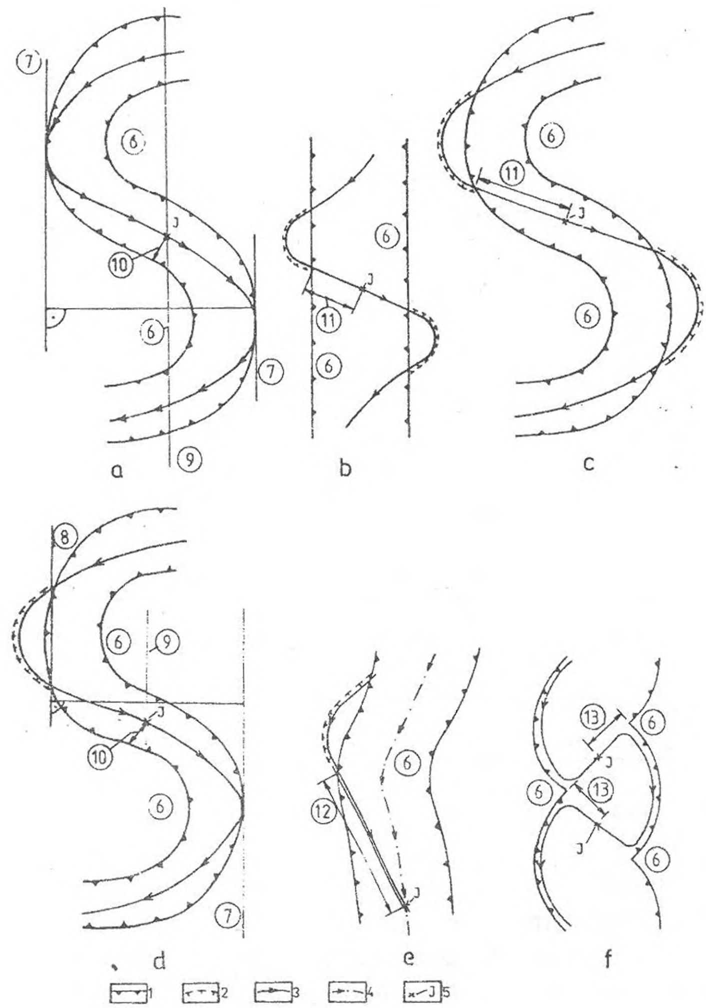

Figure 17: Plotting of inflection points of troughs with various morphology
Legend: a. plotting of inflection points of a meandering river (after J. Cholnoky), and of a trough that has no overhanging wall, b. in the case of straight or almost straight trough, where there are overhanging walls at both sides (developing meander), c. at meandering trough, where the overhanging wall developed at both loops (loop or meander remnant), d. at meandering trough, where the overhanging wall developed only at one loop, e. at falsely meandering trough (the trough sections are at about right angle), where there is only one overhanging wall, f. at trough with meander remnants and without overhanging wall, 1. trough edge, 2. end of overhanging wall at the plain of trough bottom, 3. present channel line, 4. previous channel line, 5. inflection point, 6. skirt, 7. bounding line, 8. The straight passing through the end of overhanging wall, which is parallel with the bounding line of the next loop, 9. middle line, 10. half width of the trough at the middle line, 11. shortest half width between the ends of opposite overhanging walls, 12. The straight line received as the extension of the original channel line at the end of the overhanging wall where it crosses the original channel line, 13. the shortest half width between opposite neighboring skirt tips

V. The Correlation of the Causes of Meandering and the Sizes of Meander Components

1. The Components of Karren Meanders

Besides the component that have been described (meander wavelength, meander arc length and meander zone width) the following are specified (*BALOGH, K.* 1991, *BORSY, Z.* 1992, *Fig. 16a, b*). The sinuosity of the meander is the ratio of the channel line and the axis length of the meander between two inflection points.

The rate of development (β) of the bend is determined with the equation (*LACZAY, I.* 1982):

$$\beta = \frac{i}{h}$$

where i is the length of arc along the channel line,

h is the wavelength of the meander or the chord of the bend,

LACZAY, I. (1982) specifies river bends with the values of β (*Table II*):

Table II: River bend types specified by their development (LACZAY, I. 1982)

type of river bend	value of β
undeveloped bend	< 1,1
developed bend	1,1-1,4
well developed bend	1,4-3,5
fully developed bend	> 3,5

The measurement of the various components of the trough bends is made possible by the drawing of the various channel lines on the survey map.

The initial channel line can be determined as the central curve between the trough rims. The opposite trough rim points can be staked out where the perpendicular of a point on the trough axis intersects the rims. The present channel line can be described with such a curve that merges to the bottom of the overhanging walls and passes through the inflection points. (Where there is no overhanging wall the channel line can be determined by the connecting of the inflection points with those points of the rim that are touched by the envelope curves.) Inflection points between neighboring bends of different morphology can be plotted using the methods shown on *Fig. 17.* (The lining of the channel line is varying during any single function. Thus it is possible that the channel line that can be plotted will approximate the channel line that occurs at high water.) The plotted channel lines of a surveyed trough (No. 7) are shown on *Fig. 18.* The validity of the plotting can be checked. The present channel line is of acceptable precision if the inflection points are situated on the original channel line. (It can be seen that this hasn't been achieved in all cases.)

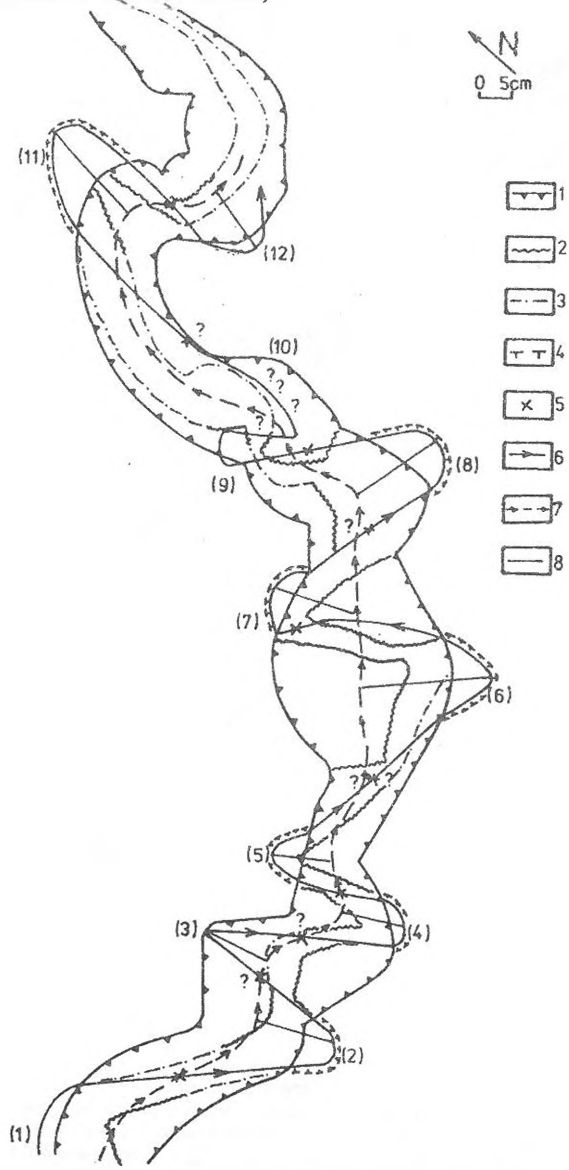

Figure 18: Constructed channel lines of trough No 7 (number in parenthesis identifies the loop)
Legend: 1. edge of type I trough, 2. lower edge of skirt, 3. end of gently sloping trough, 4. bottom of overhanging wall at the plane of the trough bottom, 5. inflection point, 6. present channel line, 7. previous channel line, 8. accessory straight along which the Sk_k and Sk_j values can be measured

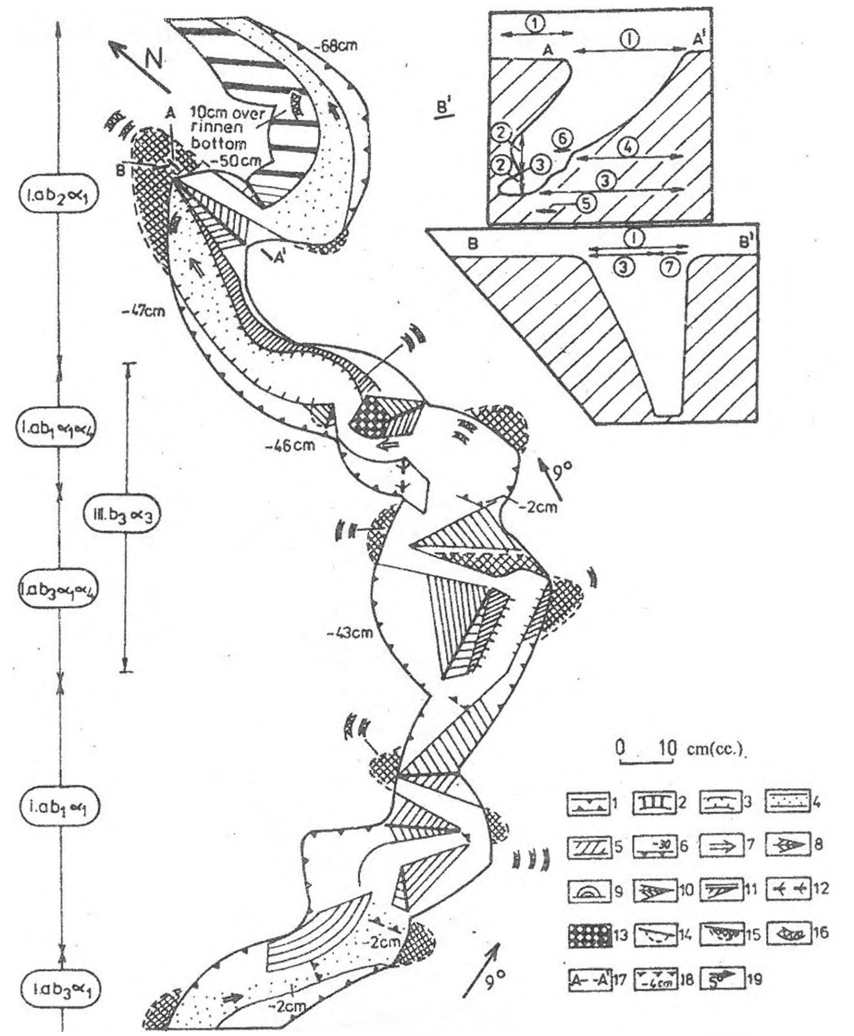

Figure 19: Morphological map of trough 7

Legend: 1. vertical side wall of type I trough, 2. gently sloping trough side of type I trough,, 3. vertical side wall of type III trough, 4. plane trough bottom, 5. trough bottom terrace, 6. depth of trough (in centimeters), 7. slope direction of trough bottom, 8. half pyramid skirt, 9. half cone skirt, 10. asymmetric skirt, 11. half skirt, 12. skirt remnant with sharp pectination, 13. meander terrace on skirt, 14. overhanging wall, 15. meander terrace at overhanging wall, 16. terrace groove and major terrace groove (the position and size of the small terrace groove in the bend is not drawn to scale), 17. position of section, , 18. solution threshold, step with depth (in centimeters), 19. The gradient and slope direction of the surrounding rock surface, a. falsely meandering trough section, b. truly meandering trough part (b_1 with meander remnants, b_2 loop meandering, b_3 developing meandering, b_4 ceasing meandering), the swinging of the channel line is due to internal (α) reason (α_1 false meandering of trough, α_2 flowing water of tributary trough, α_3 the bend or its skirt, α_4 edge of trough), section: 1. overhanging wall of concave trough rim, 2. terrace on concave trough side, 3. skirt, 4. upper skirt remnant, 5. lower skirt remnant, 6. terrace groove on the skirt, 7. trough bottom

In the knowledge of the present channel line and the inflection points the length of the meander arc and the wavelength of the meander can be measured and from these results the stage of development of the meander can be calculated.

The maximum of the slippage can be determined at a bend determining the difference between the present and original channel line (Sk_j) and the difference between the initial slippage and the original channel line (Sk_k) in the plane of the map (*Fig. 20*). This is nothing else but the biggest measure of the overhanging of the concave trough rim that can be measured in the plane of the trough bottom with a few exceptions (not detailed here). The slippage intensity (L_i) belonging to a certain trough depth can be determined:

$$L_i = \frac{Sk_j - Sk_k}{m}$$

where (Sk_j) is the difference between the present and original channel lines measured on the map.

(Sk_k) is the difference between the initial slippage and the original channel lines measured on the map.

m is the depth of the trough in the bend.

The number expressing the intensity of the slippage determines the measure of the swing (lateral shift) of the channel line at unit entrenchment. The number expressing the intensity of the slippage is negative at opposite slippage because $Sk_k > Sk_j$.

2. The Analysis of the Meander Components of Surveyed Troughs

Correlation between the slope gradient and the components of meanders (slippage intensity, channel line swing) is sought for in the following. *HUTCHINSON, D. W.* (1996) found correlation between the sinuosity of meandering troughs and the slope gradient. He found that the smaller is the slope gradient, the bigger is the sinuosity. It is not clear in the quoted communication from which measures of the trough has been the channel line calculated. This has an importance because using the length of the bending trough rim the sinuosity of the trough before the entrenchment can be determined.

Nine meandering troughs were surveyed and the scale 1:5 and 1:10 contour (*BARNA, J.* 1998) and morphological (*VERESS, M.* 1998) maps were drawn. On four of the contour maps the channel lines were successfully drawn and from one of the other maps data for the calculation of the slippage intensity were measured (*VERESS, M.* 1998). The topographic map (showing the channel lines) and the morphological map of trough No. 7 of the mentioned troughs is presented in the paper (*Figures 18, 19, Picture 8*).

The values of the slippage intensity were studied in relation with the gradient of the host surface. The numeric data of the various troughs were grouped by meander type considering if the development of the meander was resulted by internal or external causes.

Data of average slippage intensity calculated for the four troughs shows (*Fig. 21*) that the slippage intensity depends on the slope gradient in a reverse linear way. From the function produced by the usage of the data it can be determined that the slippage is 0 at 15.49° slope gradient while it is the biggest, 0.3501 at 0 °. This letter value can not actually occur as at 0 ° slope there is no flow and so there is no channel line swinging. At the producing of the function the No. 6 trough has been disregarded because of a reversed slippage. Quite naturally more data would be needed for the more accurate determination of the relation of the slippage intensity and slope gradient.

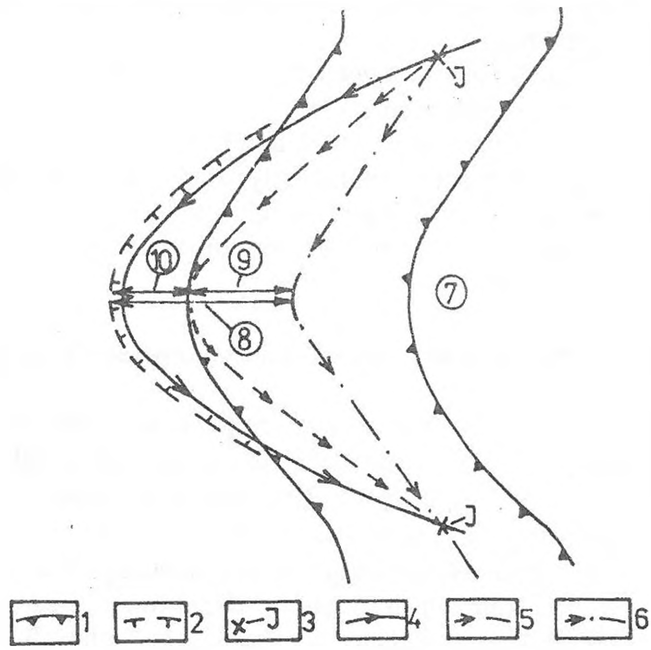

Figure 20: Swinging of channel line and its components
Legend: 1. trough rim, 2. end of overhanging wall at the trough bottom plane, 3. inflection point, 4. present channel line, 5. channel line at the start of slippage, 6. previous channel line, 7. skirt, 8. Sk_j, 9. Sk_k, 10. $Sk_j - Sk_k$

The dependence of the slippage intensity on slope gradient can be probably explained with the fact that at large gradients there is no sufficient time for the swinging of the channel line. (Intensive trough entrenchment is explained by the quick flow of the solvent.) Consequently at larger slope gradient less swing occurs at unit entrenchment. The quick entrenchment of the trough can factually cause the swing as the existing trough wall decreases the measure of the channel line swing. When the trough wall develops quickly the swing is hindered right at the beginning thus the process of self generation is hindered as well. (In self generation it is understood that because of the channel line swing an asymmetrical trough shape is resulted that just promotes later swinging.) The fact that the ever accelerating flow does not result lateral but vertical dissolution hints that the slope gradient has a greater role in the shaping of flow properties than those effects responsible for the channel line swing (internal and external causes). It hints to the relative independence of swinging from the slope gradient that the slippage intensity varies with the internal and external causes. In the case of an internal cause the average of the slippage intensity is 0.0928, while 0.2439 or 0.2966 at external causes (*Table III*). The fact that the slippage intensity is bigger at an external cause may signal that the external cause effects the swinging in a greater degree than the internal one. It seems that at some such troughs where the swinging of the channel line is caused by false meandering the increase of the slope gradient increases the magnitude of the swinging. (The swinging of the channel line is 1.85 cm in the No. 3 trough on a 3.29° slope and it is 4.45 cm in No. 7 at a 8.1° gradient slope.) This might be explained that the quicker is the flow of the solvent it has the more chance that the channel line hits the entrenching trough rim. For this reason the lateral solution is not slowed down during entrenchment. In the No. 1 trough however the channel line swing is large at small slope gradient, therefore for the analysis of the relation between the slope gradient and the swinging of the channel line of false meandering in origin further survey is needed. In any case the listed data indicate that the swinging of the channel line can occur on land surfaces of various gradients.

According to the data shown in Table III the stage of development of the meander depends on what caused the swinging of the channel line (internal or external cause), because the meanders made by external causes are more developed than those made by internal causes (2.5135 and 1.8724).

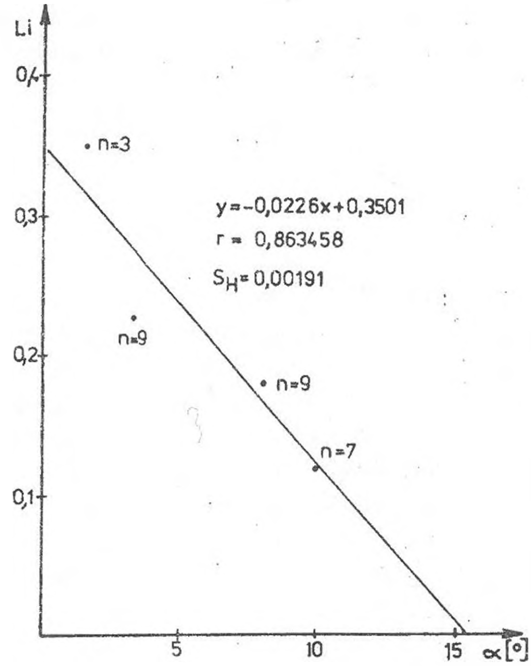

Figure 21: Relation of the slope angle and slippage intensity

4. Conclusions

a. The classification of the forms of karren meanders and the explanation of the development of the forms offer information to the understanding of the processes of solution on the trough bottom and to the knowledge about one variant of meandering that is connected with the process of karren development.

b. The development of the karren meanders and their forms have been deduced from the swinging of the channel lines of linearly flowing solvent.

c. With the classification of the meanders of the karren troughs two main types of trough development were recognized - the rainwater runnels and the regressive troughs. Those troughs that contain meander remnants, perishing meanders or looping meanders (these letter are asymmetric from their rims), are probably rainwater runnels. Falsely meandering troughs and those containing developing meanders (if their upper end is falsely meandering) are of regressive development.

d. The qualification of the simple but mainly the composite karren trough meanders offers data for the development of individual troughs. With the explanation of the troughs occurring on any particular part of a karren ground surface the explanation of the development of a major karren ground surface becomes possible.

e. The slippage intensity (L_i), that is, the lateral shift of the channel line at unit entrenchment depends on the gradient of the host ground slope. The occurrence of the swinging of the channel line and thus the development of a meander does not depend on the slope of the host surface if it has any.

f. The development of the bend (that is expressed mostly in the growth of the arc of the channel line) is big if the solvent swings in the shallow trough at the beginning of the entrenchment and the swinging persists during the entrenchment. Thus the development of bends (and the stage of development) is influenced by two effects: the effect of the channel line swinging and the slope gradient. The letter has an indirect influence such as the swinging of the channel line slows down in a smaller or bigger degree. It is suggested that the slope gradient influences the swinging of the channel line directly too if it is caused by false meandering.

Table III: The averages of components (using the data measured in the Nos. 3, 4, 6, 7 troughs)

meander type	loop	developing			remnant			all types	
cause of the swinging	external n=3	internal n=7	external n=13	all n=20	internal n=2	external n=6	all n=8	internal n=10	external 21
length of the bend	45,75	23,5	18,6153	21,0576	27,5 (66,71)*	33,5833	30,54	25,5	32,6495
wave length	15,125	12,0	10,38	11,19	16,0 (16,87)*	13,8333	14,9166	14,0	13,1128
stage of development	3,0233	2,0210	1,8992	1,9601	1,7239 (4,08)*	2,6181	2,171	1,8724	2,5135
intensity of slippage	0,3336	0,1056	0,2300	0,1678	0,08 (-3,32)*	0,1608	0,1204	0,0928	0,2439 0,2966**

* the number in parenthesis belongs to trough No. 6 (n=7)
** with the data of trough No. 3 (n=3)

IRODALOM

ALLEN, J. R. L. (1982): Sedimentary Structures. Their Character and Physical Basis I.-II. - Amsterdam - Oxford - New York, Elsevier

BALÁZS, D. (1990): Karrformák-karregyüttesek - Karszt és Barlang II. p. 117-122.

BALOGH, K. (1991): Szedimentológia I. k. - Akadémia kiadó, Bp.

BARNA, J. (1998): Karrmeanderek szintvonalas ábrázolásának tapasztalatai - Karsztfejlődés II. (Totes Gebirge karrjai) - BDTF Természetföldrajzi Tanszék, Szombathely, p. 91-98.

BORSY, Z. (1992): Általános természeti földrajz - Tankönyvkiadó, Bp.
BÖGLI, A. (1976): Die Wichtigsten Karrenformen der Kalkalpen - In: Karst Processes and Relevant Landsforms. ISU Comission on Karst Denudation, Ljubljana pp. 141-149.
CHOLNOKY, J.: Hegyek-völgyek - Franklin Társulat, Bp.
DUNKERLEY, D. L. (1979): The Morphology and Development of Rillenkarren - Z. Geomorph. 23. p. 332-348.
FRIDTJOF, B. (1954): Verkarstung und Badenschwund im Dachsteingebiet Mitteilungen der Höhlenkomission 1.p. 53-56.
HUTCHINSON, D. W. (1996): Runnels, Rinnenkarren and Meanderkarren: Form, Classification and Relationships - In: *FORNOS, I. J. - GINES, Á.* (editor): Karren Landforms p. 209-223, Universitat de les Illes Balears, Palma de Mallorca
LACZAY, I. (1982): A folyószabályozás tervezésének morfológiai alapjai - Vízügyi Közl. p. 235-254.
PÉCSI, M. (1975): Geomorfológia - MÁFI, Bp.
SZUNYOGH, G.-LAKOTÁR, K.-SZIGETI, I. (1998): Nagy területet lefedő karrvályúrendszer struktúrájának elemzése - Karsztfejlődés II. (Totes Gebirge karrjai) - BDTF Természetföldrajzi Tanszék, Szombathely, p. 125-148.
VERESS, M. (1998): Karrmeanderek - Karsztfejlődés II. (Totes Gebirge karrjai) - BDTF Természetföldrajzi Tanszék, Szombathely, p. 35-58.
VERESS, M.-BARNA, J. (1998): Karrmeanderek morfológiai térképezésének tapasztalatai - Karsztfejlődés II. (Totes Gebirge karrjai) - BDTF Természetföldrajzi Tanszék, Szombathely, p. 59-74.
VERESS, M. (1995): Karros folyamatok és formák rendszerezése Totes Gebirge-i példák alapján - Karsztfejlődés I (Totes Gebirge karrja) - Pauz Kiadó, Szombathely, p. 7-30.
VERESS, M. (1998): Adatok karrvályúk meanderfejlődéséhez - Karsztfejlődés II. (Totes Gebirge karrjai), BDTF Természetföldrajzi Tanszék, Szombathely, p. 35-58.
ZENTAI, Z.-HORVÁTH, E. T. (1995): Totes-hegységi lejtőkarrok morfometriai vizsgálatainak eredményei - Karsztfejlődés I. (Totes Gebirge karrjai) - Pauz Kiadó, Szombathely, p. 79-88.

PICTURES

1. False meander (Asiago Plateau, Italy)

2. True meander (Totes Gebirge)
Legend: 1. skirt, 2. overhanging wall

3. Meander terraces (Totes Gebirge)
Legend: 1. type I trough, 2. type II trough, 3. skirt terrace, 4. terrace at overhanging wall, 5. giant terrace groove

4. True meander developed at false meander (a meander of the trough shown on picture 3)
Legend: 1. skirt, 2. overhanging wall, 3. giant terrace groove, 4. skirt terrace, 5. terrace on skirt, 6. type III trough

5. Meander remnant (Totes Gebirge)

6. Loop meander (Julian Alps, Slovenia)

7. Meanders of a composite trough (Totes Gebirge)
Legend: 1. falsely meandering type I trough, 2. freely meandering type III trough, 3. loop meander, 4. developing meander, 5. skirt, demolished by type III trough

8. Trough No. 7 and its meanders (Totes Gebirge, see the qualification of the meanders on Fig 19,)

1.

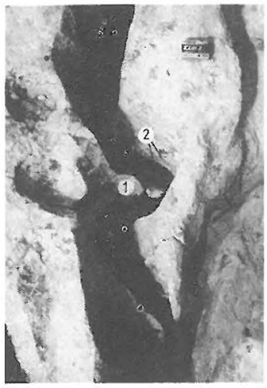

2.

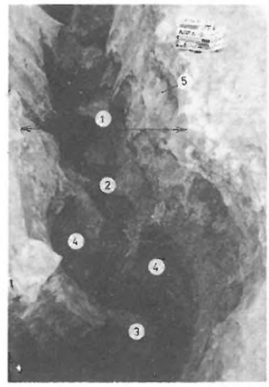

3.

4.

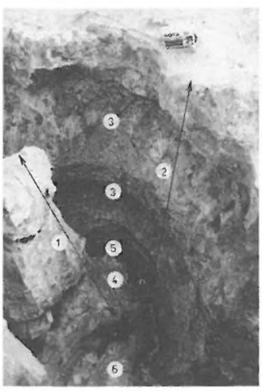

5.

6.

7.

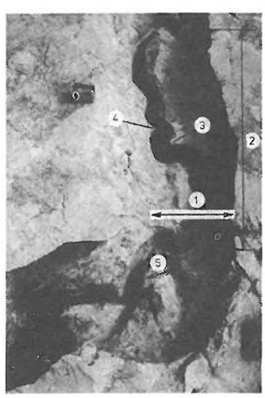

8.

KARSZTFEJLŐDÉS IV.
Szombathely, 2000. pp. 77-108.

THE STUDY OF THE HISTORY OF DISSOLUTION OF KARREN GROUND SURFACES DEVELOPING TO KARREN MONADNOCKS AND INSELBERGS - WITH SOME EXAMPLES

MÁRTON VERESS* - TAMÁS NACSA**
*„Berzsenyi Dániel" College, Department of Geography
9700 Szombathely, Károlyi G. tér 4.
** 8600 Siófok, Jókai u. 8

Abstract: Scale 1:10 morphological surveys were prepared about six selected parts of the karren landforms in the Austrian Totes Gebirge. The concepts of karren inselberg and monadnock are introduced and these residual ground surfaces are specified. Karren inselbergs and monadnocks developed by karren troughs are studied in detaile. These can develop by the merging of tributary ends or tributary and main troughs, as well as by the false and true beheading of bends. By the examination of the merging of troughs (that is possible with the observation of the locations of appearance of trough bottom divides and steps in the course of merging by solution) the way of the development of inselbergs and monadnocks and the sequence of the various karren forms can be determined. In the knowledge of the relative ages of development the history of dissolution of a single part of the ground surface can be determined. Considering the relative ages of development of the various karren forms such series of maps were prepared that illustrate the history of dissolution of the surrounding of the monadnocks.

1. Introduction

An inselberg is a hill spared by erosion in its proximity. It is called a monadnock if the top of the hill retains the original land surface (*BULLA, B.* 1954, *BALÁZS, D.* 1987). (Table mountain, mesa, butte etc. are locally used in the English language without geomorphological distinction.)

The karren parts of the ground surface of the karst are denuded by solution of intensity and duration varying with the location. Parts of the surface that are denuded at relatively lesser degree as their proximity or not at all are called karren inselbergs and karren monadnocks respectively.

Karren inselbergs and karren monadnocks show differences in more than one aspects to erosion made inselbergs and monadnocks. These differences are the following:

- Inselbergs and monadnocks made by erosion can be of several kilometers wide and long and they can be many hundreds of meters high. The karren inselbergs and monadnocks are only several meters of lateral size and several decimeters high.
- Erosion made inselbergs and monadnocks are sculpted from their vicinity by erosion, karren inselbergs and monadnocks by solution. The sides of the letter are much steeper than those of the former. The bordering slopes are

often overhanging. Their surface is rougher too. Several centimeters tall small size cones occur frequently on their tops as well as shallow, wide initial karren troughs and some centimeter deep and wide type III troughs.

Karren inselbergs and monadnocks can be developed by various karren processes. Thus they can be developed by the partial merging of neighboring solution pots, heel marks or karren troughs. (*VERESS, M.* 1995). They can develop at karren tables (*BÖGLI, A.* 1976, *BALÁZS, D.* 1990). While the surface is denuded by solution in the vicinity of the karren table, this does not happen under the rock of the table (*Fig. 1a*). This paper reports about studies aimed at karren inselbergs and monadnocks developing during the development of karren troughs.

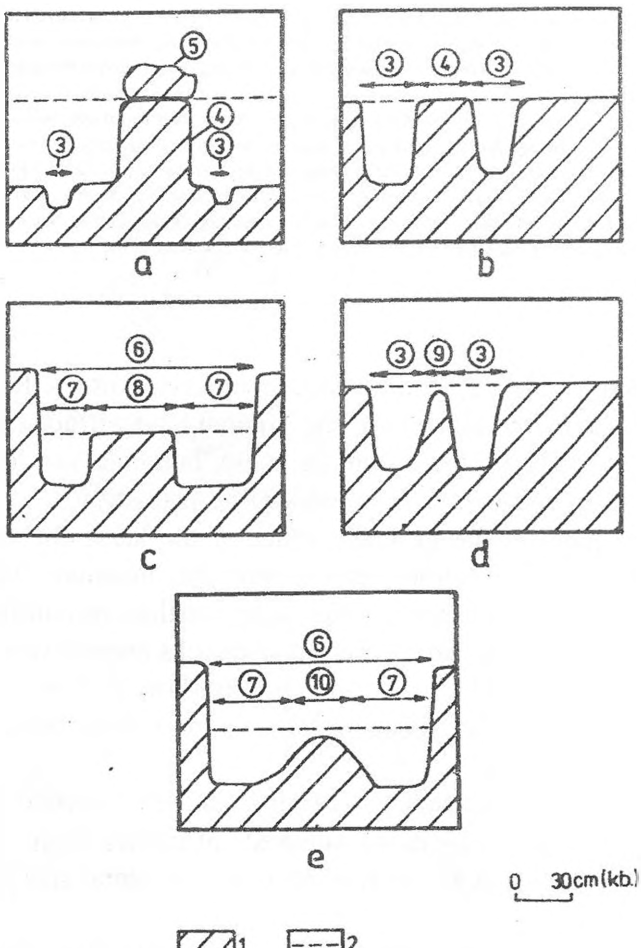

Figure 1: Cap-rock protected karren monadnock (a), monadnock developed by troughs (b), monadnock on the bottom (c), karren inselberg (d) and karren inselberg on the bottom (e)

Legend: 1. karren developing on rock. 2. elevation of karren ground surface before the separation of the residual ground surface, 3. type I karren trough, 4. karren inselberg, 5. boulder, 6. older type I karren trough, 7. I. or II type younger karren trough, 8. monadnock on the bottom, 9. karren inselberg, 10. karren inselberg on the bottom

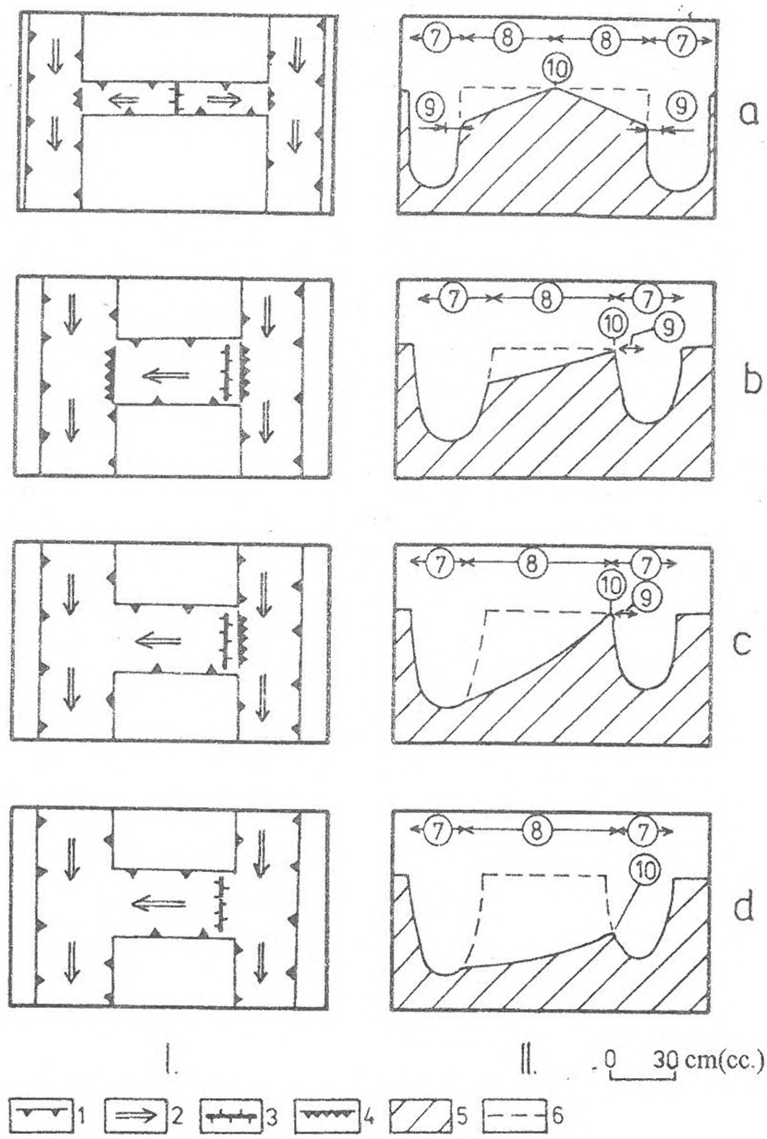

Figure 2: Meeting of trough ends (a) and false beheading (b, c, d)
Legend: 1. type I karren trough, 2. direction of slope of type I karren trough bottom, 3. trough bottom watershed, 4.step, 5. karren developing the rock surface, 6. ground surface before trough entrenchment , 7. master trough, 8. regressive tributary trough, 9. step, 10. trough bottom watershed, I. view from above II. side view (sections along the side of troughs connected by beheading), the regressive trough ends join (a), the beheading trough deepens constantly (b), the beheading trough retreats (c), the beheading trough entrenches to the bottom of the main trough (d)

For the presentation and the interpretation of the history of processes (history of denudation by solution) occurring on the terrain of inselbergs and monadnocks geomorphological surveys were completed. The data needed for the field maps that is the basis of the geomorphological surveys were obtained with the surveying method developed and applied by *SZUNYOGH, G.* (1995, 1998). For a more detailed survey instead of the 50x50 cm rectangular network a 10x10 cm network was applied.

2. Site of the Study

The site of the study was an area under the Widerkar Peak in the Totes Gebirge on the slope of a valley of glacial origin at an elevation of 1800 m. The study area is a closed-drainage karstification unit (*VERESS, M.-ZENTAI, Z.-HORVÁTH, E. T.* 1996) isolated from its surroundings. The rocks of the karstification unit are tilted, the closed-drainage conditions have been only magnified by surface solution. For this reason the site has been divided to smaller sub-units during its development. The fractures and faults bordering the sub-units at 55-235° strikes have developed to fissures by solution. The upper fringe of a particular sub-unit joins the upper unit with a threshold of karstic origin while its lower fringe ends at the edge of the fissure bordering the unit at its lower end. The karstic thresholds that border the units are bed-edges, the surface of the sub-units are bedding planes. Karren troughs occupy the bedding plane surfaces. In the major (type I) troughs sporadically type II and more often type III troughs develop (*VERESS, M.* 1995). As long the type I troughs are in the range of decimeter width, type III troughs are only several centimeter wide or deep. The karren troughs conduct to the fissures bordering the sub-unit or to trough-end pits. The karren troughs often form bends or are composed of sections of various direction. It occurs frequently that side troughs branch off from the main troughs this making karren trough systems.

3. Types of Karren Monadnocks and Inselbergs

Karren monadnocks and inselbergs are remnants of the original ground surface. These remnants can be classified by the processes responsible for their development or by the way they were isolated from their surroundings.

3.1. The Specification of Monadnocks and Inselbergs by the Development of Their Surfaces

Karren monadnocks are those remnants of ground surface whose elevation was identical with the elevation of the ground surface that they had been separated from (*Fig. 1*). A monadnock one with dissected surface (the surface dissected by karren indentations and rises) is a karren surfaced monadnock. Karren development could occur before the isolation from the original surface (monadnock with primary karren) or after (monadnock with secondary karren).

It shall be noted that some of the surveyed ground surfaces can be expected to be the remnants of trough bottoms. These are older than the presently existing trough bottoms so the trough bottom monadnocks can be taken as monadnocks with primary karren. It may occur that karren development characterized the top of the monadnock before as well as after the isolation. Bottom monadnocks develop at the bottoms of older karren forms. Most frequent are the trough bottom monadnocks (*Picture 1*). In these cases the remnants of the ground surface develop on the trough bottoms. The bottom monadnocks make a transition between the monadnocks and terraces. Terraces are older trough bottom remnants that developed because the younger, widening troughs digest in part the bottom of the older troughs (on which it is developing; *VERESS, M.* 1995).

Inselbergs are those remnants of the ground surface of which the top elevation decreased during the isolation (*Fig. 1*). Such remnants that had been lower than their surroundings before isolation are considered inselbergs too. Bottom inselbergs can develop on trough bottoms.

Resulted by the lateral growth of karren troughs the ground surface remaining between them may become inselbergs (crest inselberg). Peninsular inselbergs develop when the remnants between the karren troughs are not separated from the surrounding ground surface.

3.2. Categories of Inselbergs and Monadnocks by Their Way of Isolation

Karren inselbergs and monadnocks can develop on ground surface isolated between main and tributary troughs as well as in the recesses (concave sides) of bends.

3. 2. 1. The Turning of Ground Surface into Inselbergs and Monadnocks Between Main and Tributary Troughs

The troughs on rocky ground surfaces retreat by solution at the effect of the solvent flowing in them (*VERESS, M.* 1995).

The possibilities of the connection of karren troughs have been studied (*VERESS, M.* 1995) applying the statements of *CHOLNOKY, J.* (1926) on the development of regressive river valleys. Studies having performed ever since need some modifications or further development.

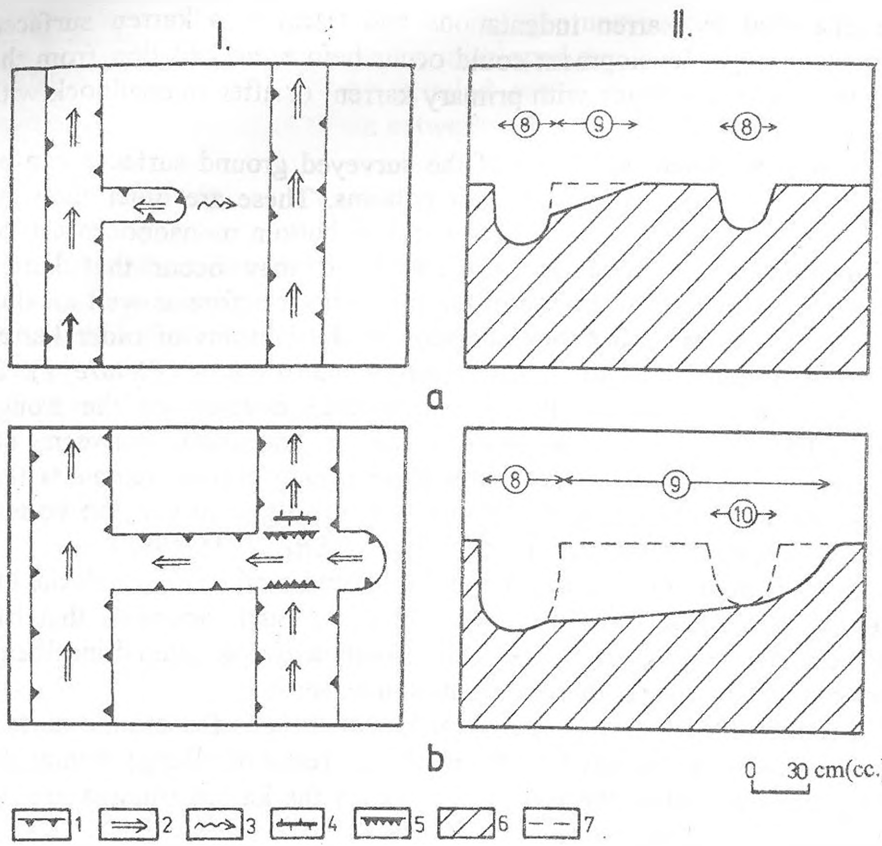

Figure 3: True beheading

Legend: 1. type I karren trough, 2. slope direction of type I karren trough bottom, 3. direction of retreating of trough end, 4. trough bottom watershed, 5. step, 6. karren development on the rock, 7. ground surface before trough entrenchment, 8. main trough, 9. regressive tributary trough, 10. ruined main trough, I. vertical view, II. side view (section along beheading trough), a. before beheading, b. after beheading

A regressive trough can reach the end of another regressive trough (*Fig. 2a*) or the side of another one (*Picture 2*).

In the first case a trough-end meeting, trough-end merging, in the second case a beheading occurs. At the merging of the troughs bottom divides develop (*VERESS, M.* 1995). The troughs bottom divides are a couple of centimeters tall and wide thresholds.

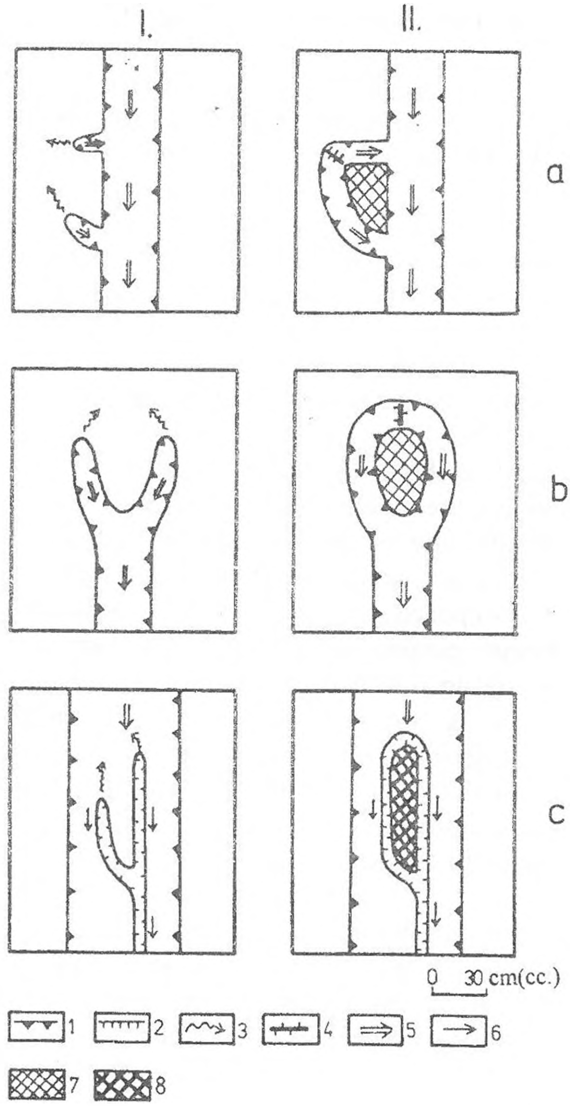

Figure 4: Development of karren inselberg and monadnock by the merging of trough ends
Legend: 1. type I karren trough, 2. type III karren trough, 3. direction of the regression of trough end, 4. trough bottom watershed, 5. slope direction of type I karren trough bottom, 6. slope direction of type III karren trough bottom, 7. monadnock, 8. bottom monadnock, I. initial condition, II. fully developed condition

In the course of trough beheading false beheading (*Fig. 2b, c, d*) and true beheading can be specified (*Fig. 3*). At false beheading the original flow conditions of the trough bottom do not change while at true beheading they do. The kinds of false beheading are as listed below.

- The retreating trough that makes the beheading entrenches at a slower pace (*Fig. 2b*). At the upper end of the beheading trough (where the false beheading is occurring) trough bottom divides develop. On the side of this at the beheaded trough a step develops that is the remnant of the trough side. The bottom of the beheading tributary trough hangs above the bottom of the main trough.
- The lower end of retreating trough entrenches at a quick pace. At the site of the beheading trough bottom divide develops with a step. The bottom of the beheading tributary trough bottom merges with that of the main trough (*Fig. 2c*).
- The retreating tributary trough entrenches at a quick pace at its whole length. The side exposed to the false beheading can be totally digested. Only a trough bottom divide develops here (*Fig. 2d*).

At true beheading the trough exposed to beheading is always digested by the trough making the beheading. At trough crossing beheading this occurs on the opposite side of the beheaded trough as well (*Fig. 3*). The developing divide does not develop in the trough responsible for beheading but in the one that is exposed to it. While at false beheading the direction of the divide is always perpendicular to the trough responsible for the beheading, it is parallel to it at true beheading (*Fig. 3*). The extension of the trough bottom divide is not the same in the described cases. At false beheading the trough bottom divide reaches from one rim to the other in the trough making the beheading. At true beheading, because it developed earlier the divide develops in the bottom of the exposed trough and its length does not exceed the width of the bottom.

At true beheading the waters of the upper part of the beheaded trough flow into the trough the beheading. If the entrenchment of the trough responsible for the beheading is intensive, one or two steps develop with directions identical with that of the trough bottom divide.

At the merging of the trough ends monadnocks may develop if the two tributary troughs of the main trough that retreat towards one another. The monadnock develops at the side of the main trough (*Fig. 4a*) but it can develop at the end as well (*Fig. 4b, c, Picture 3*). In the letter case the main trough forks to two tributary troughs.

At false beheading monadnocks develop when the retreating end of the tributary trough reaches up to the rim of the main trough. This may occur if an arced tributary develops from a straight main trough (*Fig. 5a*), but it may occur if at an arced section of the main trough one or two straight tributaries (*Fig. 5b*) develop.

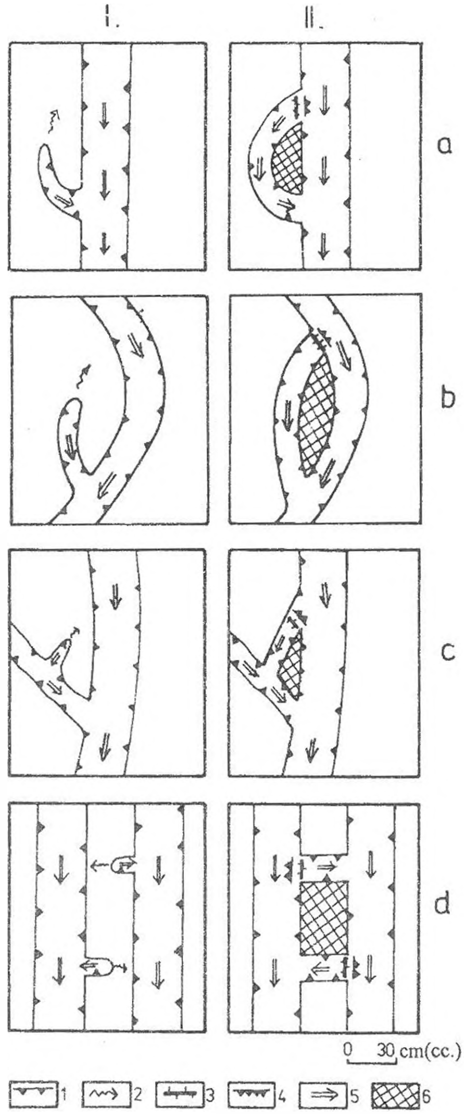

Figure 5: Developing of karren monadnocks with false beheading
Legend: 1. type I karren trough, 2. direction of regression of trough end, 3. trough bottom watershed, 4. step, 5. slope direction of type I karren trough bottom, 6. monadnock. I. initial condition, II. fully developed condition

Karren monadnocks can develop between major troughs too. In this case two tributary troughs take part in the development of the monadnock (*Fig. 5d*).

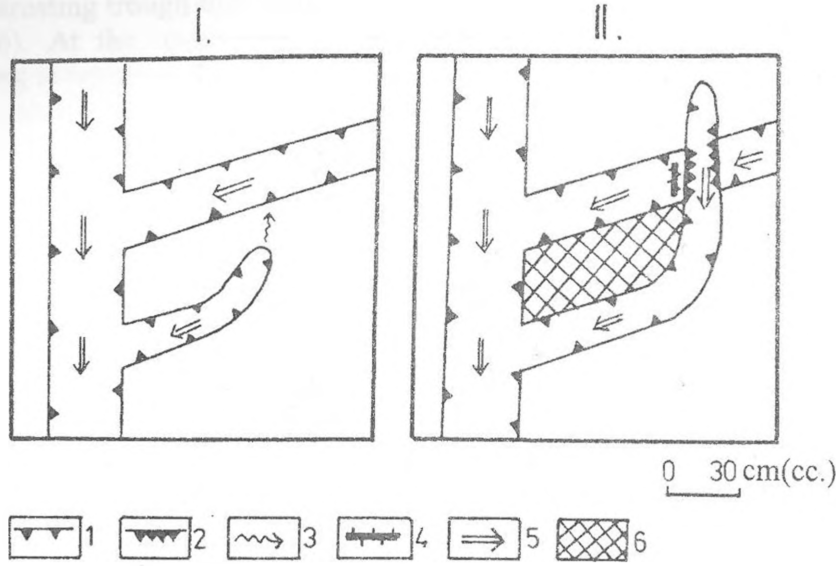

Figure 6: Developing of karren monadnocks with true beheading
Legend: 1. type I karren trough, 2. step, 3. direction of regression of trough end, 4. trough bottom watershed, 5. slope direction of type I karren trough bottom, 6. monadnock, I. initial condition, II. fully developed condition

Monadnocks can develop at true beheadings as well. In this case some major trough and its two tributaries surround the monadnock. The isolation of the monadnock is completed when the tributary trough developing quicker reaches the side of the trough that has developed at an earlier time (*Fig. 6*).

Monadnocks can develop other ways than the described ones, two of them is mentioned here.

Seldom, but it may occur that karren cavities play a role in the development of monadnocks. In this occurrence the tributary trough reaches the main trough above its section that contains a karren cavity (or a second tributary trough belonging to it). The development of the monadnock is complete when the roof of the cavity vanishes (*Fig. 7a*).

If the main trough is shallow and it bends too, the solvent flow in it hits the trough rim and spills over. The spilling water dissolves a trough downwards on the sloping ground surface (progressive trough). The lower end of the tributary trough may reach the main trough again. As a result, a monadnock develops independently from any bend (*Fig. 7b*). The progressive tributary trough quickly becomes hanging (at both ends joining the main trough with steps) because the main trough flows with more solvent and consequently its entrenchment is quicker. Such tributaries don't receive water from the main trough any more. Trough bottom divide does not develop in the progressive trough.

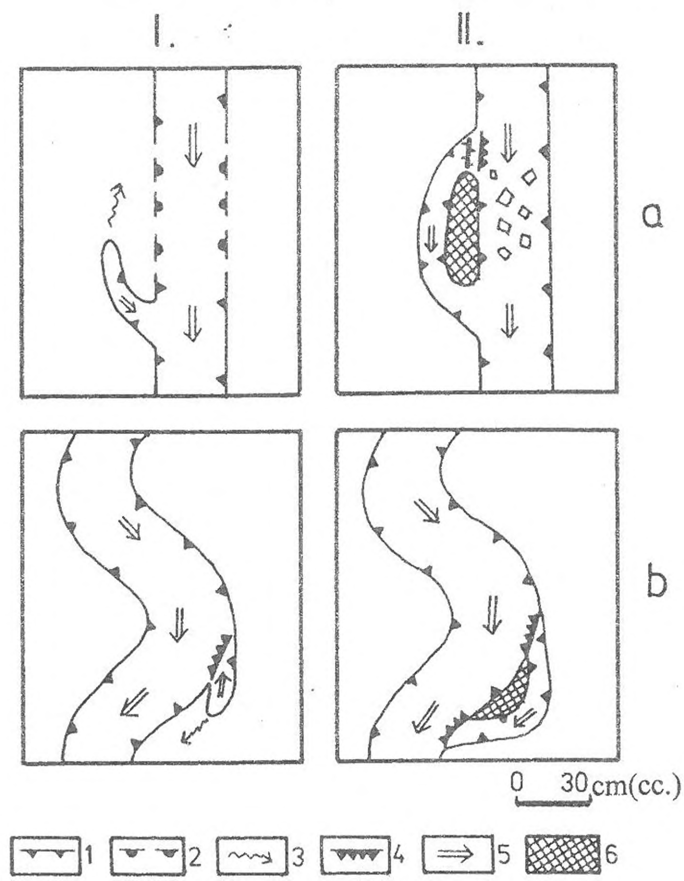

Figure 7: Developing of karren monadnocks after opening up the karren cavity (a) and development of progressive trough (b)
Legend: 1. type I karren trough, 2. karren cavity, 3. direction of regression of trough end, 4. step, 5. slope direction of type I karren trough bottom, 6. monadnock, I. initial condition, II. fully developed condition

3.2.2. Development of karren inselbergs and monadnocks in the recesses (concave sides) of bends.

The recesses of karren troughs can develop at true- or false meandering. The cutoff of the recesses may happen with false- or true beheading. At false beheading it is not the solvent flowing in the trough that executes the cutoff. In this case rainfall on the recess and its neck develop karren troughs. These are the tributaries of the trough making the bend and they are hanging in position. False beheading can happen at the neck or at any other part of the recess. It may happen by the retreating of a single karren trough (*Fig. 8a*) or by the connecting of two retreating troughs (*Fig. 8b and Picture 4*). In the first case the trough bottom divide develops at the end of the tributary trough (the step develops at both ends of it) while in the letter case at the joint of the two troughs. Steps develop at both trough mouths.

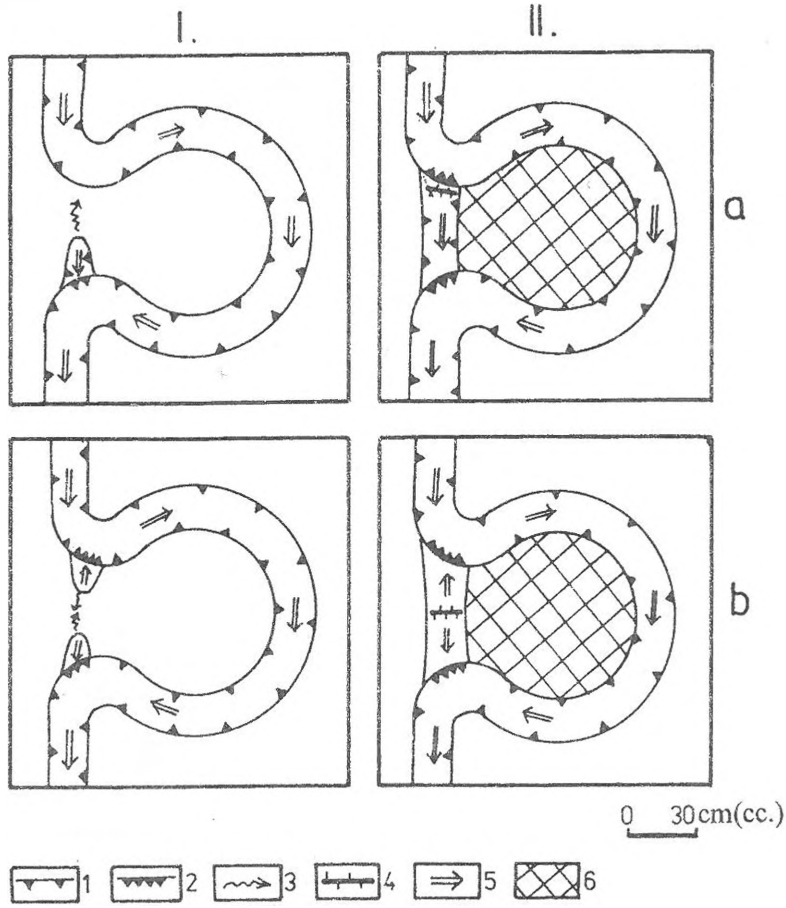

Figure 8: Developing of karren monadnocks with false beheading of bends in the case of regression of 1 (a) or 2 (b) tributary troughs
Legend: 1. type I karren trough, 2. step, 3. direction of regression of trough end, 4. trough bottom watershed, 5. slope direction of type I karren trough bottom, 6. monadnock, I. initial condition, II. fully developed condition

Troughs developing at various parts of the bend can cut up the recesses to monadnocks of various sizes. In the case of the retreating of two tributaries the divide develops within the neck zone. In the case of one retreating tributary the divide develops where its upper end reaches the main trough. The ends of the neck troughs hang above the bottom of the main trough.

At true beheading the recess is separated by the solvent flow in the trough.

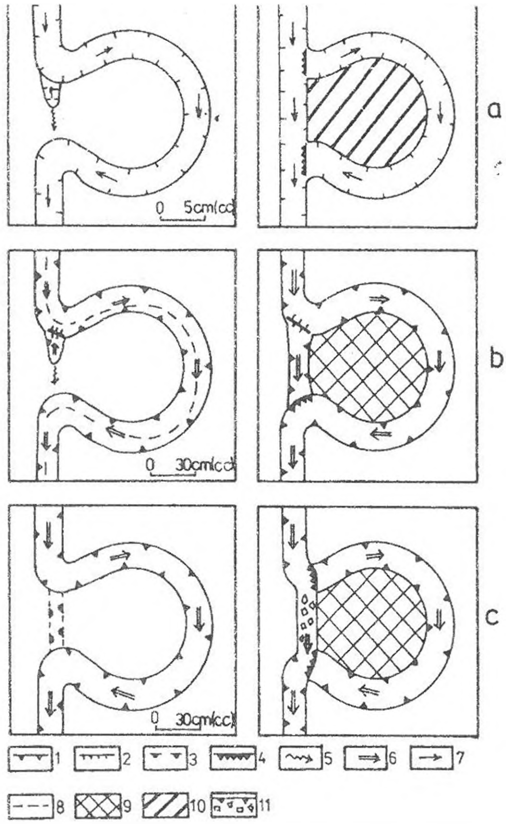

Figure 9: Developing of karren monadnocks with true beheading of bends
Legend: 1. type I karren trough, 2. type III karren trough, 3. karren cavity, 4. step, 5. direction of regression of trough end, 6. slope direction of type I karren trough bottom, 7. slope direction of type III karren trough bottom, 8. channel line, 9. monadnock, 10. karren inselberg on the bottom, 11. opened-up karren trough, I. initial condition, II. fully developed condition a. b. developing progressive trough, c. cave-in of karren cavity

True beheading occurs most simply in type III troughs, because they are only a few centimeters deep. When the gradient of the master trough (type I trough) is moderate and the meander zone of the type III trough is wide, the meander arc is long, the solvent flow in the trough does not follow the arc of the loop but spills over. Thus an intensively developing progressive trough is made on the neck.

Beheading occurs if the depth of the progressive trough exceeds the depth of the trough in the bend. The separated trough section becomes hanging with both ends connecting to the new trough section in the neck with steps. As bend slippage may happen on the surface of the recess, lateral small extension pointed inselbergs may develop (*Fig. 9a and Picture 5*). The phenomenon can be observed in type II troughs too. In these cases the cutoff of the recess occurs during the development of type III troughs.

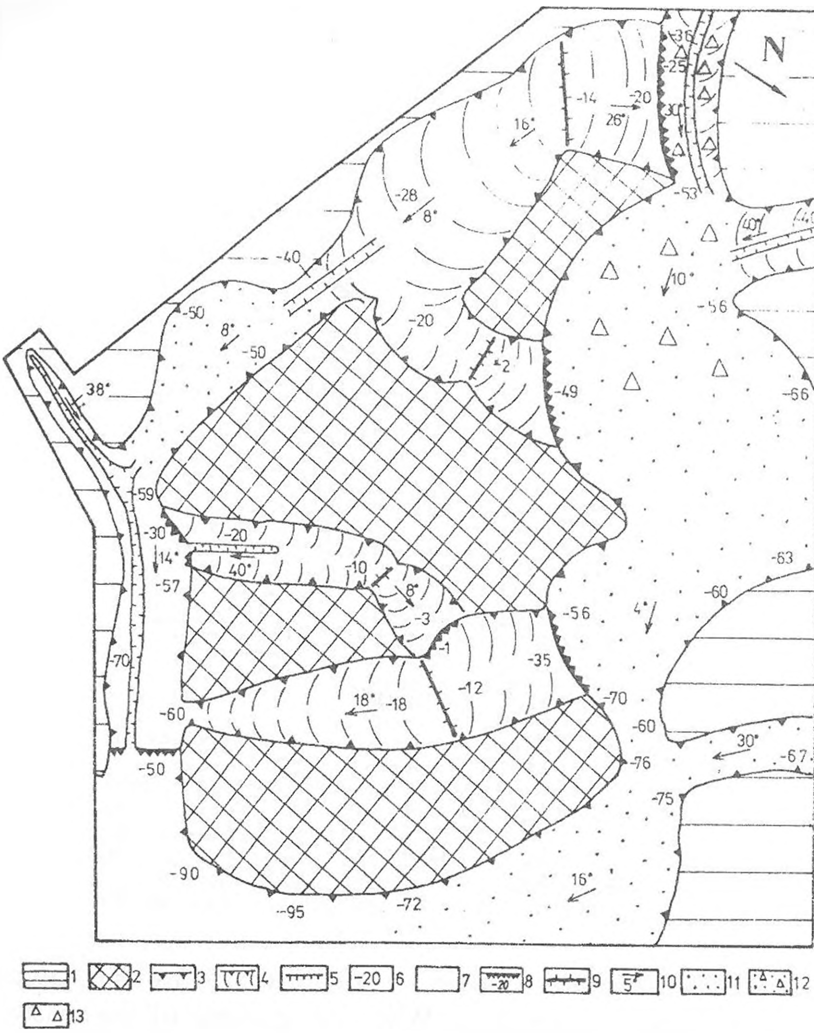

Figure 10: Morphological map of the "A" karren ground surface detail
Legend: 1. karren development on the rock near the mapped ground surface part, 2. monadnock, 3. type I karren trough (vertical-sided), 4. type I karren trough (gently sloping-sided), 5. type III karren trough, 6. trough with depth in centimeters (it is indicated at the point where it was measured between the bottom and rim), 7. trough bottom without sediment, 8. step with depth in centimeters, 9. trough bottom watershed, 10. direction of slope of karren trough bottom, 11. soil and weathering products, 12. soil with rock debris, 13. rock debris

True beheading can develop in type I troughs too mostly when the trough consists of a single meander (loop meander in an overdeveloped trough). The channel line hits the trough rims at the necks. If the depth of the trough is moderate at these places part of the flow in the trough spills over that results the partial cutoff of the loop (*Fig. 9b*). The developing progressive trough at the neck and the bottom of the meander can entrench together. Both trough sections remain active because water can flow in both the progressive trough and in the cutoff part of the main trough. The lower end of the progressive trough hangs above the bottom of the master trough, at its upper end a trough bottom divide develops. The monadnock developed by the progressive trough can be cut up to monadnock remnants by further troughs by false beheading.

Karren cavity may develop in the necks. The development of the monadnock is complete with the destruction of the roof of the karren cavity (*Fig. 9c*). The beheaded bend is hanging, it joins the existing trough sections with steps at the necks.

4. The History of Dissolution of the Mapped Karren Ground Surfaces

The history of dissolution of ground surfaces mapped at the Widerkar Peak will be presented in the followings. At the sketching of the history of dissolution not only results obtained in the analysis of the karren inselbergs and monadnocks were applied but the results of the study of meander development as well (*VERESS, M.* 1998).

4.1. The "A" Karren Ground Surface Detail (Fig. 10, Picture 6)

The arcing type I and II karren troughs develop by retreating. The letter is the tributary trough of the former (*Fig. 11a*). These two karren troughs develop parallel to each other in part.

The ends of the type I and II karren troughs reaching up to one another create a series of monadnocks (*Fig. 11b, c, d*). First the No. V, then the No. VI, VII and finally the No. VIII monadnocks develop. The trend of the described series of development can be especially caught in the case of the monadnocks Nos. V and VI. That is, the No. III tributary trough can develop only (a premise of the development of monadnock No. VI) when the Nos. II and III troughs connect. (The development of these two letter troughs results the development of monadnock No. V.)

Of the tributary troughs retreating towards each other those retreating from the No. II trough are the older. This is proved by the trough bottom divides being closer to the No. I trough. Another proof is that the difference of elevation of the bottoms of the No. II trough and its tributaries are smaller than that of the No. I trough and its tributaries.

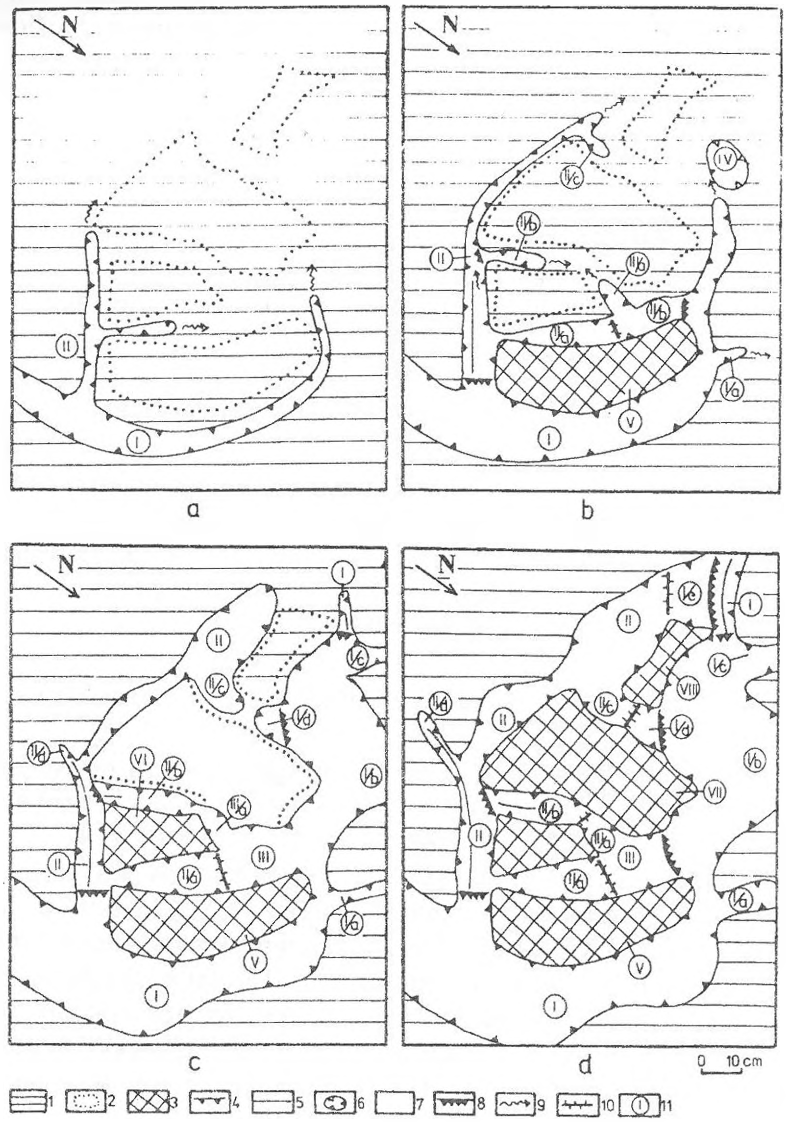

Figure 11: Solution history of "A" ground surface detail
Legend: 1. surface without karren, or showing no reconstructable karren forms, 2. monadnock developed at a later time, 3. monadnock, 4. type I karren trough, 5. type III karren trough, 6. initial solution pan, 7. trough bottom and solution pan bottom without covering sediment, 8. step, 9. direction of regression of trough end, 10. trough bottom watershed, 11. identifying sign of trough, solution pan and monadnock (a, b, c former condition, d present condition)

4.2. The "B" Karren Ground Surface Detail (Fig. 12, Picture 7)

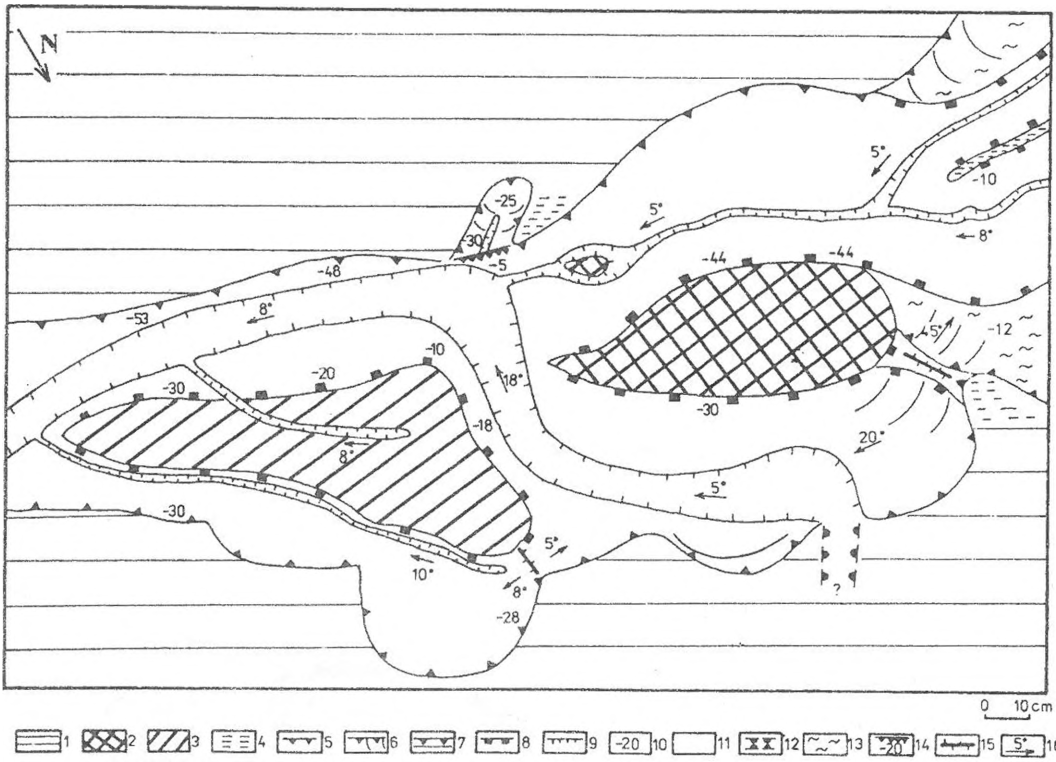

Figure 12: Morphological map of the "B" ground surface detail
Legend: 1. karren development on the rock near the mapped ground surface detail, 2. bottom monadnock, 3. karren inselberg on the bottom, 4. karren half-inselberg, 5. type I karren trough (vertical-sided), 6. type I karren trough (gently sloping-sided), 7. type I karren trough (overhanging-sided), 8. type II karren trough (vertical-sided), 9. type III karren trough, 10. trough with depth in centimeters (it is shown where it was measured), 11. trough bottom without covering sediment, 12. karren cavity, 13. terrace, 14. step with depth in centimeters, 15. trough bottom watershed, 16. direction of slope of grade of karren trough bottom

The type I, No. I karren trough develops. The development of a type II trough, No. II begins in the bottom of this trough (*Fig. 13a*). The intensive widening of trough No. II then that of trough No. V digests the bottom of trough No. I in the direction of its rim. In these locations the remnants of the

No. I. trough do not remain even in the form of terraces. (Such remain only in its interior as bottom inselbergs and monadnocks.) The No. IIa and IIb troughs develop forking from trough No. II as well as its No. III tributary trough (*Fig. 13b, c*). Because of the less intensive widening of the No IIa and IIb troughs terraces develop in this section of trough No I.

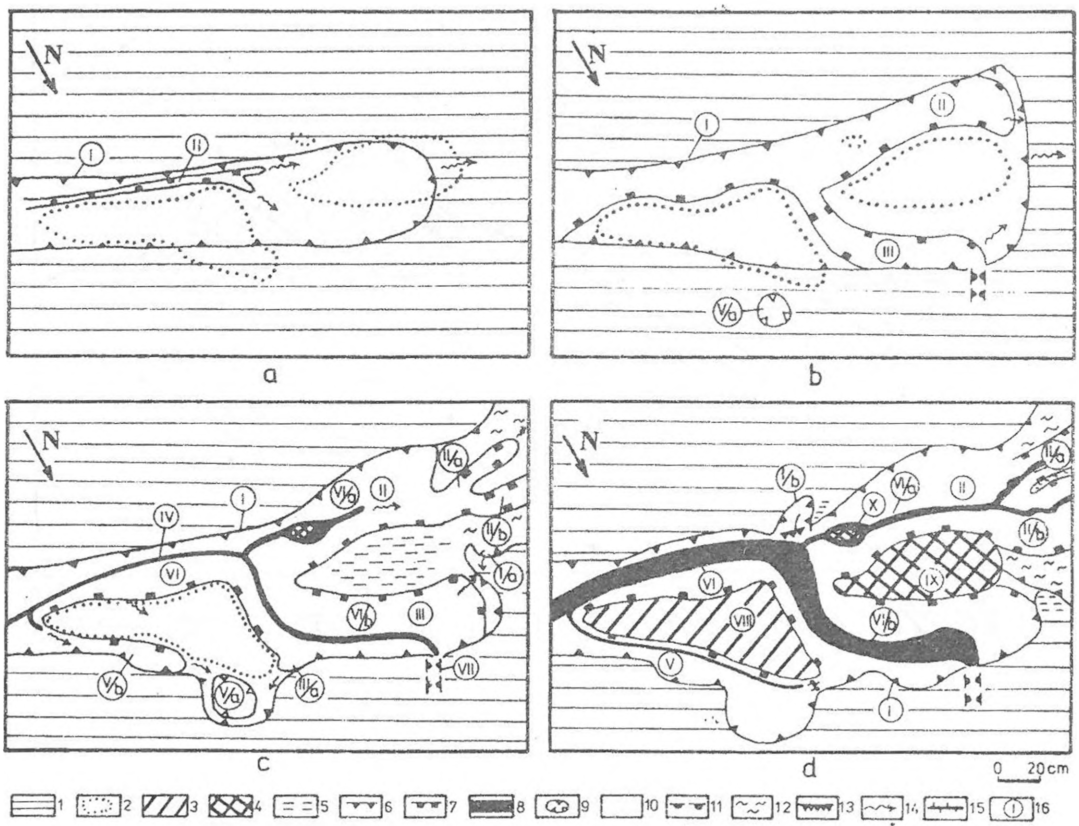

Figure 13: Solution history of "B" ground surface detail
Legend: 1. surface without karren, or showing no reconstructable karren forms, 2. karren inselberg and monadnock developed at a later time, 3. karren inselberg on the bottom, 4. bottom monadnock, 5. karren half-inselberg, 6. type I karren trough, 7. type II karren trough, 8. type III karren trough, 9. little solution pan , 10. trough bottom and solution pan bottom without covering sediment, 11. karren cavity, 12. terrace, 13. step, 14. direction of regression of trough end, 15. trough bottom watershed, 16. identity sign of trough, solution pan , karren cavity, monadnock and karren inselberg (a, b, c former condition, d present condition)

With the connecting of the troughs Nos. V and III the No. VIII bottom monadnock and with the connecting of the troughs Nos. III and I the No. IX bottom monadnock develops. (The No. VIII monadnock rises only a few centimeters above the trough No. V that hints at the intensive destruction of its surface.) As a result of the forking of trough VI. such a bottom monadnock develops that is a residue of the bottom of the No. II trough (*Fig. 13c, d*).

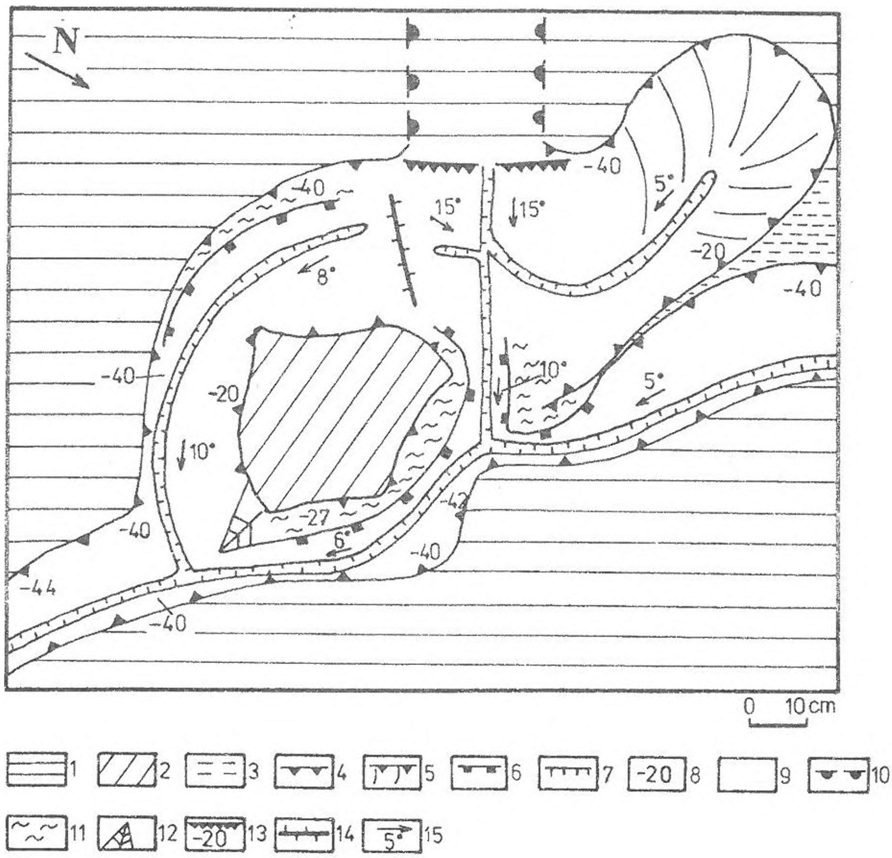

Figure 14: Morphological map of the "C" ground surface detail
Legend: 1. karren development on the rock near the mapped ground surface detail, 2. karren inselberg, 3. karren half-inselberg, 4. type I karren trough (vertical-sided), 5. type I karren trough (gently sloping-sided), 6. type II karren trough (vertical-sided), 7. type III karren trough, 8. trough with depth in centimeters (it is shown where it was measured), 9. trough bottom without covering sediment, 10. karren cavity, 11. terrace, terrace remnant, 12. skirt, 13. step with depth in centimeters, 14. trough bottom watershed, 15. direction of slope of grade of karren trough bottom

4.3. The "C" Karren Ground Surface Detail (Fig. 14, Picture 8)

From the No. I karren trough retreating to the northwest the Nos. II and III karren troughs develop (*Fig. 15a*). The age of the No. II karren trough is more or its development is quicker than that of trough No. III. For this reason the No. IIIa tributary trough reaches the rim of trough No. II during its westward retreating (*Fig. 15b*). Because the development of the former is quicker, it beheads the letter (*Fig. 15c, d*).

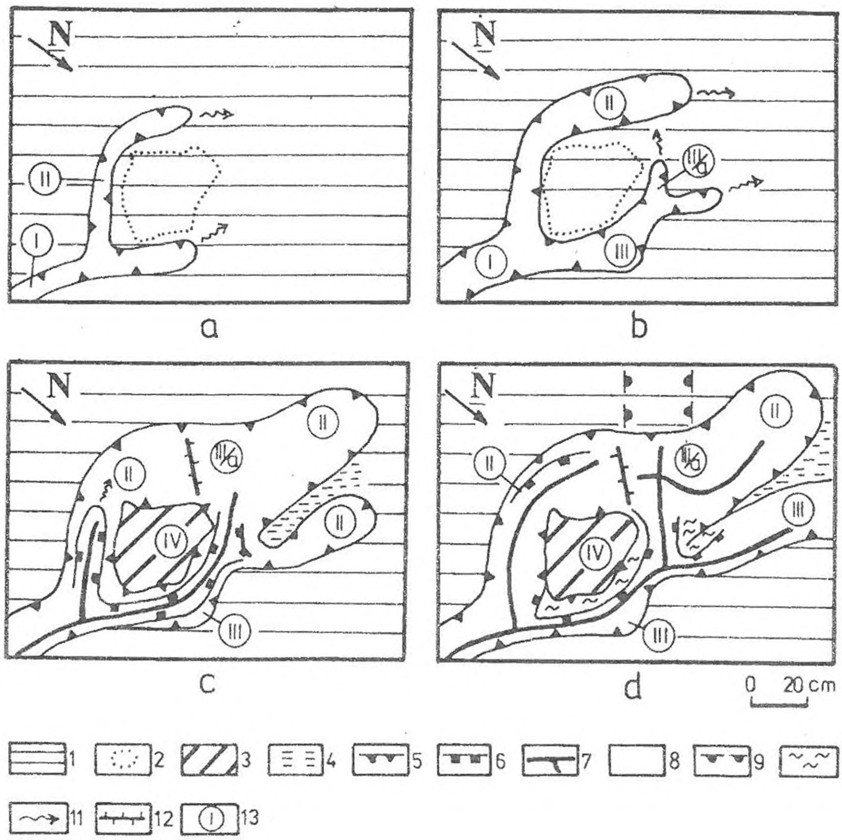

Figure 15: Solution history of the "C" ground surface detail
Legend: 1. surface without karren, or showing no reconstructable karren forms, 2. karren inselberg developed at a later time, 3. karren inselberg, 4. karren half-inselberg, 5. type I karren trough, 6. type II karren trough, 7. type III karren trough, 8. trough bottom without covering sediment, 9. karren cavity, 10. terrace, 11. direction of regression of trough end, 12. trough bottom watershed, 13. identity sign of trough and karren inselberg (a, b, c former condition, d present condition)

Type II troughs develop on the bottoms of type I troughs (Nos. II and III). The widening of these cause the development of terraces in troughs Nos. II and III. The development of the type II troughs is completed to the time of beheading. This is hinted by the fact that the type II troughs and terraces do not develop in the beheaded trough sections.

The No. IV inselberg develops as a result of the beheading. Its top is lower than the elevation of the surrounding surface. There is no trace of any such effect during the development of troughs Nos. II and III that would have caused the denudation of the surface of the top of the monadnock. That's why it is possible that the karren development of the top of the monadnock has been the result of karren processes independent of the above described processes.

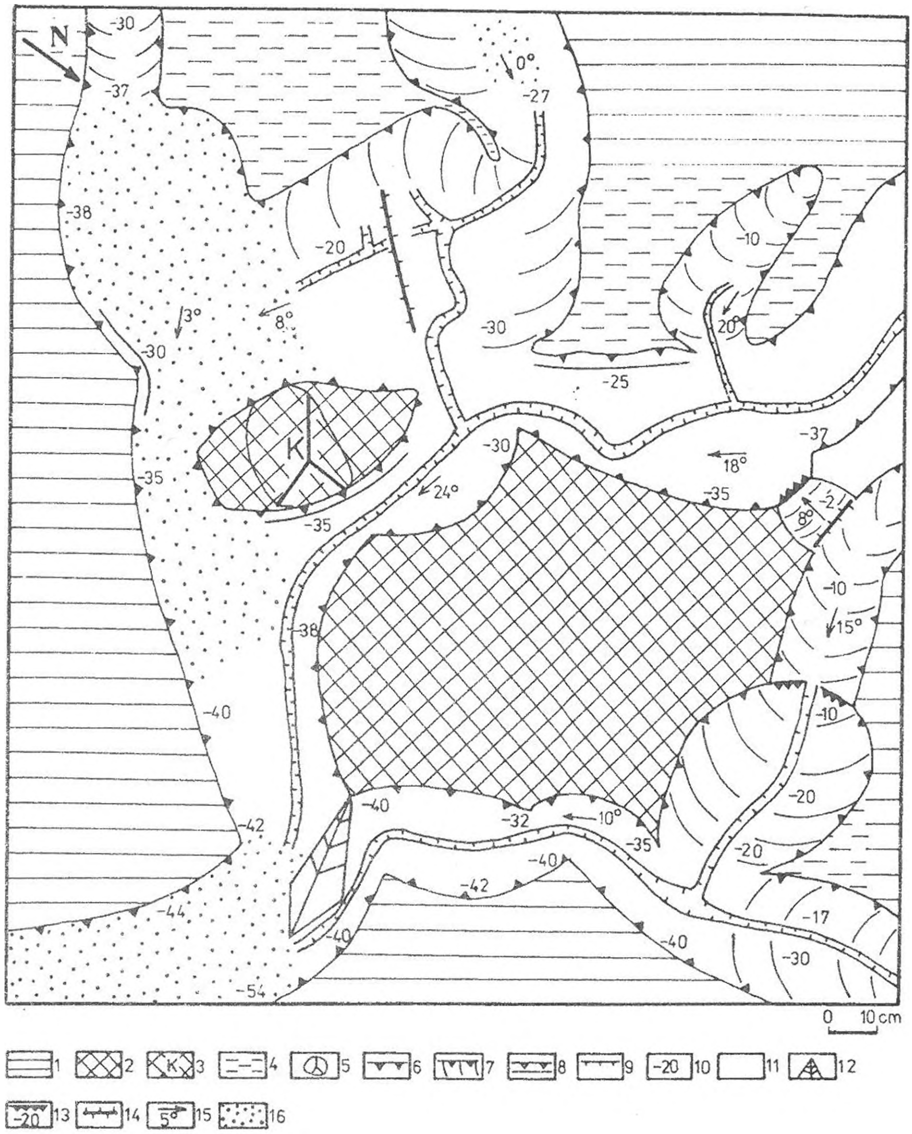

Figure 16: Morphological map of the "D" ground surface detail
Legend: 1. karren development on the rock near the mapped ground surface detail, 2. monadnock, 3. karren monadnock, 4. karren half-inselberg, 5. karren rise, 6. type I karren trough (vertical-sided), 7. type I karren trough (gently sloping-sided), 8. type I karren trough (overhanging-sided), 9. type III karren trough, 10. trough with depth in centimeters (it is shown where it was measured), 11. trough bottom without covering sediment, 12. skirt (at slippage), 13. step with depth in centimeters, 14. trough bottom watershed, 15. direction of slope of karren trough bottom, 16. soil and weathering products

4.4. The "D" Karren Ground Surface Detail (Fig. 16)

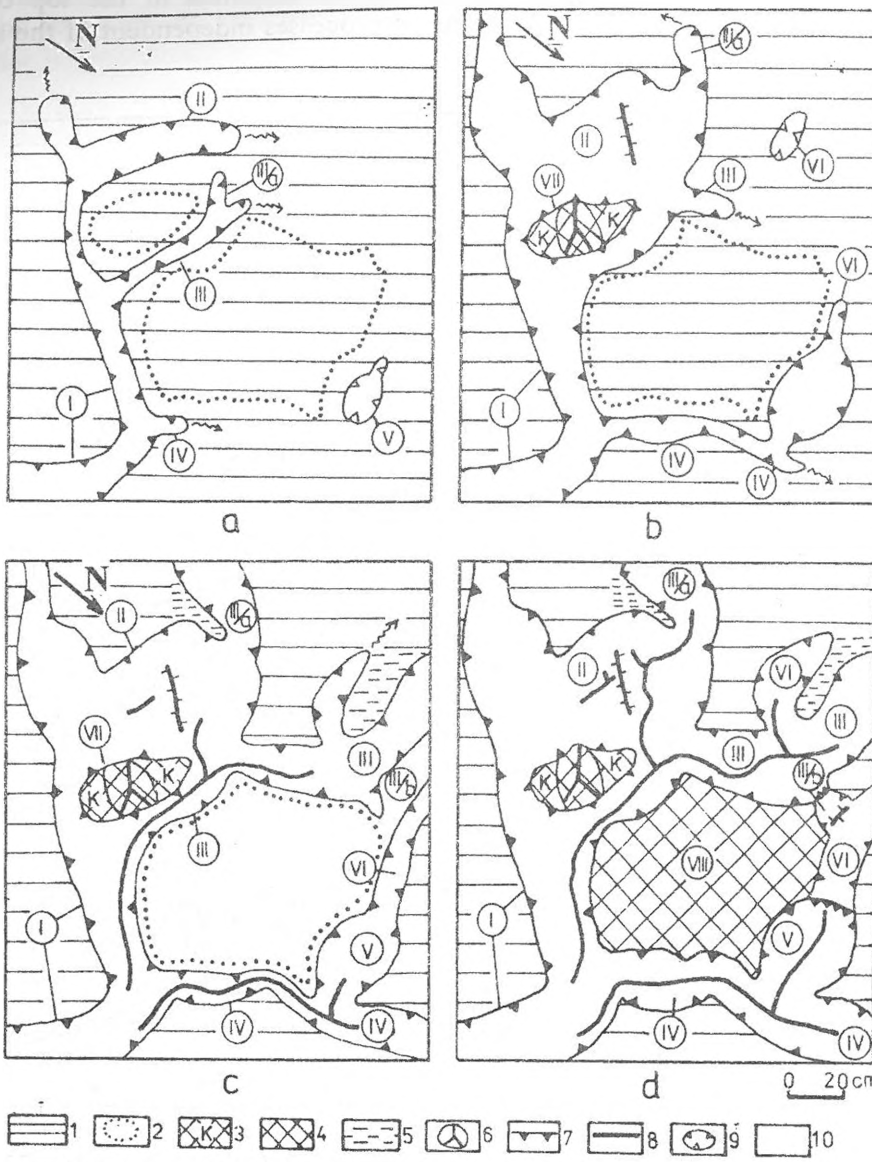

Figure 17: Solution history of the "D" ground surface detail
Legend: 1. surface without karren, or showing no reconstrutable karren forms, 2. karren inselberg and monadnock developed at a later time, 3. karren monadnock, 4. monadnock, 5. karren half-inselberg, 6. karren rise, 7. type I karren trough, 8. type III karren trough, 9. small solution pan , 10. trough bottom without sediment, 11. step, 12. direction of regression of trough end, 13. trough bottom watershed, 14. identity sign of trough and monadnock (a, b, c former condition, d present condition)

The No. I trough develops from the east to the west and making a bend to southwest it develops further ever retreating. Retreating westwards from the karren trough tributary karren troughs develop (Nos. II, III, IV, *Fig. 17a*). The older No. II is beheaded by the younger, more intensively developing No. III that is proved by the trough bottom divide in the former. The No. VII rough surfaced karren monadnock develops (*Fig. 17b*). Its surface probably carries the traces of older trough bottoms that hints at previous karren development. Following this (*Fig. 17c*) the No. IIIb karren trough reaches the No. VI. karren trough (false beheading) that proves the higher age of development of the No. III trough being higher than that of No. VI, or its higher rate of development. The monadnock No. VIII develops (*Fig. 17d*).

4.5. The "E" Karren Ground Surface Detail (Fig. 18, Picture 9)

The No. I karren trough develops with its tributary trough (I.a). The No. I karren trough makes a system (with a karren trough swallet) with the No. V karren cavity. A solution pan (No. III) develops above this karren cavity that is joined by the No. II karren trough. (*Fig. 19a*).

The roof of the karren cavity had possibly thinned so much at the bottom of the No. II karren trough and solution pan that part of it may have developed to an opening up karren trough (*Fig. 19b*). This way the connection between the No. II karren trough and the solution pan has been severed. The merging by solution of the No. Ia karren trough and the solution pan can be expected as well as the collapse of the roof of the karren cavity in its whole length (*Fig. 19d*). Resulted by these processes the remnant of the original ground surface becomes a monadnock between the remnant of the solution pan (V) and the bottom of the No. II karren trough becomes an inselberg (VI).

4.6. The "F" Karren Ground Surface Detail (Fig. 20, Picture 10)

The karren trough No. I develops as a rainwater runnel with three meanders (*Fig. 21a*). The two smaller meanders (m_1 and m_2) are true meanders this proven by the skirts on the trough sides. In the big meander (m_3) that is a loop meander, a skirt can not be recognized. In spite of this the development of this bend has probably happened by true meandering proven by the overhanging wall in the concave side of the band.

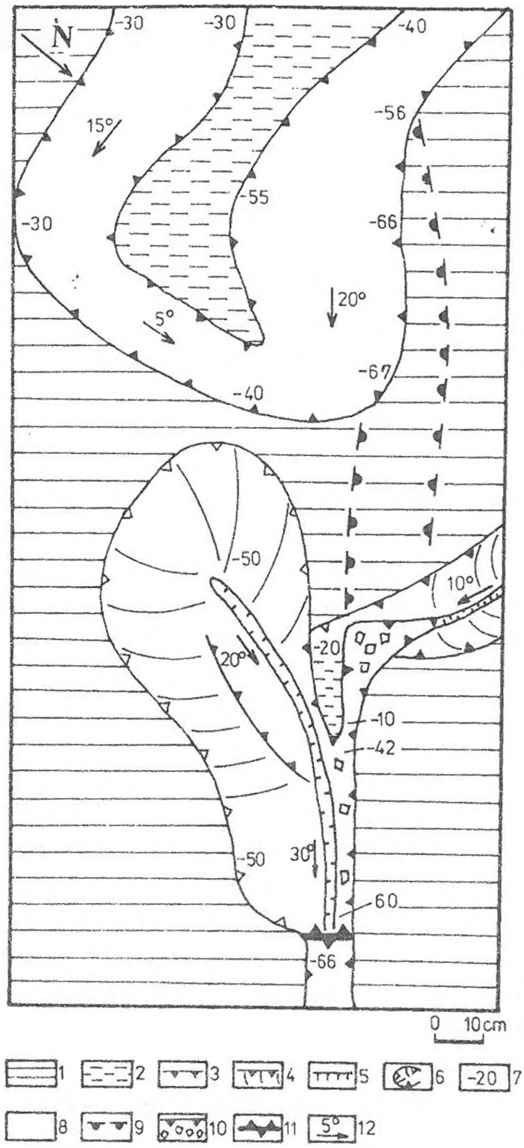

Figure 18: Morphological map of the "E" ground surface detail
Legend: 1. karren development on the rock near the mapped ground surface detail, 2. karren half-inselberg, 3. type I karren trough (vertical-sided), 4. type I karren trough (gently sloping-sided), 5. type III karren trough, 6. vertical-sided and gently sloping-sided solution pan remnant, 7. trough and solution pan with depth in centimeters (it is shown where it was measured), 8. trough bottom without covering sediment, 9. karren cavity, 10. trough developed by opening up, 11. trough arch, 12. direction of slope of karren trough bottom

Early begins the development of the No. II trough in the m_3 meander, that separates the No. XV monadnock by false beheading (*Fig. 21b*). The early beheading is proven by the smallest step height than can be associated with the big entrenchment of the trough.

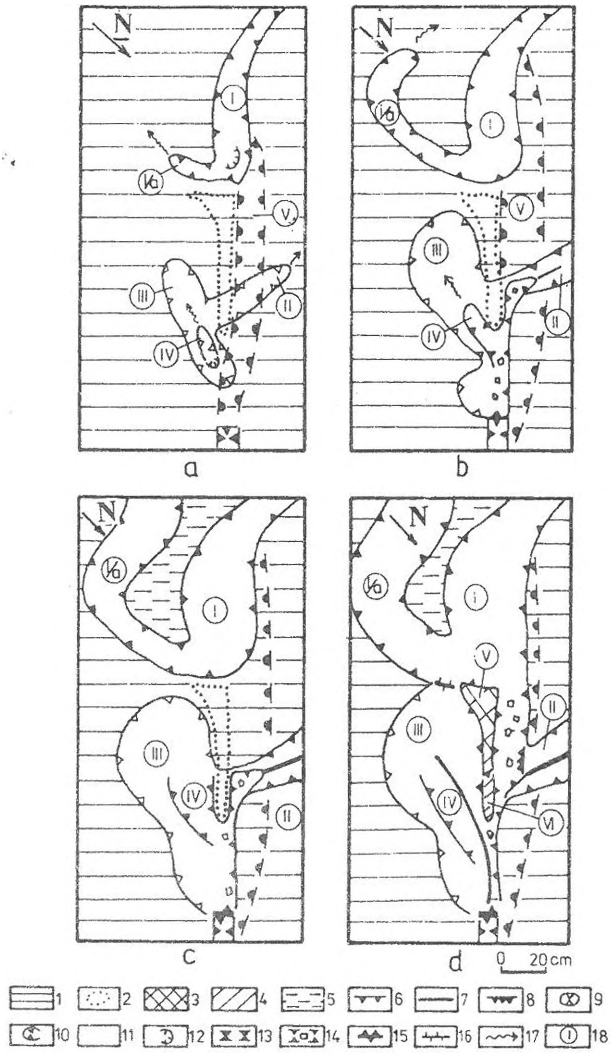

Figure 19: Solution history of the "E" ground surface detail
Legend: 1. surface without karren, or showing no reconstructable karren forms, 2. karren inselberg and monadnock developed at a later time, 3. monadnock, 4. karren inselberg, 5. karren half-inselberg, 6. type I karren trough, 7. type III karren trough, 8. step, 9. solution pan , 10. destructed solution pan , 11. trough and solution pan bottom, 12. trough sink, 13. karren cavity, 14. trough developed by opening up, 15. trough arch, 16. trough bottom watershed, 17. direction of regression of trough end, 18. identity sign of trough, solution pan and monadnock (a, b, former condition, c present condition, d condition in the future)

The channel line swing intensifies in the quickly widening trough No. I resulting the progressive development of troughs Nos. III and IV (*Fig. 21b, c*). The loop type development of trough No. III develops the No. XIV monadnock. (The surface of both the Nos XIV and XV monadnocks are karren. The time of the karren development can not be specified.) Many more tributary troughs develop in the No. I trough (Nos. VII, VIII, X, XI). The No. XII karren cavity develops and trough end connecting occurs between the troughs Nos. V and VI.

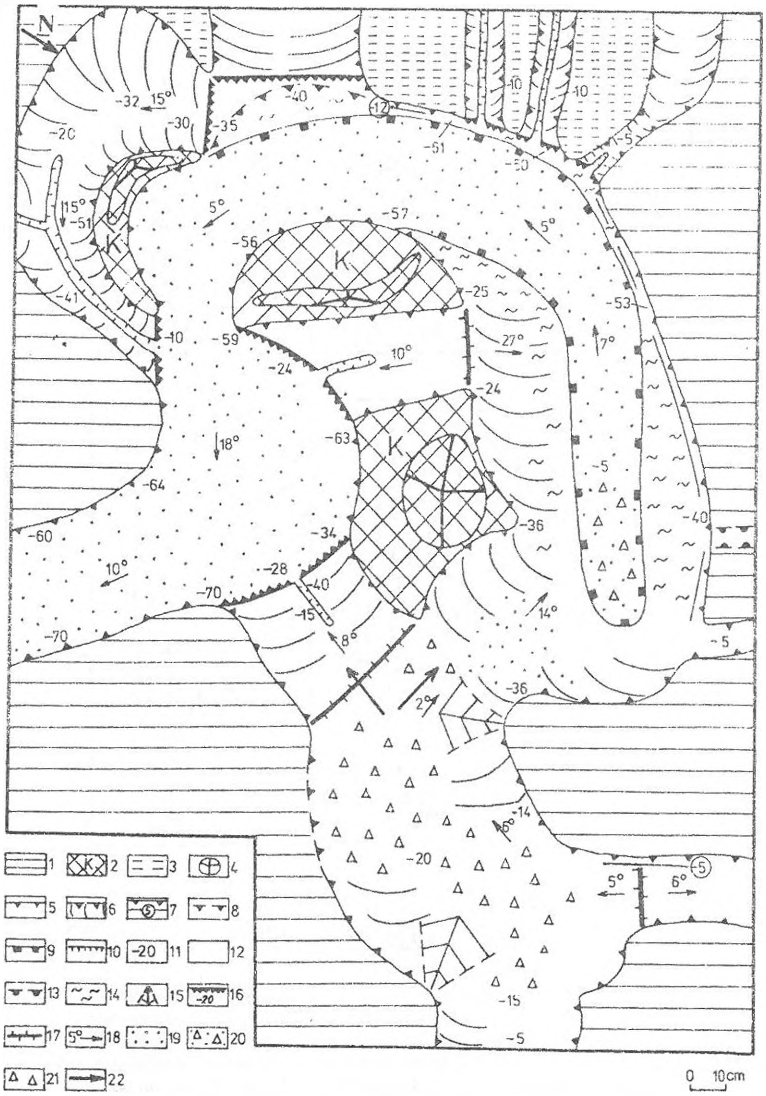

Figure 20: Morphological map of the "F" ground surface detail
Legend: 1. karren development on the rock near the mapped ground surface detail, 2. karren monadnock, 3. karren halfinselberg and monadnock, 4. karren rise, 5. type I karren trough (vertical-sided), 6. type I karren trough (gently sloping-sided), 7. type I karren trough (overhanging-sided, the number shows the biggest horizontal distance in centimeters between overhanging side and edge of trough), 8. ruined edge of trough, 9. type II karren trough (vertical-sided), 10. type III karren trough, 11. trough with depth in centimeters (it is shown where it was measured), 12. trough bottom without covering sediment, 13. karren cavity, 14. terrace, 15. skirt remnant (at slippage), 16. step with depth in centimeters , 17. trough bottom watershed, 18. direction of slope of grade of karren trough bottom, 19. soil and weathering products , 20. soil debris, 21. debris, 22. water flow directions at the time of mapping

The beheading of the recess is done by the No. IV progressive trough, the No. XVI monadnock develops (*Fig. 21d*).

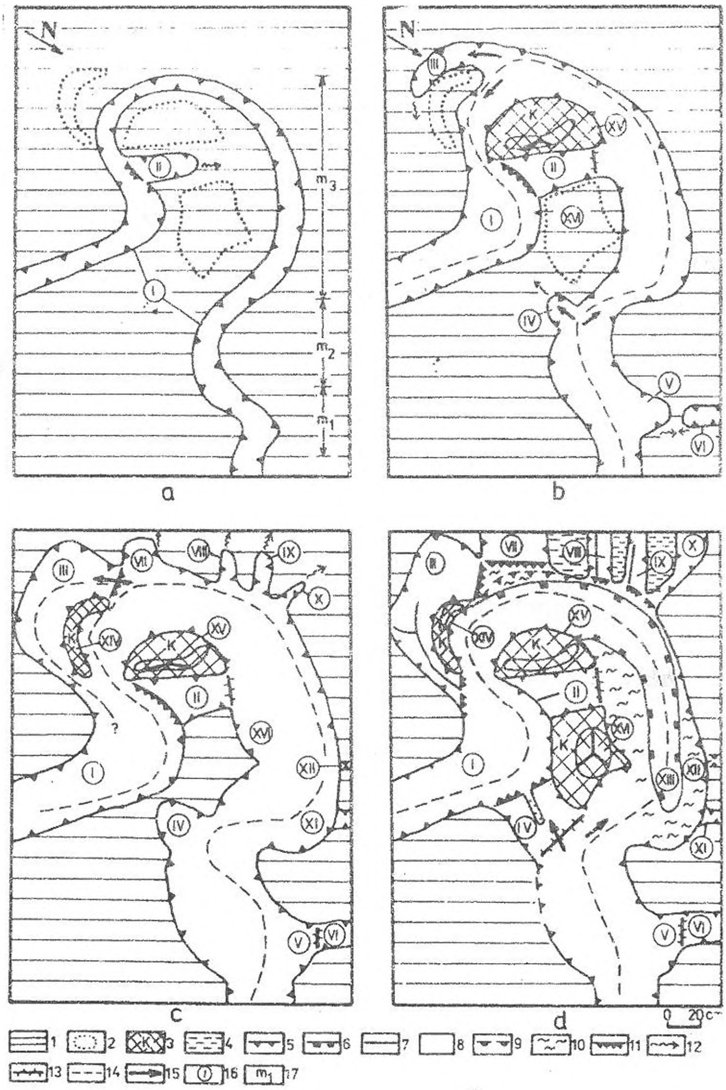

Figure 21: Solution history of the "F" ground surface detail
Legend: 1. surface without karren, or showing no reconstructable karren forms, 2. karren inselberg and monadnock developed at a later time, 3. karren monadnock, 4. karren half inselberg, 5. type I karren trough, 6. type II karren trough, 7. type III karren trough, 8. trough bottom without covering sediment, 9. karren cavity, 10. terrace, 11. step, 12. direction of regression of trough end, 13. trough bottom watershed, 14. channel line, 15. probable water flow directions, 16. identity sign of trough and monadnock, 17. identity sign of meander (a, b, c former condition, d present condition)

The solvent that flows from the karren cavity develops a type II trough (No. XIII) with the partial entrenchment of the No. I trough. This results the development of terraces at parts of the trough No. I. The overhanging walls of trough No. I collapse.

5. Consequences

a. Those troughs that are separated by trough bottom divides and steps have developed regressively. The location and position of these features give ground to the determination of the type of connecting.
b. Considering the trough-end merges, the false and true beheading of troughs and bends the type of development of inselbergs and monadnocks and the sequence of the development of karren forms can be determined on some specific karren ground surface.
c. Using the detailed morphological survey of some specific karren ground surface and the relative sequence of the development of karren forms such a series of maps can be prepared that can describe the process of dissolution to a certain profundity.

REFERENCES

BALÁZS, D. (1987): Szigethegyek-tanuhegyek - Természet Világa 7. sz. p. 261-265.
BALÁZS, D. (1990): Karrformák-karregyüttesek - Karszt és Barlang II. p. 117-122.
BÖGLI, A. (1976): Die Wichtigsten Karrenformen der Kalkalpen - In: Karst Processes and Relevants Landforms. ISU Comission on Karst Denudation. Ljubljana p. 141-149.
BULLA, B. (1954): Ált. természeti földrajz II. - Tankönyvkiadó, Bp.
CHOLNOKY, J. (1926): A földfelszín formáinak ismerete (Morfológia) - Bp.
SZUNYOGH, G. (1995): Mészkőfelszinek kisformáinak grafikus ábrázolása - Karsztfejlődés I. (Totes Gebirge karrjai) p. 41-60.
SZUNYOGH, G. (1998): Nagy területet lefedő karrvályúrendszer struktúrájának elemzése - Karsztfejlődés II. (Totes Gebirge karrjai) BDTF Természetföldrajzi Tanszék, Szombathely, p. 7-34.
VERESS, M. (1995): Karros folyamatok és formák rendszerezése Totes Gebirge-i példák alapján - Karsztfejlődés I. (Totes Gebirge karrjai) p. 7-30.
VERESS, M.-ZENTAI, Z.-HORVÁTH, E. T. (1996): Egy magashegységi karsztterület vertikális formáinak vizsgálata (Totes Gebirge, Ausztria) - BDTF Tud. Közl. X. Természettudományok 5. p. 141-157.
VERESS, M. (1998): Karrmeanderek - Karsztfejlődés II. (Totes Gebirge karrjai) BDTF Természetföldrajzi Tanszék, Szombathely, p. 35-58.

Picture *1: Developing trough bottom monadnock (Totes Gebirge)*
Legend: 1. type I trough, 2. type III trough, 3. bottom monadnock, 4. terrace

Picture 2: Trough beheading (Asiago Plateau)
Legend: 1. beheaded trough, 2. beheading trough, 3. step, 4. slope direction of trough, 5. fissure karren

Picture 3: Karren inselberg developed by the connecting of tributary troughs (Totes Gebirge)
Legend: 1. tributary trough, 2. karren inselberg, 3. type I trough, 4. older type II trough, 5. younger type II trough, 6. remnant of trough bottom developed by inside trough shifting, 7. ridge between older and younger type II troughs

Picture 4: Karren inselberg developed by false beheading
Legend: 1. loop meander, 2. recess surrounded by meander, 3. karren monadnock, 4. regressive trough, 5. trough bottom divide , 6. step

Picture 5: Karren inselberg developed by true beheading (there are meander remnants in the trough section above the karren inselberg, Totes Gebirge)
Legend: 1. karren inselberg (beheaded skirt), 2. older, cut off trough bottom, 3. skirt, 4. developing meandering trough section, 5. trough section with meander remnants

Picture 6: The „A" Karren Ground Surface Detail (Totes Gebirge)
Legend: 1. karren monadnock, 2. vertical-sided type I trough, 3. gently slooping-sided type I trough, 4. trough bottom divide

Picture 7: The „B" Karren Ground Surface Detail (Totes Gebirge)
Legend: 1. trough bottom monadnock, 2. trough bottom inselberg, 3. type I trough, 4. type II trough, 5. type III trough, 6. karren cavity, 7. trough bottom divide

Picture 8: The „C" Karren Ground Surface Detail (Totes Gebirge)
Legend: 1. karren inselberg, 2. karren halfinselberg, 3. vertical-sided type I trough, 4. gently slooping-sided type I trough, 5. type III trough, 6. type II trough, 7. karren cavity, 8. terrace, 9. trough bottom divide

Picture 9: The „E" Karren Ground Surface Detail (Totes Gebirge)
Legend: 1. karren kalfinselberg, 2. vertical-sided type I trough, 3. type III trough, 4. kamenitza remain, 5. karren cavity, 6. opening karren trough, 7. trough arch

Picture 10: The "F" Karren Ground Surface Detail (Totes Gebirge)
Legend: 1. loop meander, 2. recess surrounded by meander, 3. karren monadnocks, 4. progressive trough, 5. regressive trough

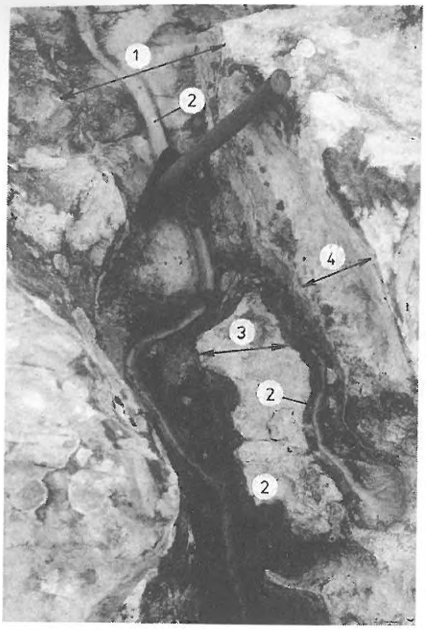

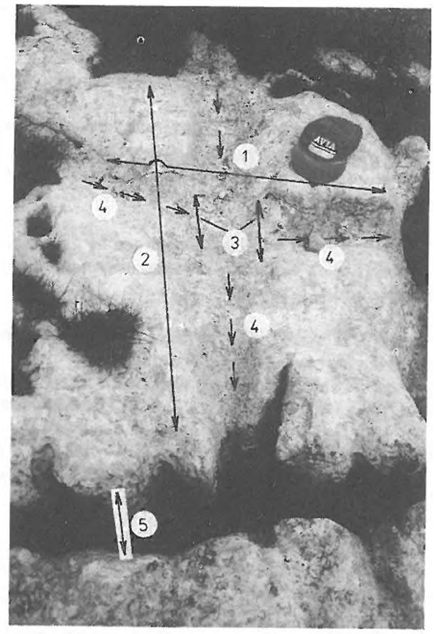

1. | 2.

3.

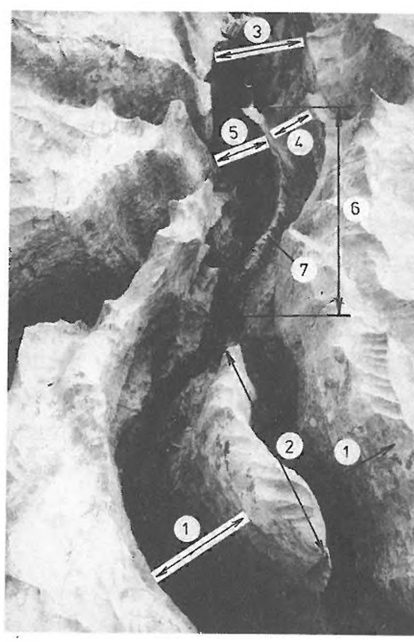

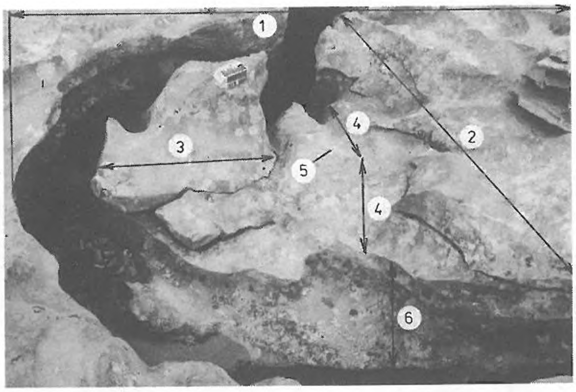

4.

6.

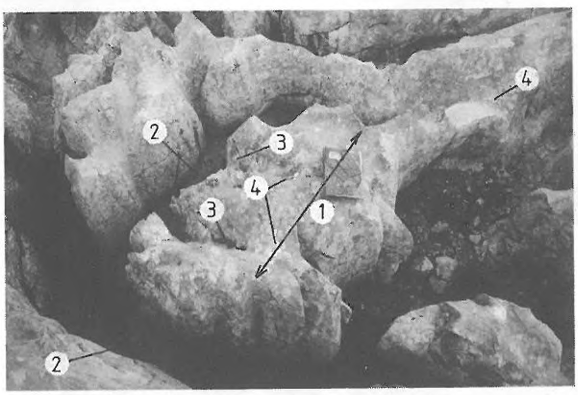

5. | 7.

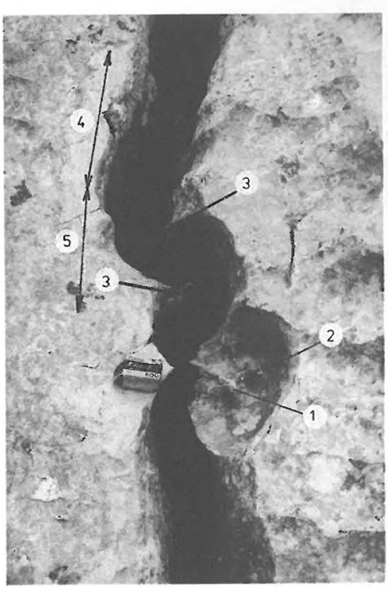

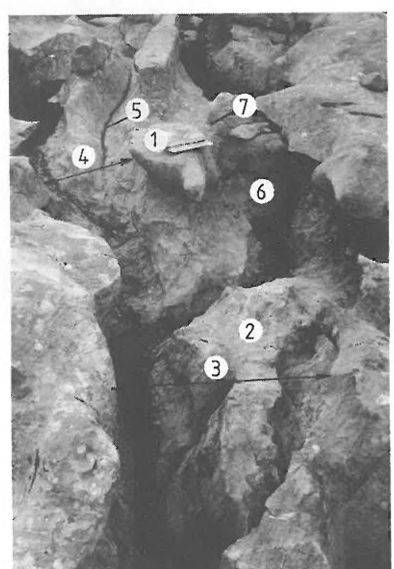

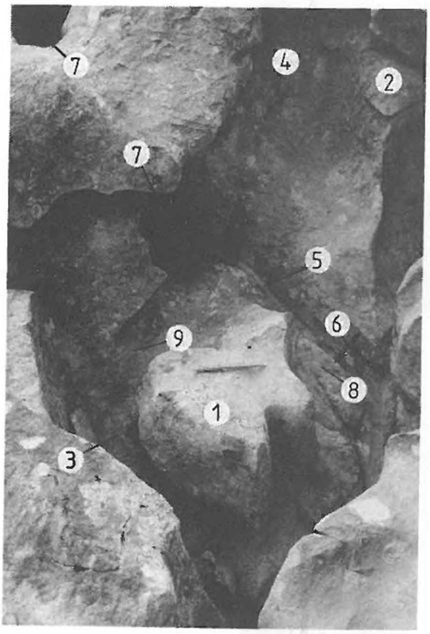

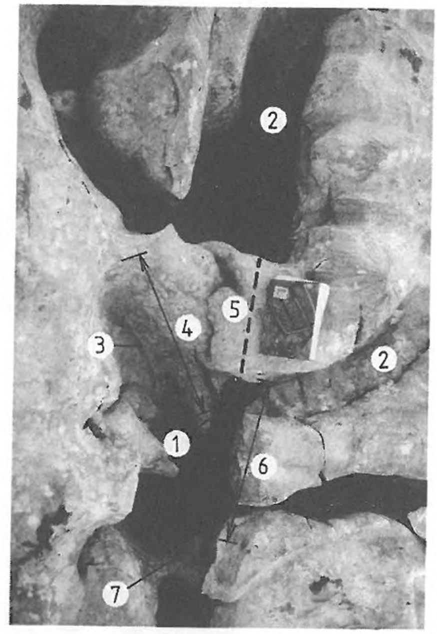

8. | 9.

10.

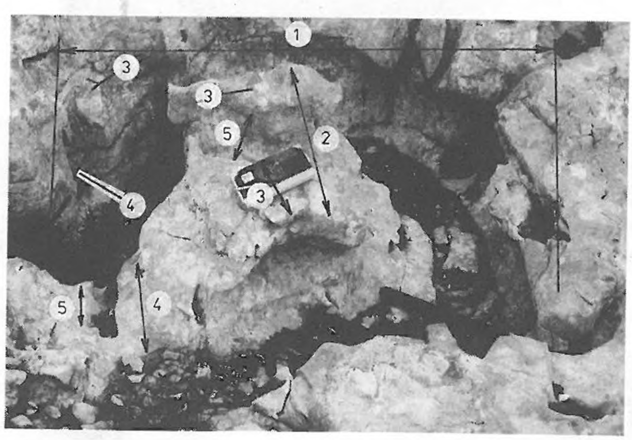

KARSZTFEJLŐDÉS IV.
Szombathely, 2000. pp. 109- 124.

SOME PROPERTIES OF THE ALPINE VERTICAL KARSTIFICATION

PÉTER GRUBER - ERNŐ TAMÁS HORVÁTH - GYÖRGY KOVÁCS - SZILÁRD SOMLAI - LEVENTE SZABÓ - ZOLTÁN ZENTAI
„Berzsenyi Dániel" College, Department of Geography
9700 Szombathely, Károlyi G. tér 4.

Abstract: The paper studies vertical karstic forms that develop in the alpine region below the snow line. Three forms are differentiated by their dimensions: karren micro-forms, meso-forms (vertical shafts) and major forms (characteristic alpine vertical shaft systems). The origin of karren micro- and meso-forms are explained by the solution of the limestone surface as a process akin to the making of the karrenfelds. The origin of the major vertical caves is understood as a different phenomenon. The paper considers these caves a phenomenon corresponding to with the potholes of the Alsó-hegy in Hungary/Slovakia. The paper studies the meso-forms in detail and specifies three types: potholes (vertical caves), channel-end shafts and caved-in shafts. The process of the origin of these phenomena is explained by individual models. The paper suspects a strong relation between the origin of the potholes and the snow accumulated in them. The channel-end shafts are explained by the decapitation of the karren-channels and classifies them as karren-swallets. The origin of the caved-in shafts is explained by more than one ways: the collapse of cavities, the merging of fissures and the weathering of channel-end shafts by freezing.

Introduction

During the karst-research program three sites in the Austrian Totes Mountains and two sites in the Italian Asiago Plateau were studied for vertical karst forms, their morphology, their origin and the frequency of their occurrence. The studies were extended to the relation of other karstic (mostly karren) and non-karstic phenomena. For a comparison studies were carried out on the Hungarian Alsó-hegy plateau.

Description of the Study Areas

I. The studies of 1996 were carried out in the Totes Mountains in Austria on two neighboring sites below the Hint. Bruder and Widerkar peaks on the bottoms and side slopes of glacial valleys at elevations about 1800 m above the sea level on terraced bedding plane surfaces devoid of vegetation or soil. On a 60.000 m^2 area 59 vertical shafts were surveyed.

II. Studies were carried out again in 1997 in the Totes Mountains in the upper part of a one time firn basin in the vicinity of the Scheibling Peak at an elevation of about 1900 m. on stepping big extension bedding plane surfaces devoid of vegetation or soil. On a 12,000 m^2 area 23 vertical shafts were surveyed.

III. The glacier valleys below the Rinner Peak (2012) in the Totes Mountains were studied as well in 1997. The plateau is broken by U shaped glacier valleys that are devoid of vegetation, only dwarf pines and some rock-grasses survive on the steep slopes on exposing narrow terraces of limestone. The glacier progressing down was probably cut in two by the ridge of the Rinner Peak towering as a nunatak. These two branches of the glacier probably joined the major glacier moving in a NNW direction as hanging glaciers. The bottom of this valley is located at about 1600 m of elevation already under the timber-line.

IV. Studies were carried out in the Italian Asiago Plateau in 1998 on two bedding plane sites that were dissected by rises and steps. One of them was elevated at 1900 m, the other at 2060 m. Both study sites were built of Jurassic dolomitic limestone.

V. Studies were carried out in 1999 on the Hungarian part of the Alsó-hegy Plateau visiting the Vecsembükki and Almási Potholes that are located at about 500 m elevation in middle elevation mountain environment.

During these studies sites of different elevation, vegetation and of various geological and geomorphological nature were compared. In spite of the differences in the conditions of origin and in the morphology many similarities can be recognized. The most outstanding in the conditions of origin is the vertical definition that is resulted by the very close fracturing in the alpine sites and by the close to vertical position of the bedding planes in the Alsó-hegy. The morphology of all study areas is characterized by vertically elongated karstic forms. This phenomenon was described in the study of the karstic micro-forms and karrenfelds of the Asiago plateau as well *(VERESS, M. - ZENTAI, Z. - KOVÁCS, GY. 1999).*

The methods of study

During the collection of data a number of varied methods were applied to achieve a many faceted approach to the subject.

The shafts situated in *Site I.* were surveyed and scale 1:100 maps and profiles were drawn. The shafts were classified to types according to their morphology and topography. During classification the following regards were observed:

- the position of the shaft-entrance related to the pre-forming fissures,
- the symmetry conditions of the shaft entrance (regular or elongated),
- the hydrographic situation of the shafts (have individual catchment areas or not),
- the neighborhood of the shafts (presence of soil covering or situated on bare rock),
- the roughness of the shaft-walls,
- the quantity and position of debris,

- the depth of the shafts,
- the number of individual shafts of potholes (complexity)

To describe the topographic distribution and relation to the fractures a scale 1:500 survey map was completed.

The survey of the shafts on *Site II.* was extended only to characteristic types. The classification was made observing identical regards as the ones used in *Site I.* A scale 1:200 survey map was completed about the site.

The catena principle was applied on *Site III.* The survey started at 1950 m of elevation and it was continued to the bottom of a former glacier valley 400 m below recording the parameters of phenomena met along the line (strip). (Length of the openings and the dimension at right angle to it, depth, measure of debris and vegetation covering.) As the alpine slopes are not easily traversed, karstic forms met along the often zigzagging tourist trail were surveyed. On a distance of roughly 2.5 km 253 occurrences were recorded.

A survey was made on *Site IV.* observing the described regards.

On *Site V* surface reconnaissance was carried out and morphological observations were made in two potholes that can be considered representative examples for the area. (Almási- and Vecsembükki-zsomboly).

Vertical karstification and the main types of karst-forms

Observations were made from the moderate climate, medium elevation karst-morphological territory to alpine (below the snow line) sites. Detailed survey was carried out on some contiguous bedding plane surfaces (some as large as 1000 m^2) of glacial/karstic origin. The common nature of these sites was the lack or minor role of vegetation and soil covering, the separation by scarps from the neighboring areas and the great degree karrenfeld development of the land surface. These are individual (autogenic) units of karstification crossed by very numerous fractures.

Three vertical types of karstification were classified on the study area in regards of extension and nature.

1. Micro-size surface and near surface karstification resulting karstic micro-forms, the karren. *VERESS, M.(1995)* classifies surface, linear, subsoil, vertical and subsurface solution. The various types of solution shall be classified to three types of karstification *(VERESS, M. - ZENTAI, Z. - KOVÁCS, GY. 1999)*, that are the following:

- Surface karren development that shall include surface, linear, local and subsoil solution.

- Vertical karren development that is the result of solution along fractures penetrating the rock, where unidirectional (fracture karren), two-direction (network karren) and local solution (pit karren) can be classified.
- The third type of karren development is represented by subsurface solution within the rock mass.

The present study concerns only vertical small forms made by local solution or connecting by solution.

2. Medium scale karstification and the generated karstic meso-forms. The development of these is tightly tied to the processes of surface solution, the karren development. They develop in part during the merging of smaller karren small-forms and in part as an "overgrowing" in size. It is the essence of the process that the simple growth in size changes the nature of the whole process (e.g. accumulation of snow commences) that activate further processes, in cases some hitherto secondary processes are activated. These meso-forms that are related to local solution and merging will be referred to as "shafts".

3. Grand scale karstification that result the typical alpine vertical forms, the major vertical caves. Processes occurring in this group do not resemble the micro- and meso- scale solution processes, the developing forms can not be derived from the processes of karren development.

This paper considers those forms vertical where the depth of the form is bigger than the biggest dimension of the entrance. Considering this the following vertical karst forms were classified:

1.1 Pit karren: An embryonic type of the vertical solution karst forms. A narrow (1-2 m) diameter cylindrical form (*VERESS, M.-PÉNTEK, K.* 1995). Their making is determined by fractures and their depth can be more than 100 m in extreme cases according to *ZÁMBÓ, L.* (1993). In these cases they can make a link between karren-forms and karstic meso-forms (shafts). Their occurrence is linked to the interior of major karstic forms and karrenfelds where they occur in great numbers. Pits developing near to one another can become connected and make a link towards shafts. *Pits becoming shafts:* can not be considered as full identity forms, they are transition between micro- and minor forms. It develops with the solution connection of pit karren.

Karstic mezo-forms can be classified into three categories: potholes (vertical caves), channel-end shafts and caved-in shafts. *COLLIGNON, B.* (1992) classifies these three types as debris type, snowy-bottomed type and potholes (vertical caves). This classification corresponds to the concepts used in this paper but some differences also occur.

2.1 Potholes: Can be identified with *COLLIGNON, B.* (1992)'s pothole concept. The name indicates vertical karst forms that do not have catchment areas, their entrances are round or clover leaf formed, their profile is narrowing (ice-cream cone shaped). Their walls are smooth, there is poor or no debris accumulation. The making of these pits is understood to be the effect of the karst-corrosion by the snow accumulation in them. Potholes in which snow accumulation commences (see later) can be identified with the snowy-bottomed type of potholes described by *COLLIGNON, B.* (1992). *FORD, D.C. -WILLIAMS, P.* (1989) calls the downwards tightening pits solution shafts that also identifies with the "pothole" (Hung. "zsomboly") word used by *VERESS, M. - HORVÁTH, T. - ZENTAI, Z. 1996, HORVÁTH, E. T.-ZENTAI, Z.* (1998).

2.2 Channel-end shafts are those vertical forms that are situated on bare bedding plane surfaces, have catchment areas and are joined by karren channels. These are nothing else than channel-end pits *(VERESS, M. 1995)* turned to "karren swallets" by growing. Their entrances are tight, irregular or plum-stone shaped, the surface of their walls very rugged. Their development is due to the water running down in the karren channels.

2.3 Caved-in shafts: This form can be identified as *COLLIGNON. B.* (1992)'s caved-in pit. These depressions are mostly situated at the edges of blocks and can be characterized by containing big accumulations of breakdown. Their origin can be explained by the way *KESSLER, H.* (1932) did - by the cave-in of cavities or by the secondary transformation of potholes or channel-end shafts by the effects of freezing that produced a big accumulation of debris.

A survey was completed in *Site III.* in a geomorphological environment and altitude different from those hitherto described (glacial valley). Partly as a consequence of the different morphological conditions and party due to the different method of data processing other vertical meso-forms were specified, part of which can be considered as a transition between vertical and horizontal forms or middle elevation forms (like dolines, *SZABÓ, L. 1998*).

2.4. Dolines transforming to pits: Such major well developed dolines (not the typical dolines of the middle elevation karst plateaus as they are different regarding their shapes and genetics) that contain pits and groups of pits merged by solution at their bottoms. Thus instead of surface solution deepening in the zone of pits is dominant.

2.5. Initial shafts: can be considered as a further developed version of 2.4.: The zone of pits is practically digested and a several meter diameter shaft replaces the merged pits with an accumulation of debris at the bottom, the remains of previous pillars.

3.1. Major potholes (vertical caves): Characteristic major alpine karst-forms. They are generally a complicated system of vertical shafts developing beside and below each other frequently reaching down to many hundreds of meters.

(*BÖRCSÖK, P. - GYOVAI, L.* 1984, *KARDOS, L.* 1988, *RYSZARD, K.* 1980, *SEBESZTHA, Z.* 1984). Their morphology and genetics is different of those described before as they are deeper by magnitude and more complex. *JAKUCS, L.* (1971) considers these caves pre-glacial forms that survived the Pleistocene as well as a result of chemical reactions of slowly and deeply percolating sub-nival cold waters. Hinting at their age the opinion of *BALÁZS, D.* (1990) was that the "giant" potholes of the Caucasian Mts. were made by the melt of retreating glaciers and that they were still being shaped by the accumulated snow and ice that they contain. The inner, deeper situated shafts of the major vertical caves frequently peter out as blind shafts at their tops (*BÖRCSÖK, P.-GYOVAI, L* 1985, *LUKÁCS, L.* 1980), the same way as shafts do in the medium elevation potholes in Hungary (*KÓSA, A.* 1963, 1965, 1989, 1992/a,b, *SZENTHE, I.* 1971). Among many, these facts verify our assumption that the development of major alpine caves does not begin starting from the surface but in the depths of the rock independently from surface karren processes. Thus they do not share any genetic relation to the surface micro and meso-forms. According to the observations of the authors the processes of development of potholes of the medium elevation plateau in Hungary show relations with the major alpine vertical caves.

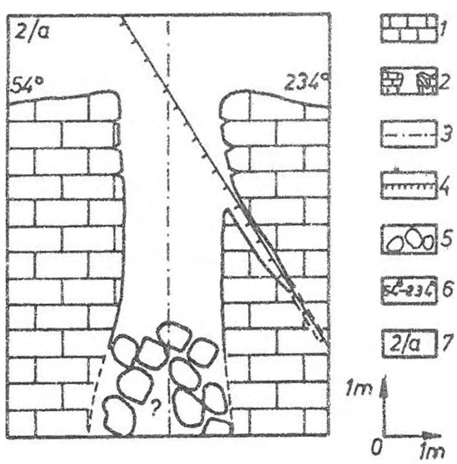

Fig. 1: Vertical section of the type 2/a pothole in the study site of the year 1996.
Legend: 1. limestone, 2. the profile of the pothole, 3. the long axis of the pothole, 4. the plane of the fracture that determines the location of the development. 5. debris (breakdown), 6. direction of the section, 7. identification code of the pothole.

The nature of the vertical meso-forms

Detailed studies were carried out about the vertical meso-forms.

Potholes: are situated at the bottom of glacial valleys and if on the sides of the valley, always on small slope terraces. On the sides of residual peaks and crests potholes were not found. More than one explanations seem to fit the phenomenon:

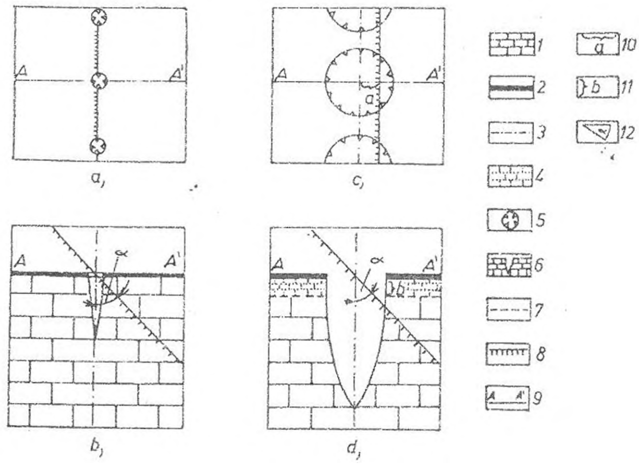

Fig. 2: A result of surface denudation by solution the long axis and the fissure line are shifted from each other (from the angle of the fracture plane to the vertical and the distance of the two lines the measure of denudation of the surface can be calculated since the time of origin of the shaft).
Legend: a, plan view of the site in the initial stage of development; b, A-Á direction section in the initial stage of development; c, plan view of the site in the advanced stage of development; d, A-Á direction section in the advanced stage of development.
1. limestone, 2. original ground surface, 3. long axis of the shaft, 4. rock mass removed by dissolution, 5. plan view of the shafts, 6. side view of the shafts, 7. new ground surface created by the removal of the original rock mass, 8. plane of fissure, 9. direction of the section, 10. distance of the long axis of the shaft and the intersection of the original fracture with the surface after denudation. 11. the measure of surface denudation, 12. the angle of the fracture plane to the vertical.

— Valleys were existing before the periods of glaciation and karstification was most intensive at the valley bottoms. This process prepared and promoted the terrain for present karstification.
— At the time of the retreating of the ice melt-waters infiltrated in the valley bottoms assigning the present locations of solution.
— The process of karstification is present everywhere but its traces are masked by intensive generation of debris on steep valley slopes.
— On terrain of small gradient vegetation is able to proliferate and soils develop generating concentrated solution.
— The axes of valleys are identical with the main tectonic directions as it is known from references *(KÓSA, A. 1967, 1992/b, ELEKES, B.-NYERGES, M.-ROSE, GY. 1992)*, and as it was verified by site studies. This is the cause of the most effective vertical solution.

According to the present knowledge of the authors probably more than one of the listed processes were effective simultaneously or in sequence. The shafts are situated along the fracture lines like beads on a necklace. Their entrances are always traversed by the fracture. The axis of the shafts is almost vertical (the "axis" is understood as the line drawn between the crossing point of the smallest and biggest dimension of the entrance to the deepest point of the shaft) but the angle of the fracture to the vertical varies. It can be seen that the vertical development of the shafts does not definitively follow the plane of the fissure (*Fig. 1*). This conclusion proves that the development of these shafts starts on the surface (at the intersection of the ground surface and the fissure) towards the inside of the rock body. In any other case the intersecting of the entrance and the fissure were not so regular. In cases when the long axis and the fissure line are not identical, possibly the two lines shifted from each other as a result of surface denudation by solution. Regarding this in the knowledge of the angle of the fracture plane to the vertical (α) and the distance of the two lines the measure of denudation (*a*) of the surface can be calculated (denudation by solution = $\boldsymbol{a \times ctg\ \alpha}$) since the time of origin of the shaft (*Fig. 2*).

The depth of the studied karst-forms does not exceed 50 m, they consist of a single shaft. As they develop as the enlargement of primary fracture lines (*VERESS, M. - PÉNTEK, K. 1995*) starting at the surface (*VERESS, M.-HORVÁTH, E.T.-ZENTAI, Z. 1996*) they show a close genetic relation to karren development. That's why these forms shall be differentiated from the many hundreds of meters deep complex alpine vertical caves.

The snow accumulated in the pothole-type meso-forms is thought to have a significant role in their development. Based on this opinion four phases in the development of the potholes can be classified *(HORVÁTH, E.T.-ZENTAI, Z. 1998):*

I. The processes in the first phase are the same as described by *VERESS, M - PÉNTEK, K. (1995)*, that is: unsaturated water percolating on the walls of the fracture dissolves the material of the wall and the fissure is enlarged. A karstic micro-form, the crack karren *(PLUHAR A.-FORD D.1970, ZÁMBÓ L. 1993*) or fracture karren *(ZÁMBÓ, L. 1993)* is resulted by the process. The development of the majority of the fractures terminates at this phase (*Fig. 3/a*).

II. Only those forms get into the second stage that deepen quickly enough to keep pace with the widening of the fracture. The condition of this is the occurrence of solution in single points. This can happen in the crossing points of joints or some other lithological, hydrological or other reasons, at the "zones of weaknesses".

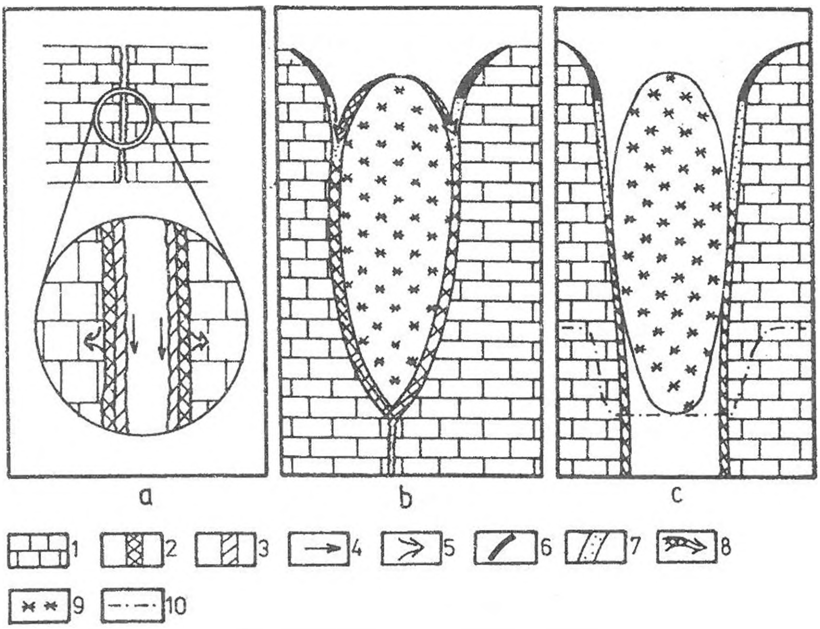

Fig. 3: Stages of development of a pothole.
Legend: a, first stage (after VERESS, M - PÉMTEK, K. 1995) widening of the primary fractures, development of fracture karren; b, second stage, snow accumulation; c, third stage, stabilized deepening after the reaching of the 0°C isotherm. 1. limestone, 2. saturated solvent, 3. unsaturated solvent, 4. direction of the flow of the solvent, 5. direction of the solution enlargement, 6. inactive zone, 7. zone of condensed water solution, 8. direction of the flow of snow melt, 9. snow, 10. maximal depth of frost penetration.

The accumulation of snow begins in the young initial shafts in this phase of development. The accumulating and compacting snow melt dissolves and deepens the shaft. During the annual period this season is the most intensive period of shaft development. After the melting of the snow the shafts (that have no catchment areas) get into a state of inactivity. The deeper, the more developed is the shaft, the longer the melting of the snow takes and the active period of shaft development elongates. For the volume of the shaft increases, not only the active period elongates but the absolute volume of the solvent increases as well. Thus a self-generating process commences in this period (*Fig 3/b*).

III. Phase No. three is not sharply different from phase II. It's the only difference that the accumulated snow would stay all around the year in the shaft. The snow accumulating in the shaft can completely fill it and spring thaw will produce water that makes a water film on the walls. The rock warms more easily than the filling snow and a gap originates between the walls and the mass of snow. The melt-water can dissolve only those parts of the wall where the snow and the rock touch. This section will be positioned ever deeper during the summer thaw. Consequently the bottom of the shaft will remain active all the time in the summer season while the upper levels

are inactivated. Where gaps develop between the walls and the snow mass the melt-water corrosion stops. Condensed-water corrosion may commence as the humid air saturates because of the cooling effect of the snow and water condenses on the rock walls. The condensed water dissolves the rock surface, the wall becomes smooth. When the radius of the shaft exceeds a certain measure, the water film disintegrates (*VERESS, M. - PÉNTEK, K.* 1995) and clover leaf cross section shafts may develop.
IV. In the fourth phase of the development the deepening of the shafts stabilizes. This is caused by the equalization of the temperature below a certain depth where the temperature does not drop below 0°C, consequently no snow can be accumulated below the 0°C isotherm. Thus the accumulation of the snow is restricted to a zone close to the entrance. The shaft that reaches this depth can store the same volume of snow from year to year. It can not be excluded in the case of these shafts that the "snow plug" is melted in the winter season caused by upsurging warmer air. Thus these shafts can remain active in the wintertime and deepen (*Fig. 3/c*).
Surface runoff can temporarily enter the potholes, melt-water running on the snow surface can get into the shafts thus the potholes may have seasonal catchment areas. According to this two types of forms, the potholes and the channel-end pits may not be sharply differentiated, transitional forms may develop.
Channel-end pits develop on rocky slopes devoid of soil covering where the karren channels are crossed by fracture lines. At these locations water piracy occurs. During this process the linear surface solution turns to be vertical at the points of the piracy. On these locations vertical karren forms, pit-karren, channel-end pits (*VERESS, M.* 1995) develop. The cavities gradually widen and neighboring pits merge. At the points of the merging the thin terrain between the runnels remain as thin crests and can even make 0.5-1,0 m wide blades in the retreating pit walls making the walls extremely rugged. The channels emptying to the pits make the catchment area of the pits. These catchment areas are not more extensive than several times 10 m^2. The size of the catchment areas influences the depth of the pits. Their entrances are generally narrow quickly narrowing with depth. Their development is due to the effect of percolating melt-waters. They can be regarded as karren-swallets (*Fig. 4*).

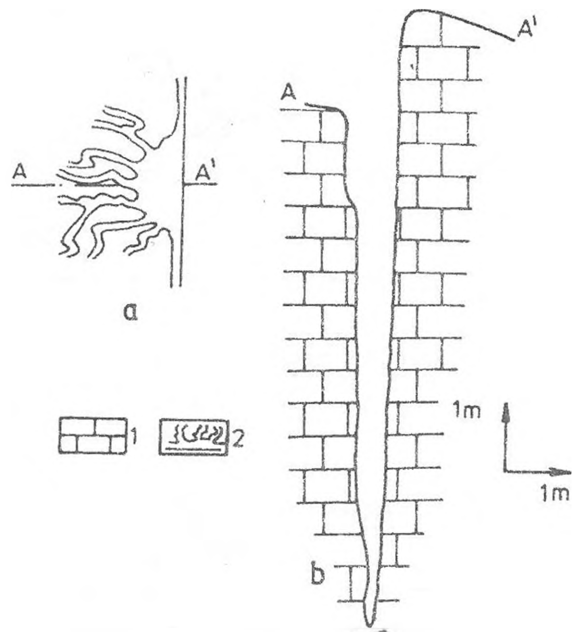

Fig. 4: Channel-end pit in the study site of the year 1996.
Legend: a: plan view, b: section,1. limestone, 2. karren channel system.

Caved-in shafts: can be of varied genetic origin.

— Caved-in shafts can develop as described by *KESSLER, H. (1932)* by the gradual cave-in of subsurface cavities or passages. According the observations of the authors if shafts of such origin are connected to extensive subsurface systems the accumulation of debris can be excessive. Explanation can be found in the great discharge of mild, humid air masses from the major cave system. The moisture in the mild air condenses to ice near the surface in the creases of the rock with much cracking force.

— Caved-in shafts can develop with the merging of fissures *(GRUBER, P.-KOVÁCS, GY.-SOMLAI, SZ. 1998)*. Fissures can develop at fractures, cracks or the planes of changing rock quality. A central role is played in the process by dissolution. Two zones of dissolution can be differentiated: the intensive and the slow zones. The intensive zones are situated at fracture- and bedding planes. Dissolution is quick here because the recharge of the solvent is quick and the process is directional. The zone of slow dissolution is the fresh rock itself that makes the shaft walls. Fractures can merge at the bedding planes if they occur frequently enough. The remnants of partition walls may collapse. The debris can break up even more by dissolution or freezing. This way large quantities of debris can be deposited in the bottoms of the merged fissure shafts.

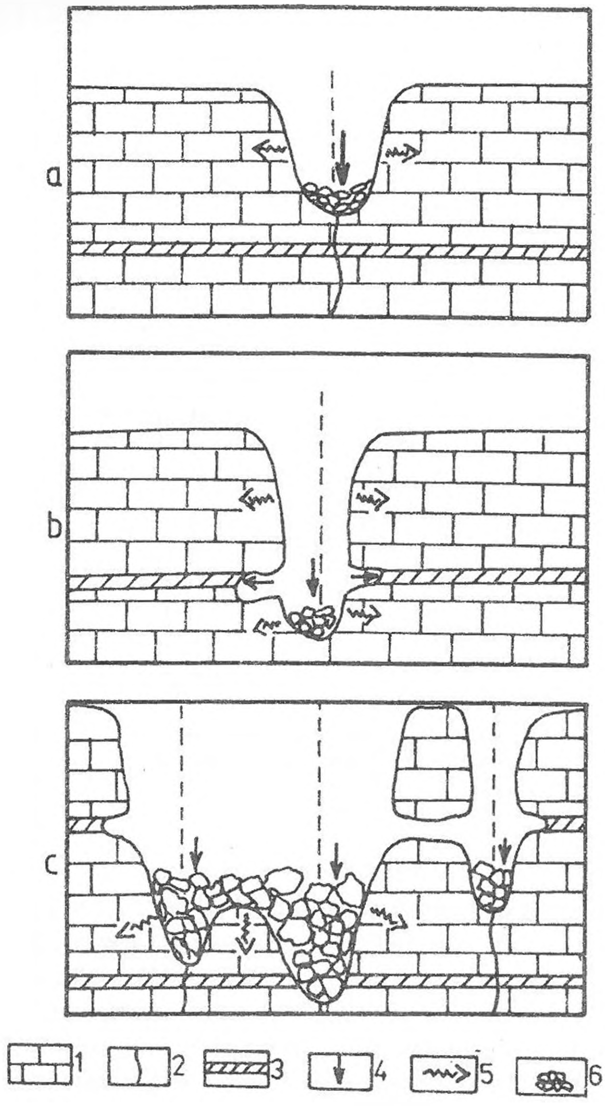

Fig. 5: The development of a caved-in shaft caused by the merging of fractures.
Legend: a. deepening along fractures, b. dissolution along bedding planes, c. merging. 1. limestone, 2. fracture, 3. bedding plane, 4. zone of intensive dissolution, 5. zone of slow dissolution, 6. breakdown.

— Caved-in shafts can develop a secondary way too when channel-end pits or potholes are transformed by frost breaking up. During the process the original forms are destroyed. The studies show that such ruining occur more frequently in the potholes than in channel-end pits. This can be explained by the continual retreating of the walls in the channel-end pits caused by the water running in the channels and always new wall surfaces are exposed by dissolution. This way the ruining of the channel-end pits occurs only when the pit looses its catchment area due to some external reason (e.g. the

transformation of the karren environment). This phenomenon can occur partially, on one side the pit wall retreats continually while the other side of the pit looses its catchment area and braking up by frost can freely occur.
The debris in the pits can be originated by frost braking up and from solution. The merging of caved-in shafts can result in large depressions filled with debris. An important cause of the pit development can be their snow fill (*HORVÁTH E. T.-ZENTAI Z.* 1998).

Morphogenetic conclusions

During the survey of pits and shafts the horizontal width and length of the entrances were measured. The following conclusions can be made. The entrance of the caved-in shafts is generally larger than that of the channel-end pits.

Table I. Average dimensions of the entrances of different types of vertical forms

type of pits	width Site No. I.	length Site No. I.	width Site No. II.	length Site No. II.
caved-in type	6.5 m	14 m	6.2 m	9.8 m
channel-end type	2.1 m	4.3 m	2.1 m	5.5 m
pothole type	-	-	4 m	6 m

The two dimensions of the entrance of the pits measured at right angles characterizes the elongation of the entrance. If the ratio of the length and width is bigger than 2, the entrance of the shaft was considered elongated. The majority of the ratio of elongation of the entrances was more than 2.

Table II. The percentage of the occurrences of elongation of more than 2 on study sites I. and II.

type of pits	Site No I.	Site No. II.	average of Sites I. and II.
caved-in type	60 %	69 %	64.5 %
channel-end type	68 %	100 %	84 %

It is suggested that the depth of the pits is proportional with their age, that is: the shallow pits are younger, the deep ones are older. The length/width data hint at the way of development of the channel-end pits. The ratio of the cross section of pits of various depth varies around 2 indicating that the pace of the growth in length and width is approximately constant during the process of development.
The development of the less elongated pit shape can be caused by more than one causes that can be the following:

— The pit develops at the intersection of fractures crossing at right angle. In this case the development happens at the same pace in all directions.

— The surrounding terrain slopes toward the pit at all sides and the preparing fracture is not very well developed. In this case karren channels join the pit at all sides. The development of all karren channels at similar pace results that the catchment area of the pit develops at similar pace in all directions. This way the pit receives similar quantities of solvent from all sides and resulting the retreat of the pit walls at equal pace.

The relation of the depth and entrances of the pits were studied. Studies of this kind were carried out by *SÁRVÁRY, I.* (1970) in the potholes of the Alsó-hegy. The width of the caved-in shafts does not change much with the increasing of the depth while the length of the entrance grows considerably. The entrances of the small depth thus small entrance shafts don't show elongation. On the contrary, the shafts of big depth will be elongated as the width of the entrance remained almost the same but its length greatly increased.

In channel-end pits both entrance dimensions increase in the function of depth and elongation with greater depth is not detectable.

SUMMARY

The paper studies alpine vertical karstic forms. Three forms were differentiated by their dimensions and origin: micro or vertical karren development, meso-forms or the development of vertical shafts and major karstification. The meso-forms were studied in detail. Vertical caves lacking catchment areas but developed by snow accumulations in their interior were classified as "potholes". Karren swallets that are resulted by overgrowing pit karren were classified as "channel-end pits". "Cave-in shafts" were understood as the final product of more than one independent processes.

It was deducted that the studied karstic meso-forms were closely related to surface karren development, they are the products of karren development wholly or in part. As the development of these forms is related to surface karren development, their age can be equal or less than that of the karren. This conclusion puts their age to the time period to the retreating of glacial ice at the end of the Pleistocene.

As a consequence close relation was found between the studied meso-forms and the vertical karren forms. The development of the vertical macro-forms, the major vertical caves can not be explained by the described processes. Their origin and development is different from the above described processes. Their development is independent of surface karren development probably their age is considerably more. The development of the potholes

(vertical caves) of the Alsó-hegy Plateau in Hungary was related to the vertical alpine caves.

REFERENCES

BALÁZS, D. (1990): Arabika és Bzib, a mélyzsombolyok birodalma - Karszt és Barlang, I. kötet. p. 63-65.
BÖRCSÖK, P.-GYOVAI, L.(1984): "Jugoszlávia '84" Brezno pri Gamsovi Glavici -Mamet -Ponorna Bunovcu - Karszt és Barlang, II. köt. p. 109-111.
BÖRCSÖK, P.-GYOVAI, L.(1985): A Jubileum-barlang bejárása -Karszt és Barlang, I-II. köt. p. 53-55.
COLLIGNON, B. (1992.): Il manuale di speleologia. - Zanichelli.
ELEKES, B.-NYERGES, M.-ROSE, GY. (1992): A Szabópallagi-zsomboly (Baglyok Szakadéka) kutatásának újabb eredményei - Karszt és Barlang p. 3-8.
FORD, D.C. - WILLIAMS, P. (1989.): Karst Geomorphology and Hydrology - London, Academic Press
GRUBER, P.-KOVÁCS, GY.-SOMLAI, SZ. (1998): Vertikális karsztformák vizsgálata az ausztriai Totes Gebirgében - Karsztfejlődés II. (Totes Gebirge karrjai). BDTF Természetföldrajzi Tanszék, Szombathely, p.201-210.
HORVÁTH, E. T.-ZENTAI, Z. (1998): Újabb adalékok a magashegységi vertikális karsztformák morfogenetikájához. - Karsztfejlődés II. (Totes Gebirge karrjai). BDTF Természetföldrajzi Tanszék, Szombathely, p. 191-200.
JAKUCS, L.(1971): A karsztok morfogenetikája -Akadémiai Kiadó, Budapest, p. 280.
KARDOS, L.(1988): Franciaország legmélyebb barlangjaiban -Karszt és Barlang, I. köt. p. 53-56.
KESSLER, H.(1932): A zsombolyok keletkezéséről -Barlangvilág, II. köt. 3-4. füzet, p. 20-22.
KÓSA, A .(1963): A szögligeti Rejtek-zsomboly -Karszt és Barlang, II. köt. p. 66-70.
KÓSA, A.(1965): A kettős zsomboly -Karszt és Barlang, I. köt. p. 17-18.
KÓSA, A. (1967): Az alsó-hegyi zsombolyok tektonikájának statisztikai vizsgálata - Karszt és Barlang p. 37-39.
KÓSA, A.(1989): A Type of Vertical Cave Considered as a "Very Deep Karrenfeld" -Procedings of the International Congres of Speleology, I. köt. p. 109-111.
KÓSA, A.(1992/a): Alsó-hegyi zsombolyatlasz, Atlas propasti Dolného Vrchu, Alsó-hegy /Dolny Vrch Pothole Atlas - Budapest, p.145.

KÓSA, A (1992/b): Nyolcvan év az Alsó-hegyen (Még egy szó a zsombolyokról) - Karszt és Barlang, p. 9-14.
LUKÁCS, L.(1980): A Jubileum-barlang - Karszt és Barlang, II. köt. p. 107-108.
RYSZARD, K.(1980): A világ legmélyebb barlangja - Karszt és Barlang, II. köt. p. 112.
SÁRVÁRY, I. (1970): A zsombolygenetika kérdéseiről - Karszt és barlang I. p. 5 - 12.
SEBESZTHA, Z.(1984): A Wielka Sniezna bejárása - Karszt és Barlang, II. köt. p. 108-109.
SZABÓ, L (1998): Karsztos mélyedések morfometriai vizsgálata a Totes-gebirgében. - Karsztfejlődés II. (Totes Gebirge karrjai). BDTF Természetföldrajzi Tanszék, Szombathely, p.169-190.
SZENTH,E I.(1971): Vizföldtani vizsgálatok a Vecsembüki-zsombolyban - Karszt és Barlang, II. köt. p. 57-60.
ZÁMBÓ, L. (1993.): A karsztosodó kőzet alaktana (karsztgeomorfológia) in: Általános Természetföldrajz (szerk.: Borsy Z.) Nemzeti Tankönyvkiadó, Budapest
VERESS, M.(1995): Karros folyamatok és formák rendszerezése Totes Gebirge-i példák alapján - Karsztfejlődés I. (Totes Gebirge karrjai), szerk. Veress M. Pauz Kiadó, Szombathely p.7-30.
VERESS, M. - PÉNTEK, K. (1995.): Kísérlet a felszíni vertikális karsztosodás kvantitatív leírására - Földrajzi Értesítő XLIV. 3.-4. p. 157.-177.
VERESS, M. - HORVÁTH, T. - ZENTAI, Z. (1996.): Egy magasehgységi karsztterület vertikális formáinak vizsgálata - BDTF Tudományos Közleményei X. Természettudományok 5., p. 141. - 157.
VERESS, M.- ZENTAI, Z.- KOVÁCS, GY. (1999): A horizontális és a vertikális karrosodás összehasonlítása az asiagoi-fennsíkon.

KARSZTFEJLŐDÉS IV.
Szombathely, 2000. pp. 125-150.

THE THEORETICAL-PHYSICAL STUDY OF THE PROCESS OF KARREN DEVELOPMENT

GÁBOR SZUNYOGH
"Berzsenyi Dániel" College, Department of Physics
9700 Szombathely, Károlyi G. tér 4.

Abstract: the results of a theoretical-physical study of the process of karren development is presented in this paper. Referring to former studies the equation system of the karstification of a sloping limestone terrain without pit formation is written considering the hydrodynamic, chemical and morphological rules of the karstification processes of a limestone rock surface. The differential geometric correlations that are necessary for the mathematical description of rock surfaces that change their shape in time are determined and the quantitative relations of physicochemical processes influencing the changes of their parameters in time are described. The basically sought for function will be the z(x,y,t) one that determines the shape of the karstified ground surface, but that demands the computation of the flow rate of the water flowing on the limestone surface as well as the calcium carbonate concentration in the water and the thickness of the liquid film. The computer solution of the algorithm of the derived partial differential equation is also presented.

Preliminaries

The Karst Research Group of the "Berzsenyi Dániel" College, Department of Geography published the general equation system of the karstification of an exposed limestone ground surface not covered by soil (*SZUNYOGH, G.* 1994). The "ultimate target" of this equation system was

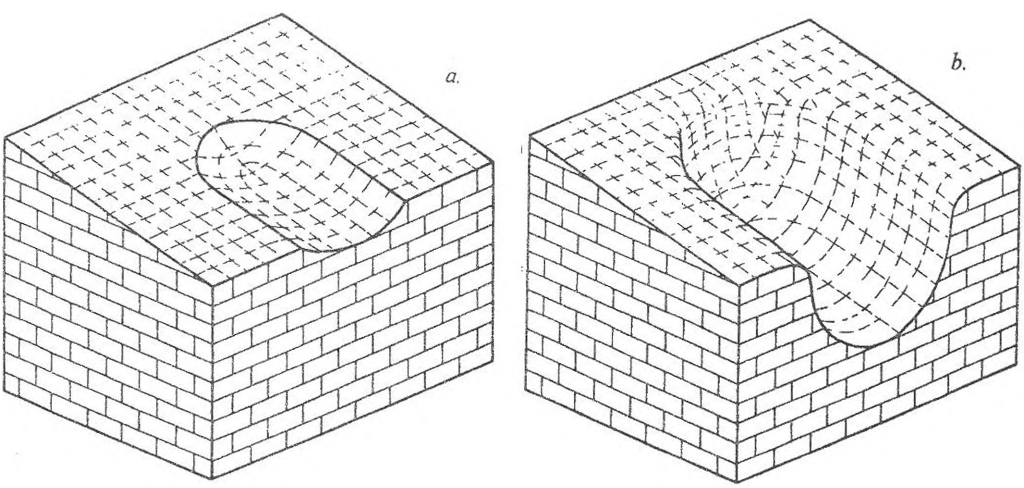

Fig. 1, a: the initial shape at the t_0 moment of the studied limestone surface uncovered by soil, b: the shape of the same limestone surface changed by karst corrosion in a later t moment (in the knowledge of the relevant physical, chemical and geological principles as well as the necessary preliminary and boundary conditions) to develop theoretically the mathematical determination of the future shape of a limestone surface that has been known at the beginning thus to support the principles of classic karst morphology (*JAKUCS, L.* 1971) in a physicochemical way (*Fig. 1*). This mathematical modeling apparently does not substitute but only adds to classic karst morphological studies enabling the checking of hypotheses (based on physicochemical principles) that are very slow processes that can not be studied by tests like the forecast of the looks of a rocky surface after a number of centuries or millennia; the study of karstification processes at conditions (hydrological, climatological etc.) that aren't there to study at the present; the forecast and quantitative study of global changes of the environment and such.

To achieve these a partial differential equation in several variables was written of which the solution is an $F(\mathbf{r})$ function that determines at what t time will the rock surface ever changed by solution pass the point in space that is characterized by the $\mathbf{r}$ position vector. The limestone surface is sought for in the form of:

$$t = F(\mathbf{r}) \qquad (1)$$

It can be derived (*SZUNYOGH, G.* 1995a) that the $\mathbf{w}$ velocity vector of the displacement (denudation) [m/s] is

$$\mathbf{w} = \frac{\mathbf{n}}{|\mathrm{grad}\, F|}, \qquad (2)$$

where $\mathbf{n}$ is the unit vector perpendicular at the rock surface (the normal of the limestone surface)

It can be computed from the measure of denudation what volume of limestone was removed from a unit surface area in unit time, thus the so called q_k mass-flux density of the limestone [kg/m^{2}s] can be expressed:

$$q_k = -\rho_k \mathbf{w} \cdot \mathbf{n}, \qquad (3)$$

where the ρ_k is the density of the limestone [kg/m^3].

Starting from the mass conservation principle it can be proved that the

$$\mathbf{v} \cdot \mathrm{grad}\, c = \frac{q_k}{h} + \frac{c}{\rho_V h} \mathbf{q}_v \mathbf{n} \qquad (4)$$

relation exists between mass-flux density of the removed limestone and the concentration of calcium carbonate in the water, where $\mathbf{v}$ is the velocity of the water flow on the limestone surface [m/s], h is the thickness of the liquid layer [m] and q_v the rainfall that replenishes the solvent, or the volume of rainfall on a unit area in unit time [kg/m^2s].

The velocity of the water flow v is determined by the gravity and the friction force (through the g gravity and η viscosity factor), that derived from the Navier-Stokes formula (*FRANK, Ph.—MIESES, R.* 1967):

$$\mathbf{v} = \frac{\rho_V h^2}{3\eta}\left[\mathbf{g} - (\mathbf{g}\cdot\mathbf{n})\mathbf{n}\right]. \tag{5}$$

The mass conservation principle is valid for the water alone too that derived from the equation of continuity takes the form:

$$\oiint_{(A)} (\rho_v \mathbf{v} - \mathbf{q}_v)\, d\mathbf{A} = 0 \tag{6}$$

where A is a closed surface of a specified static volume in the water film, p_v the density of the water (kg/m^3).

The last equation of the dissolution reflects the chemical principles of karst development expressing that the more limestone is turned into solution as the water is more aggressive, that is, the more is the difference between the maximal measure of solubility and the calcium carbonate that is actually in the solution:

$$q_k = k(c_e - c). \tag{7}$$

where k is the constant of the reaction velocity of the dissolution [m/s] (*DREYBROT, W.* 1988).

The (2)-(7) equation system is general in the sense that its validity is independent of the choice of a coordinate system thus it can be flexibly fitted to the system of coordinates that is most suitable to the geometry of the modeled karstic phenomenon. This generality comes together with some disadvantage: the published equations (in their original form) are not suitable for the solution of any specific problem, but first they have to be adjusted to some coordinate system fit to the specific task.

In the present paper this adjustment will be done to the Cartesian coordinate system, because that's the one most fit to the mathematical analysis of the karstic processes occurring on alpine limestone surfaces.

The Equation System of the Dissolution of Open Limestone Surface with the Application of Cartesian coordinate system

For the specification in space of the limestone surface such an orthogonal coordinate system shall be applied that has horizontal x and y axes and an upwards pointing z axis. (*Fig. 2*).

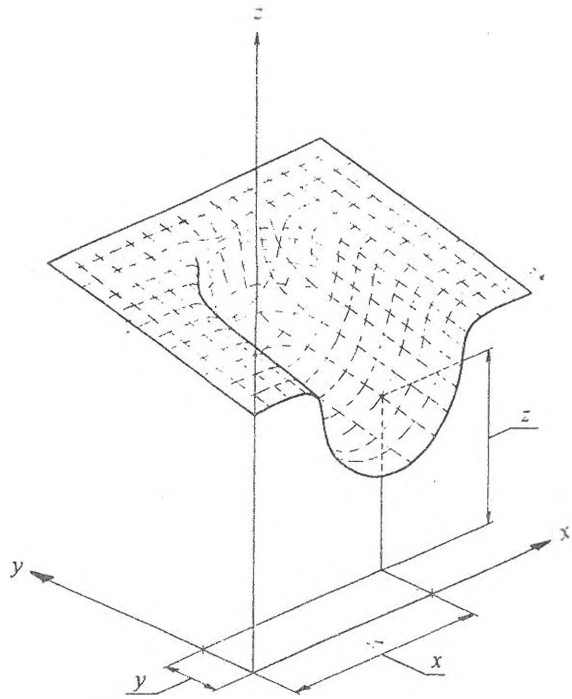

Fig. 2: The position of the coordinate system that describes the location of the limestone surface at any moment

All the unknowns in the (2)-(7) equation are the functions of x and y space coordinates and t time. The determination of these functions is aimed at, the seeking of a

$$z = f(x,y,t) \tag{8}$$

function that is the mathematical specification of the limestone surface.

The Normal Vector of the Limestone Surface in the Cartesian Coordinate System

As the normal of the limestone surface occurs more than once in the described equation aystem first **n** shall be determined as the derivative of the *z(x,y,t)* function that determines the surface (*Fig. 3*). The gradient in the x direction will be α, at y it will be β. For the components of the normal vector: n_x, n_y and n_z (*Fig. 4*) it can be written:

$$n_x = -n_z \operatorname{tg} \alpha, \tag{9}$$

$$n_y = -n_z \operatorname{tg} \beta, \tag{10}$$

and

$$n_x^2 + n_y^2 + n_z^2 = 1. \tag{11}$$

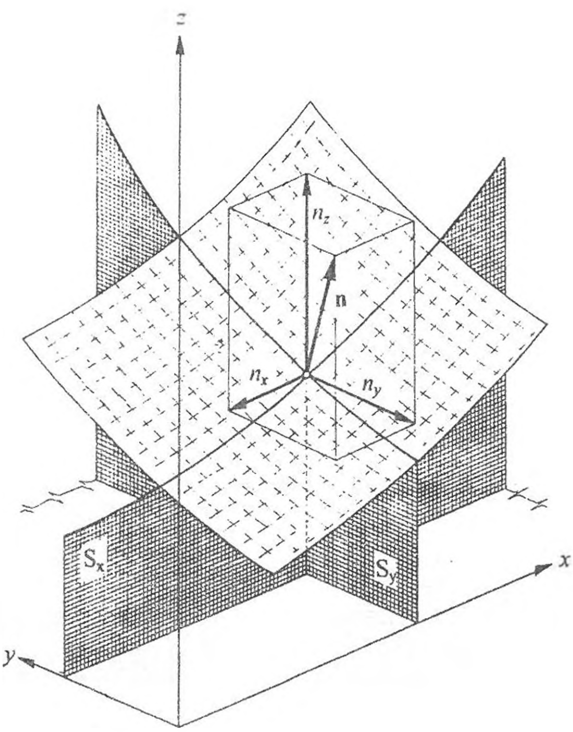

Fig. 3: The position of the so called normal vector that is at right angle at the rock surface and its resolution to components

The tgα and tgβ quantities will be equal with the gradient of the limestone surface in the x and y directions so they can be expressed by the partial derivatives of the function determining the rock surface:

$$\mathrm{tg}\,\alpha=\frac{\partial z}{\partial x}, \tag{12}$$

$$\mathrm{tg}\beta=\frac{\partial z}{\partial y}. \tag{13}$$

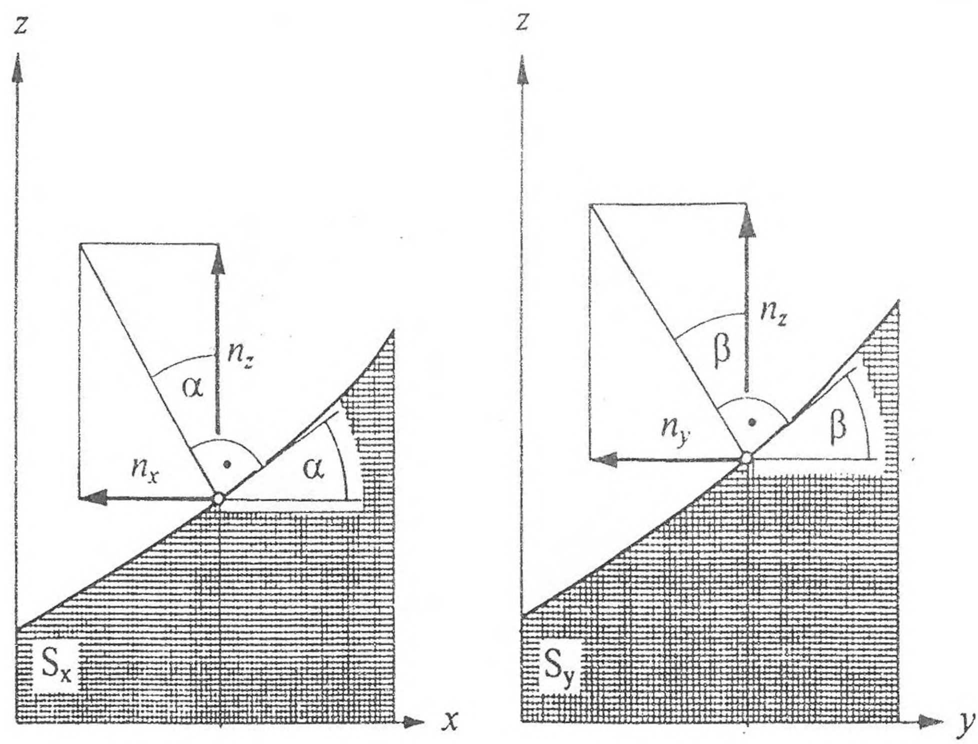

Fig. 4: The n_x, n_y and n_z components of the normal vector of the rock surface drawn in the S_x and S_y plane sections as showed in Fig. 3

The solutions of the (9)—(13) equations regarding n_x, n_y and n_z are:

$$n_x = \frac{-\dfrac{\partial z}{\partial x}}{\sqrt{\left(\dfrac{\partial z}{\partial x}\right)^2 + \left(\dfrac{\partial z}{\partial y}\right)^2 + 1}}, \tag{14}$$

$$n_y = \frac{-\dfrac{\partial z}{\partial y}}{\sqrt{\left(\dfrac{\partial z}{\partial x}\right)^2 + \left(\dfrac{\partial z}{\partial y}\right)^2 + 1}}, \tag{15}$$

and

$$n_z = \frac{1}{\sqrt{\left(\dfrac{\partial z}{\partial x}\right)^2 + \left(\dfrac{\partial z}{\partial y}\right)^2 + 1}}. \tag{16}$$

The (14)—(16) equations enable the calculation of the components in the Cartesian coordinate system of the unit vector perpendicular at the rock surface in the knowledge of the equation of the surface.

The Velocity of the Denudation of the Surface

As a result of karst corrosion the rock surface is shifting, sinking very slowly but continuously with a **w** velocity. The **w** is understood as the thickness of the surface layer that is removed by solution in unit time. Its direction is at right angle to the rock surface and it points to the interior of the fresh limestone (*Fig. 5*).

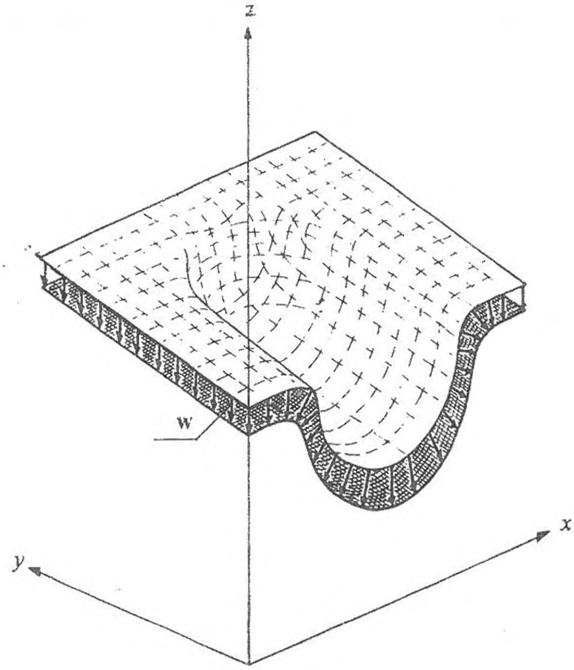

Fig. 5: The specification of the velocity vector of denudation

Writing the gradient expression in the formula of w to a coordinate form the

$$\frac{1}{|\operatorname{grad} F|}=\frac{1}{\sqrt{\left(\frac{\partial t}{\partial x}\right)^2+\left(\frac{\partial t}{\partial y}\right)^2+\left(\frac{\partial t}{\partial z}\right)^2}} \tag{17}$$

function is received that considering the rules of derivation of inverse functions can be transformed:

$$\frac{1}{|\operatorname{grad} F|}=\frac{\frac{\partial z}{\partial t}}{\sqrt{\left(\frac{\partial z}{\partial x}\right)^2+\left(\frac{\partial z}{\partial y}\right)^2+1}} \tag{18}$$

According to (2) for the determination of w (18) shall be multiplied with the normal of the surface that considering (14)—(16) produces the equations:

$$w_x = \frac{-\dfrac{\partial z}{\partial t}\dfrac{\partial z}{\partial x}}{\left(\dfrac{\partial z}{\partial x}\right)^2 + \left(\dfrac{\partial z}{\partial y}\right)^2 + 1}, \tag{19}$$

$$w_y = \frac{-\dfrac{\partial z}{\partial t}\dfrac{\partial z}{\partial y}}{\left(\dfrac{\partial z}{\partial x}\right)^2 + \left(\dfrac{\partial z}{\partial y}\right)^2 + 1}, \tag{20}$$

and

$$w_z = \frac{\dfrac{\partial z}{\partial t}}{\left(\dfrac{\partial z}{\partial x}\right)^2 + \left(\dfrac{\partial z}{\partial y}\right)^2 + 1} \tag{21}$$

The absolute value of the velocity will be

$$|\mathbf{w}| = \sqrt{w_x^2 + w_y^2 + w_z^2}\,. \tag{22}$$

that after the execution of the assigned operations take the form:

$$|\mathbf{w}| = \frac{\left|\dfrac{\partial z}{\partial t}\right|}{\sqrt{\left(\dfrac{\partial z}{\partial x}\right)^2 + \left(\dfrac{\partial z}{\partial y}\right)^2 + 1}}\,. \tag{23}$$

The Mass-Flux Density of the Dissolving Rock

The expression (3) for the mass-flux density considering the (14)—(15) and (20)—(22) expressions and after the scalar composition and ordering equation (3) gets into the form:

$$q_k = -\rho_\kappa \frac{\dfrac{\partial z}{\partial t}}{\sqrt{\left(\dfrac{\partial z}{\partial x}\right)^2 + \left(\dfrac{\partial z}{\partial y}\right)^2 + 1}} \tag{24}$$

It is apparent from equation (24) that when the rock is denuding $q_k \geq 0$ than $\frac{\partial z}{\partial t} \leq 0$, thus the surface gets to ever lower elevation, it is sinking.

The Chemical Equation of the Dissolution of Calcium Carbonate

The chemical equation of the dissolution expresses how much more limestone transfers to solution in unit time (how much more is the mass-flux density of the dissolving calcium carbonate) when the water is the more aggressive, that is the difference between the actual calcium carbonate content of the water and the total limestone solubility, is the bigger. This relation is mathematically incorporated in (7) (*VERESS, M.—PÉNTEK, K.* 1990, 1992). Writing the mass-flux density defined by (24) to the left side a relation is resulted between the derivatives of the function defining the rock surface and the concentration of calcium carbonate in the solution.

$$-\rho_k \frac{\frac{\partial z}{\partial t}}{\sqrt{\left(\frac{\partial z}{\partial x}\right)^2 + \left(\frac{\partial z}{\partial y}\right)^2 + 1}} = k(c_e - c). \tag{25}$$

Expressing $\frac{\partial z}{\partial t}$ from this an equation is resulted for the velocity of sinking of the rock surface:

$$\frac{\partial z}{\partial t} = -k\frac{c_e - c}{\rho_k}\sqrt{\left(\frac{\partial z}{\partial x}\right)^2 + \left(\frac{\partial z}{\partial y}\right)^2 + 1}. \tag{26}$$

It can be seen in (26) that the more aggressive is the water, (the difference between the equilibrium (c_e) and actual (c) calcium carbonate concentration is the bigger) the quicker is the denudation of the rock. It can be also seen that the gradient of the slope of the area (that is expressed by the $\frac{\partial z}{\partial x}$ and $\frac{\partial z}{\partial y}$ after (12) and (13) plays a boosting role in the velocity of the sinking of the surface.

The algebraic sign of the $\frac{\partial z}{\partial t}$ shall be examined considering (26) than can be done by the analysis of its constituents. The k, the first factor at the right side of the equation is a chemical constant, that is a positive number. The density of the rock (ρ_k) in the denominator is a positive number too.

The second factor in the numerator of (26) can not be negative, because that would represent an oversaturated solution that is impossible in the case of corrosion, that is:

$$c_e - c \geq 0. \tag{27}$$

The last factor in (26) is the positive root computed from the sum of squares:

$$\sqrt{\left(\frac{\partial z}{\partial x}\right)^2 + \left(\frac{\partial z}{\partial y}\right)^2 + 1} \geq 0. \tag{28}$$

It is clear from the above described that all values on the right side of (26) are positive thus their products are positive as well. But because (26) is completed with a (-) sign, it can be stated that

$$\frac{\partial z}{\partial t} \leq 0, \tag{29}$$

that is, the rock surface can not get any higher as a result of karst corrosion, it can only sink. (With the passing of time the elevation of the limestone surface becomes ever lower.) This is virtually apparent but the mathematical "reflection" of the well known principle proves the validity of the deductions.

The Spatial Development of the Calcium Carbonate Content of the Water Flowing on the Rock Surface

While the water flows on the surface it continually dissolves calcium carbonate. The velocity of dissolution is different at the various points of the rock surface as it is depending on numerous factors and first of all the quantity of calcium carbonate that has been previously dissolved in the water (c) and the velocity of the flow of the water film (*Fig.6*). This written in the Cartesian coordinate system:

$$\frac{\partial c}{\partial x} v_x + \frac{\partial c}{\partial y} v_y = \frac{q_k}{h} + \frac{c}{\rho_V h} \mathbf{q}_v \mathbf{n}, \tag{30}$$

where v_x and v_y are the x- and y components of the velocity vector of the water, h is the thickness of the water film on the rock surface, $\mathbf{q}_v$ is the quantity of rainfall. Thus (30) creates a relation between the flow velocity of the water, its chemical constitution, the volume of the corroded rock and the rainfall on the area.

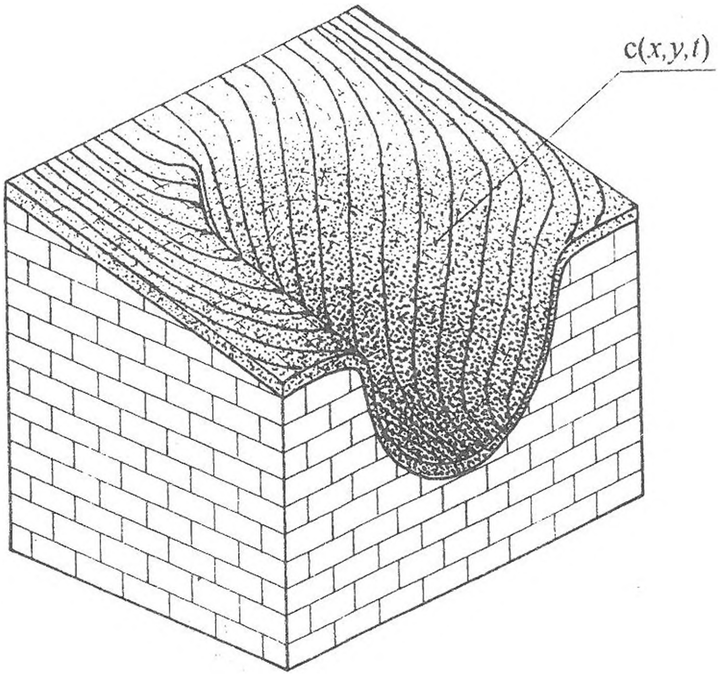

Fig. 6: The spatial distribution of calcium carbonate dissolved in the water film flowing on the rock surface

The components of the $\mathbf{q}_v$ vector in the Cartesian coordinate system

$$\mathbf{q}_v = \begin{cases} 0, \\ 0, \\ -q_v. \end{cases} \tag{31}$$

where q_v is a positive number. Its unit is: kg/m^{2}s.

Substituting the form of q_k determined in (7) to the first factor in the right of (30) and $\mathbf{q}_v$ as it is determined in (31) to the second factor. Considering the (14)—(16) equations of the normal of the rock surface the assigned scalar composition shall be executed. At length the

$$\frac{\partial c}{\partial x} v_x + \frac{\partial c}{\partial y} v_y = k \frac{c_e - c}{h} - \frac{c}{\rho_V h} q_v \tag{32}$$

equation is resulted for the spatial distribution of dissolved calcium carbonate.

(32) tells that the aggressivity (c_e-c) of the water flowing on the rock surface has a boosting effect on the concentration of calcium carbonate, because the water dissolves the limestone as long as the rainfall reduces the concentration (dilutes the solution) as it is written with a negative sign in the right of (32).

The Velocity of the Water Flowing on the Rock Surface

The flow of the water is caused by gravity, it is slowed by friction. The forces of inertia should be calculated with but in the relatively slowly flowing water film the letter can be neglected beside the former two. (*Fig. 7*). Naturally the forces of inertia shall be calculated with at high velocity flow in its full form on the left of the Navier-Stokes equation (*SZUNYOGH, G.* 1995b).

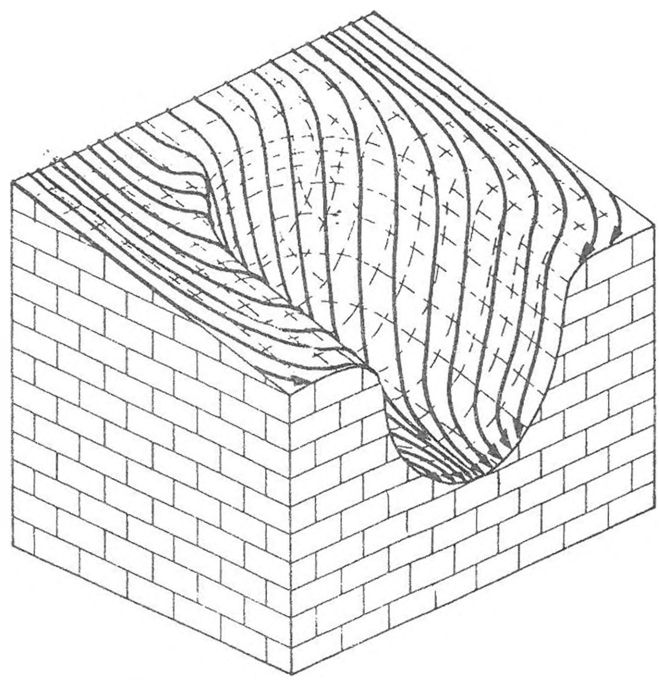

Fig. 7: The flow lines of the water film that covers the rock surface

In the (5) formula written for the velocity the g vector of the gravity occurs. As the gravity is apparently vertical and points downwards, it has only a z-directed vector component, that is:

$$\mathbf{g} = \begin{cases} 0, \\ 0, \\ -g, \end{cases} \tag{33}$$

where the absolute value of gravity is (10 m/s^2). Executing the **gn** scalar composition on the right side of (5) after the necessary ordering the following equations can be achieved for the vector components of the flow velocity of the water.

$$v_x = -\frac{\rho_V g h^2}{3\eta} \frac{\dfrac{\partial z}{\partial x}}{\left(\dfrac{\partial z}{\partial x}\right)^2 + \left(\dfrac{\partial z}{\partial y}\right)^2 + 1} \tag{34}$$

$$v_y = -\frac{\rho_V g h^2}{3\eta} \frac{\dfrac{\partial z}{\partial y}}{\left(\dfrac{\partial z}{\partial x}\right)^2 + \left(\dfrac{\partial z}{\partial y}\right)^2 + 1}, \tag{35}$$

$$v_z = -\frac{\rho_V g h^2}{3\eta} \frac{\left(\dfrac{\partial z}{\partial x}\right)^2 + \left(\dfrac{\partial z}{\partial y}\right)^2}{\left(\dfrac{\partial z}{\partial x}\right)^2 + \left(\dfrac{\partial z}{\partial y}\right)^2 + 1} \tag{36}$$

The negative sign in the (34)—(36) formulas expresses that if the surface seen in the direction of the x or y rises, the water flows backwards, toward the origin, so:

$$\text{if } \frac{\partial z}{\partial x} \geq 0, \text{ then } v_x \leq 0,$$

or $$\text{if } \frac{\partial z}{\partial x} \geq 0, \text{ then } v_y \leq 0. \tag{37}$$

The equations tell that if the surface is steep, so $\frac{\partial z}{\partial x}$ or $\frac{\partial z}{\partial y}$ is large, the water flows with greater velocity. It is visible too that the flow velocity of the water increases in a quadratic way with the flow thickness. It can be deducted that the assumption that the flow in a thin water film is slow has been proved.

The Equation of the Thickness of the Liquid Film

For the determination of the thickness of the liquid film flowing on the limestone surface the continuity equation that expresses the mass conservation of the water can be applied in a way that for the closed A surface used for the application of equation (6) a minute tilted prism shall be taken that includes the full m thickness of the flow and its base is Δx x Δy. The integration in (6) performed and decreasing the values of Δx and Δy beyond all limits (converging them to zero) then a variation of (6) is received:

$$\frac{\partial(mv_x)}{\partial x} + \frac{\partial(mv_y)}{\partial y} = -\frac{\mathbf{q}_v \mathbf{n}}{\rho_V} \tag{6}$$

The m value expressing the depth of the water occurs on the left side of the equation. As in the rest of the equations the h thickness of the water layer is used (that is apparently less than the vertical depth of the flow on sloping surfaces), it is practical to change to h to m in (6).

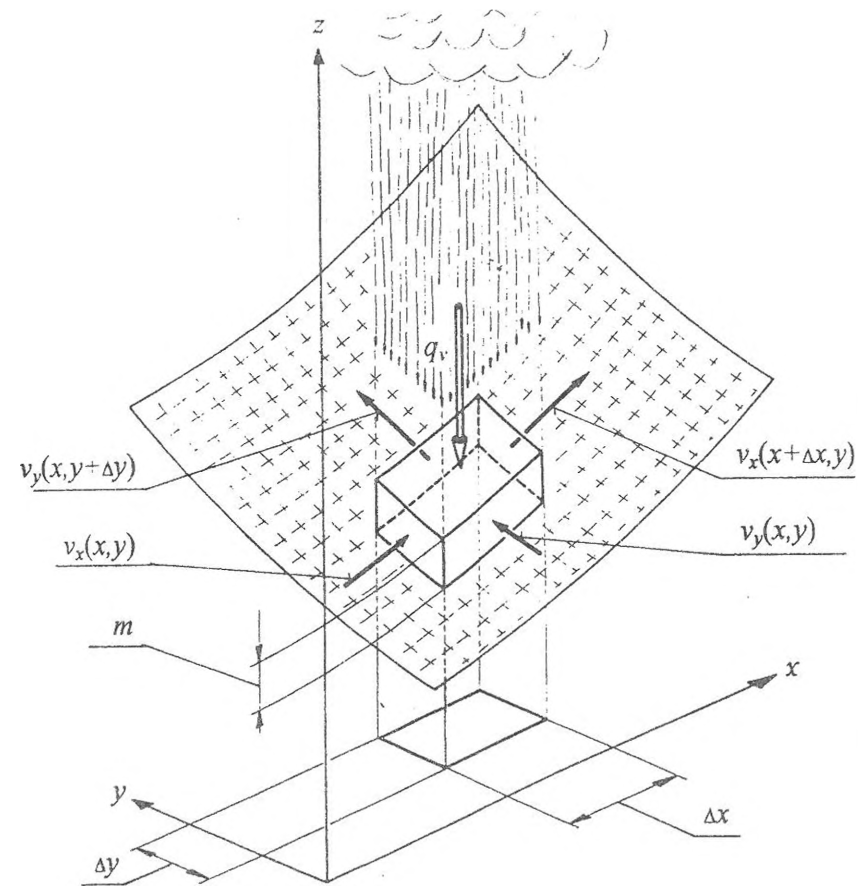

Fig 8: The "infinitely small" element of volume that contains the full depth of the water flowing on the limestone surface, for the application of the mass conservation principle

Due to geometrical considerations the relation between h and m is valid:

$$m = h\sqrt{\left(\frac{\partial z}{\partial x}\right)^2 + \left(\frac{\partial z}{\partial y}\right)^2 + 1} \tag{38}$$

Substituting expression (38) to (6) and executing the assigned derivations after a longish (but elemental) computation the following is received:

$$h\left(\frac{\partial v_x}{\partial x}+\frac{\partial v_y}{\partial y}\right)+v_x\frac{\partial h}{\partial x}+v_y\frac{\partial h}{\partial y}+v_x h\frac{\frac{\partial z}{\partial x}\frac{\partial^2 z}{\partial x^2}+\frac{\partial z}{\partial y}\frac{\partial^2 z}{\partial y\partial x}}{\left(\frac{\partial z}{\partial x}\right)^2+\left(\frac{\partial z}{\partial y}\right)^2+1}+v_y h\frac{\frac{\partial z}{\partial x}\frac{\partial^2 z}{\partial x\partial y}+\frac{\partial z}{\partial y}\frac{\partial^2 z}{\partial y^2}}{\left(\frac{\partial z}{\partial x}\right)^2+\left(\frac{\partial z}{\partial y}\right)^2+1}=$$

$$.=\frac{q_v}{\rho_v}\frac{1}{\sqrt{\left(\frac{\partial z}{\partial x}\right)^2+\left(\frac{\partial z}{\partial y}\right)^2+1}} \tag{39}$$

(39) connects the differential geometric parameters (gradients in various directions and curvatures) of the rock surface, the flow velocity of the water and the thickness of the flow.

Summary

For the quantitative study of the processes of corrosion of the limestone surface the $v_x(x,y,t)$ and $v_y(x,y,t)$ components of the flow velocity vector, the $h(x,y,t)$ thickness of the liquid film, the $c(x,y,t)$ concentration of dissolved calcium carbonate and the $z=f(x,y,t)$ function determining the limestone surface shall be determined. The listed five unknowns can be derived by the listed five partial differential equations

$$v_x=-\frac{\rho_V g h^2}{3\eta}\frac{\frac{\partial z}{\partial x}}{\left(\frac{\partial z}{\partial x}\right)^2+\left(\frac{\partial z}{\partial y}\right)^2+1}, \tag{40}$$

$$v_y=-\frac{\rho_V g h^2}{3\eta}\frac{\frac{\partial z}{\partial y}}{\left(\frac{\partial z}{\partial x}\right)^2+\left(\frac{\partial z}{\partial y}\right)^2+1}, \tag{41}$$

$$h\left(\frac{\partial v_x}{\partial x}+\frac{\partial v_y}{\partial y}\right)+v_x\frac{\partial h}{\partial x}+v_y\frac{\partial h}{\partial y}+v_x h\frac{\frac{\partial z}{\partial x}\frac{\partial^2 z}{\partial x^2}+\frac{\partial z}{\partial y}\frac{\partial^2 z}{\partial y\partial x}}{\left(\frac{\partial z}{\partial x}\right)^2+\left(\frac{\partial z}{\partial y}\right)^2+1}+v_y h\frac{\frac{\partial z}{\partial x}\frac{\partial^2 z}{\partial x\partial y}+\frac{\partial z}{\partial y}\frac{\partial^2 z}{\partial y^2}}{\left(\frac{\partial z}{\partial x}\right)^2+\left(\frac{\partial z}{\partial y}\right)^2+1}=$$

$$=\frac{q_v}{\rho_v}\frac{1}{\sqrt{\left(\frac{\partial z}{\partial x}\right)^2+\left(\frac{\partial z}{\partial y}\right)^2+1}}, \tag{42}$$

$$\frac{\partial c}{\partial x}v_x+\frac{\partial c}{\partial y}v_y=k\frac{c_e-c}{h}-\frac{c}{\rho_V h}q_v, \tag{43}$$

$$\frac{\partial z}{\partial t}=-k\frac{c_e-c}{\rho_k}\sqrt{\left(\frac{\partial z}{\partial x}\right)^2+\left(\frac{\partial z}{\partial y}\right)^2+1}. \tag{44}$$

The solution of (40)—(44) will be dealt with later.

The Computerized Possibilities for the Solution of the Equations of Karst Corrosion

Unfortunately the general solution for the (40)—(44) equations can not be provided, only particular solutions exist that fit to the initial and boundary conditions (*DUBLJANSZKIJ, J. V. 1989, SZUNYOGH, G. 1995.c*). Apparently some schemes for the solution can be worked out that help in the study of some individual types of tasks.

The(40)—(44) equation system is very befitting for computerized solution because its equations are separable by the unknowns in them thus it is sufficient to solve smaller (three unknowns at most) equation systems. The steps of a numerical solution are described in the followings.

Initial and Boundary Conditions

Be the function reflecting the rock surface at the beginning of the t_o period of study of the karst corrosion:

$$z(x,y,t)=z_0(x,y), \qquad \text{if} \qquad t=t_0 \tag{45}$$

known. The $H_0(x,y,t)$ thickness of the liquid film and the concentration of the calcium carbonate in the solution $C_0(x,y,t)$ at the upper fringes of the sloping rock surface (there where the water arrives to the study site) thus

$$h(x,y,t) = H_0(x,y,t), \qquad \text{if} \quad x,y \in \Gamma, \quad t_0 \leq t, \tag{46}$$

and

$$c(x,y,t) = C_0(x,y,t), \qquad \text{if} \quad x,y \in \Gamma, \quad t_0 \leq t, \tag{47}$$

shall be known where Γ is the set of the points of the upper limestone surface fringe (*Fig. 9*).

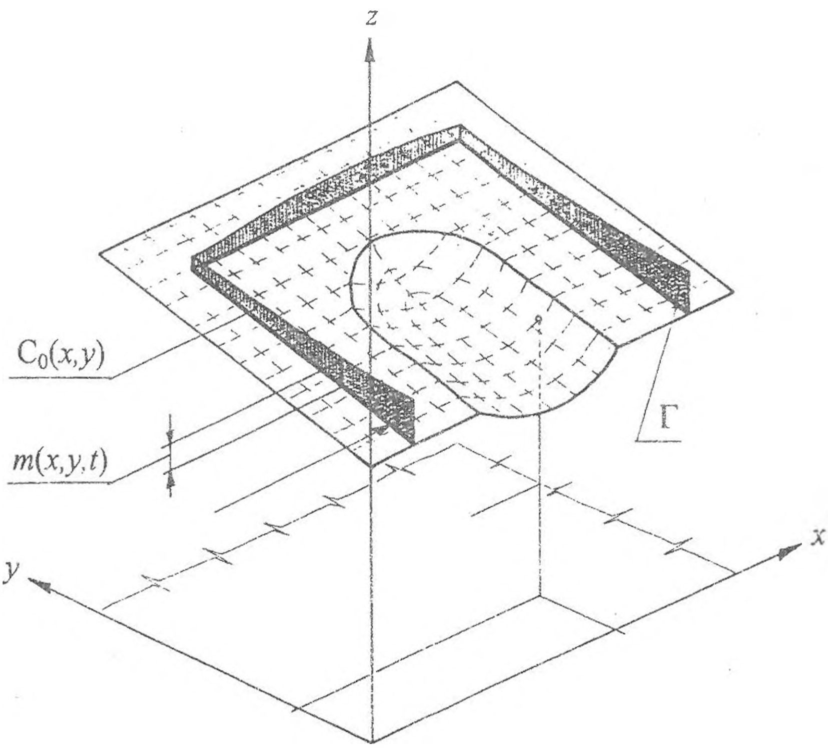

Fig. 9: The initial and boundary conditions of the differential equation system of karst corrosion

The Development of the Karst Corrosion at the Beginning of the Denudation

$$\frac{\partial z_0}{\partial x} = \xi_x^{(0)}(x,y), \qquad \text{if} \qquad t = t_0 \tag{48}$$

$$\frac{\partial z_0}{\partial y} = \xi_y^{(0)}(x,y), \qquad \text{if} \qquad t = t_0, \tag{49}$$

$$\frac{\partial^2 z_0}{\partial x^2} = \zeta_{xx}^{(0)}(x,y), \qquad \text{if} \qquad t = t_0, \tag{50}$$

$$\frac{\partial^2 z_0}{\partial x \partial y} = \zeta_{xy}^{(0)}(x,y), \qquad \text{if} \qquad t = t_0, \tag{51}$$

$$\frac{\partial^2 z_0}{\partial y^2} = \zeta_{yy}^{(0)}(x,y), \qquad \text{if} \qquad t = t_0. \tag{52}$$

The $\xi_x^{(0)}$, $\xi_y^{(0)}$, $\zeta_{xx}^{(0)}$, $\zeta_{xy}^{(0)}$ and $\zeta_{yy}^{(0)}$ functions in (48)-(52) are apparently known. (The $^{(0)}$ index indicates that these derivatives are related to t_0 time). The performance of the derivation (allowing to the computer program) shall not be done by an analytic but a numerical way.

These functions substituted to the equations (40)—(42) a differential equation with three unknowns is gained for the initial v_{x0} és v_{y0} velocity and h_0 thickness of the flow:

$$v_{x0} = -\frac{\rho_V g h_0^2}{3\eta} \frac{\xi_x^{(0)}}{\left(\xi_x^{(0)}\right)^2 + \left(\xi_y^{(0)}\right)^2 + 1}, \tag{53}$$

$$v_{y0} = -\frac{\rho_V g h_0^2}{3\eta} \frac{\xi_y^{(0)}}{\left(\xi_x^{(0)}\right)^2 + \left(\xi_y^{(0)}\right)^2 + 1}, \tag{54}$$

$$h_0\left(\frac{\partial v_{x0}}{\partial x} + \frac{\partial v_{y0}}{\partial y}\right) + v_{x0}\frac{\partial h_0}{\partial x} + v_{y0}\frac{\partial h_0}{\partial y} + v_{x0}h_0 \frac{\xi_x^{(0)}\zeta_{xx}^{(0)} + \xi_y^{(0)}\zeta_{xy}^{(0)}}{\left(\xi_x^{(0)}\right)^2 + \left(\xi_y^{(0)}\right)^2 + 1} + v_{y0}h_0 \frac{\xi_x^{(0)}\zeta_{xy}^{(0)} + \xi_y^{(0)}\zeta_{yy}^{(0)}}{\left(\xi_x^{(0)}\right)^2 + \left(\xi_y^{(0)}\right)^2 + 1} =$$

$$= \frac{q_v}{\rho_v} \frac{1}{\sqrt{\left(\zeta_x^{(0)}\right)^2 + \left(\zeta_y^{(0)}\right)^2 + 1}}. \tag{55}$$

The value of the $H_0(x,y,t)$ function of (46) at $t=t_0$ substituted to (53) and (54) the boundary conditions for velocity, V_{x0} and V_{x0} are gained:

$$V_{x0} = -\frac{\rho_V g H_0^2(x,y,t_0)}{3\eta} \frac{\xi_x^{(0)}}{\left(\xi_x^{(0)}\right)^2 + \left(\xi_y^{(0)}\right)^2 + 1}, \quad \text{if} \quad x,y \in \Gamma \quad \text{and} \quad t = t_0, \tag{56}$$

or

$$V_{y0} = -\frac{\rho_V g H_0^2(x,y,t_0)}{3\eta} \frac{\xi_y^{(0)}}{\left(\xi_x^{(0)}\right)^2 + \left(\xi_y^{(0)}\right)^2 + 1}, \quad \text{if} \quad x,y \in \Gamma \quad \text{and} \quad t = t_0. \tag{57}$$

With these boundary conditions the (53)—(55) equations can be solved with the method of finite differences (for the $v_{x0}(x,y)$, $v_{y0}(x,y)$ and $h_0(x,y)$ variables) directly or (with the elimination of v_{x0}, v_{y0}) only for $h_0(x,y)$ by the computer. The solution written to (43)

$$\frac{\partial c_0}{\partial x} v_{x0} + \frac{\partial c_0}{\partial y} v_{y0} = k\frac{c_e - c_0}{h_0} - \frac{c_0}{\rho_V h_0} q_v, \tag{58}$$

where the only unknown is the c_0 initial concentration of the solution. Apparently (58) is a partial differential equation and its solution is a two variable function ($c_0 = c_0(x,y)$), but fortunately it is only a linear and simple equation this way its solution on the computer does not raise difficulties. For the solution considering (47) the $c_0(x,y) = C_0(x,y,t)$, if $t = t_0$ boundary condition serves as a supplement.

It can be determined at length what is the velocity of the sinking of a specific (arbitrary) point of x—y coordinates. Equation (44) for $t = t_0$:

$$\left.\frac{\partial z}{\partial t}\right|_{t=0} = -k\frac{c_e - c_0}{\rho_k}\sqrt{\left(\zeta_x^{(0)}\right)^2 + \left(\zeta_y^{(0)}\right)^2 + 1}. \tag{59}$$

The Shape of the Limestone Surface a Short time after the Initial Moment

In the knowledge of the velocity of sinking it can be determined what function describes the shape of the rock surface after the passing of a Δt minute time interval in the next moment ($t_1 = t_0 + \Delta t$).

With the integration of (59):

$$z(x,y,t)\big|_{t=t_1} - z(x,y,t)\big|_{t=t_0} = \int_{t=t_0}^{t_1} -k\frac{c_e - c}{\rho_k}\sqrt{\left(\frac{\partial z}{\partial x}\right)^2 + \left(\frac{\partial z}{\partial y}\right)^2 + 1}\, dt. \tag{60}$$

$z(x,y,t)\big|_{t=t_0}$ means the shape of the rock surface at t=t_0 time and $z(x,y,t)\big|_{t=t_1}$ at t=t_1 time, that is:

$$z(x,y,t)\big|_{t=t_0} = z_0(x,y), \qquad \text{if} \qquad t = t_0. \tag{61}$$

$$z(x,y,t)\big|_{t=t_1} = z_1(x,y), \qquad \text{if} \qquad t = t_1 \tag{62}$$

The first average value principle of the integration applied at the right side of (60) particularly that it is valid for all continuous and integrable $f(t)$ function in the t_A és t_B interval, that:

$$\int_{t_A}^{t_B} f(t)dt = (t_B - t_A)\cdot f(t^*), \tag{63}$$

where about t^*only that much is known that it is an internal point of the t_A, t_B interval (that is: $t_A \le t^* \le t_B$). t_0 chosen for t_A and t_1 for t_B (60) takes the form:

$$z(x,y,t)\big|_{t=t_1} - z(x,y,t)\big|_{t=t_0} = (t_1 - t_0)\left[-k\frac{c_e - c}{\rho_k}\sqrt{\left(\frac{\partial z}{\partial x}\right)^2 + \left(\frac{\partial z}{\partial y}\right)^2 + 1}\,\right]_{t=t^*} \tag{64}$$

If the difference of t_1 and t_0

$$\Delta t = (t_1 - t_0) \tag{65}$$

is sufficientléy small than t_0, t_1 and t^* are only "slightly" different so writingt^* instead of t_0 into the argument of values at the left of (64) a substantial fault has not been committed. The fault is the smaller as smaller is Δt.

Considering the (48), (49), (61), (62) and (65) signs for the shape of the rock surface in a particular moment will be

$$z_1(x,y) = z_0(x,y) - k\frac{c_e - c_0}{\rho_k}\sqrt{\left(\zeta_x^{(0)}\right)^2 + \left(\zeta_y^{(0)}\right)^2 + 1}\cdot\Delta t \tag{66}$$

$v_{x0}(x,y)$, $v_{y0}(x,y)$, $h_0(x,y)$, $c_0(x,y)$ and $\left.\frac{\partial z}{\partial t}\right|_{t=0}$ expresses all the necessary data to characterize the denudation of the limestone surface at the t=0 moment.

The Shape of the Limestone Surface in an Arbitrary Moment

The relations derived in the foregoing retain their validity even when not a t_0 but a t_1 moment is chosen for the initial moment only the indices change, (1) shall be written replacing the "old" (0) indices and (2)-s replace the "old" (1)-s.

$$z_2(x,y) = z_1(x,y) - k\frac{c_e - c_1}{\rho_k}\sqrt{\left(\zeta_x^{(1)}\right)^2 + \left(\zeta_y^{(1)}\right)^2 + 1} \cdot \Delta t. \tag{67}$$

(67) can be computed in the knowledge of (66).

Continuing the same order of ideas the shape of the rock surface can be specified at any arbitrary t_n moment.

1. The derivatives expressing the differential geometric parameters shall be specified in the knowledge of $z_n(x,y,t)$:

$$\xi_x^{(n)}(x,y) = \frac{\partial z_n}{\partial x} \qquad \text{if} \qquad t = t_n \quad (t_n = t_{n-1} + \Delta t) \tag{68}$$

$$\xi_y^{(n)}(x,y) = \frac{\partial z_n}{\partial y}, \qquad \text{if} \qquad t = t_n \quad (t_n = t_{n-1} + \Delta t), \tag{69}$$

$$\zeta_{xx}^{(n)}(x,y) = \frac{\partial^2 z_n}{\partial x^2}, \qquad \text{if} \qquad t = t_n \quad (t_n = t_{n-1} + \Delta t), \tag{70}$$

$$\zeta_{xy}^{(n)}(x,y) = \frac{\partial^2 z_n}{\partial x \partial y}, \qquad \text{if} \qquad t = t_n \quad (t_n = t_{n-1} + \Delta t), \tag{71}$$

$$\zeta_{yy}^{(n)}(x,y) = \frac{\partial^2 z_n}{\partial y^2}, \qquad \text{if} \qquad t = t_n \quad (t_n = t_{n-1} + \Delta t), \tag{72}$$

2. Substituting the substitute value of $H_0(x,y,t)$ from (46) at $t=t_0$ to (53) and (54) the boundary conditions for velocity V_{xn} and V_{xn} will be:

$$V_{xn} = -\frac{\rho_V g H_0^2(x,y,t)}{3\eta}\frac{\xi_x^{(n)}}{\left(\xi_x^{(n)}\right)^2 + \left(\xi_y^{(n)}\right)^2 + 1}, \quad \text{if } x,y \in \Gamma, \text{ and } t = t_n, \tag{73}$$

or

$$V_{yn} = -\frac{\rho_V g H_0^2(x,y,t)}{3\eta}\frac{\xi_y^{(n)}}{\left(\xi_x^{(n)}\right)^2 + \left(\xi_y^{(n)}\right)^2 + 1}, \quad \text{if } x,y \in \Gamma, \text{ if } t = t_n. \tag{74}$$

Considering these boundary conditions the (53)—(55) equation system can be solved by computer for the $t=t_n$ moment with the method of finite differences regarding ($v_{xn}(x,y)$, $v_{yn}(x,y)$ and $h_n(x,y)$):

$$v_{xn}(x,y) = -\frac{\rho_V g h_n^2(x,y)}{3\eta} \frac{\xi_x^{(n)}}{\left(\xi_x^{(n)}\right)^2 + \left(\xi_y^{(n)}\right)^2 + 1}, \tag{75}$$

$$v_{yn}(x,y) = -\frac{\rho_V g h_n^2(x,y)}{3\eta} \frac{\xi_y^{(n)}}{\left(\xi_x^{(n)}\right)^2 + \left(\xi_y^{(n)}\right)^2 + 1}, \tag{76}$$

$$h_n\left(\frac{\partial v_{xn}}{\partial x} + \frac{\partial v_{yn}}{\partial y}\right) + v_{xn}\frac{\partial h_n}{\partial x} + v_{yn}\frac{\partial h_n}{\partial y} + v_{xn}h_n \frac{\xi_x^{(n)}\zeta_{xx}^{(n)} + \xi_y^{(n)}\zeta_{xy}^{(n)}}{\left(\xi_x^{(n)}\right)^2 + \left(\xi_y^{(n)}\right)^2 + 1} + v_{yn}h_n \frac{\xi_x^{(n)}\zeta_{xy}^{(n)} + \xi_y^{(n)}\zeta_{yy}^{(n)}}{\left(\xi_x^{(n)}\right)^2 + \left(\xi_y^{(n)}\right)^2 + 1} =$$

$$= \frac{q_v}{\rho_v} \frac{1}{\sqrt{\left(\zeta_x^{(n)}\right)^2 + \left(\zeta_y^{(n)}\right)^2 + 1}}. \tag{77}$$

Writing the solution to (43) a differential equation is received for $c(x,y,t_n)$:

$$\frac{\partial c_n}{\partial x}v_{xn} + \frac{\partial c_n}{\partial y}v_{yn} = k\frac{c_e - c_n}{h_n} - \frac{c_n}{\rho_V h_n}q_v, \tag{78}$$

That substituted with

$$c_n(x,y) = C_0(x,y,t), \qquad \text{if} \quad x,y \in \Gamma \text{ és } \quad t = t_n \tag{79}$$

boundary condition it can be solved by computer.

By the ideas followed in (60)

$$z_{n+1}(x,y) = z_n(x,y) - k\frac{c_e - c_n(x,y)}{\rho_k}\sqrt{\left(\zeta_x^{(n)}\right)^2 + \left(\zeta_y^{(n)}\right)^2 + 1}\cdot\Delta t \tag{80}$$

The procedure of the solution will be (*Fig. 10*):

1. The $z_1(x,y)$ shape of the rock surface is determined at t_1 moment.
2. In the knowledge of $z_1(x,y)$ the shape $z_2(x,y)$ of the rock surface is determined $z_2(x,y)$ for the t_2 moment.
3. This procedure is continued for the series of t_3, t_4, t_5 ... moments as long as the $z_n(x,y)$ function belonging to the t_n moment is achieved. The sought for solution is:

$$z(x,y,t) = z_n(x,y), \quad \text{if} \quad t = t_n. \tag{78}$$

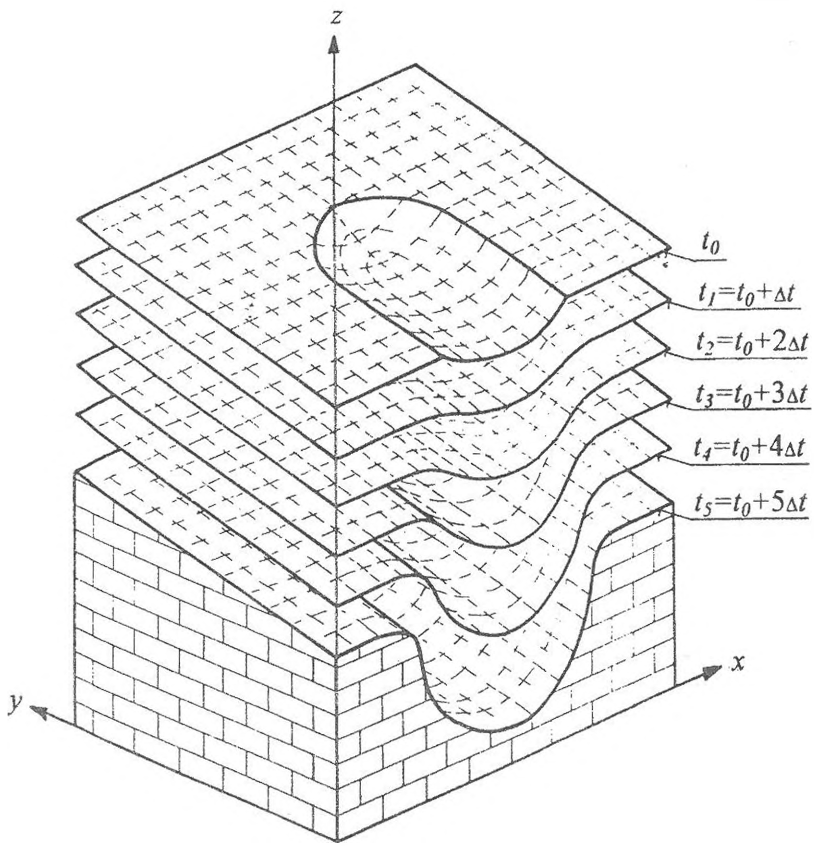

Fig. 10: Basic diagram of the development of a small limestone surface irregularity (e.g. a heel print) to a karren trough for computer modeling

REFERENCES

DREYBROT, W. (1988): Processes in Karst Systems. Springer-Verlag. 283.p. Berlin, 1988

DUBLJANSZKIJ, J. V. (1989): A víztükör alatti gömbfülke-képződés elméleti vizsgálata—*Karszt és Barlang* I-II. p.29-31

FRANK, Ph.—MIESES, R. (1967): A mechanika és fizika differenciál- és integrálegyenletei. Műszaki könyvkiadó, Budapest, 1967
JAKUCS, L. (1971): A karsztok morfogenetikája. Akadémiai kiadó, Budapest, 1971
SZUNYOGH, G. (1994): Szabad, talajjal nem borított mészkőfelszín karsztosodásának általános egyenletrendszere—*Karsztfejlődés I. (Totes Gebirge karrjai)*. Pauz kiadó, Celldömölk. p. 145-164
SZUNYOGH, G. (1995.a): A matematikai modellezés helye és szerepe a karsztosodással járó folyamatok leírásában — *Karszt és Barlangkutatás*. X. évf. 1981-95. p. 251-269
SZUNYOGH, G. (1995.b): Karrcsatornák vízszállító képességének elméleti meghatározása — *IV. Karsztológiai Szeminárium*. Szombathely, 1995
SZUNYOGH, G. (1995.c): Mészkőfelszíni alakzatok kialakulásának fizikája — *Studia Physica Savariesia. III.* Szombathely, 1995. p. 9.1-9.11
VERESS, M.—PÉNTEK, K. (1990): Kísérlet a karsztos felszínek denudációjának kvantitatív leírására—*Karszt és Barlang* I. p. 19-28
VERESS, M.—PÉNTEK, K. (1992): Felszíni karsztos formák vizsgálata matematikai módszerekkel—*Oktatási intézmények karszt és barlangkutató tevékenységének II. országos konferenciája*, Szombathely. p.21-29

KARSZTFEJLŐDÉS IV.
Szombathely, 2000. pp. 151-174.

DIFFERENTIAL EQUATIONS DESCRIBING THE CHANGES OF SHAPE CAUSED BY KARST CORROSION OF ANY ARBITRARY LIMESTONE SURFACE

GÁBOR SZUNYOGH
"Berzsenyi Dániel" College, Department of Physics
9700 Szombathely, Károlyi G. tér 4.

Abstract: A sort of karstic processes happens in circumstances when the rock surface exposed to solution is identical with the surface that determines the macroscopic shape of the rock, i.e. the solution takes place directly on the surface of the rock that is not covered by soil or debris. Such processes occur at the making of karrenfelds, rillenkarren, rock-bowls as well as at the making of vertical elements (potholes, vertical shafts). Though these forms seem to be substantially different, their development can be described with a universal differential equation. This paper describes the setting up of the differential equation system.

Introduction

A sort of karstic processes happens in circumstances when the rock surface exposed to solution is identical with the surface that determines the macroscopic shape of the rock, i.e. the solution takes place directly on the surface of the rock that is not covered by soil or debris. Such processes occur at the making of karrenfelds, rillenkarren, rock-bowls as well as at the making of vertical elements (potholes, vertical shafts). Though these forms seem to be substantially different, their development can be described with a universal differential equation.

This paper describes the setting up of the differential equation system. The equation system (due to its universal validity) is relatively complicated but in concrete cases it reduces naturally if the symmetries and other reducing conditions of the studied case are made use of.

The setting up of such a differential equation system is justified because it unifies the efforts (virtually very different from one another regarding the different nature of their specific aims) of others having studied the dissolution of the free limestone surface *(VERESS, M.—PÉNTEK, K. 1990, 1992, DUBLJANSZKIJ, J. V. 1989, JAKUCS, L. 1971, SZUNYOGH, G. 1995 etc.)* and the method offers new theoretical views on other phenomena that have not been yet studied. The basic novelty of the method is that it offers possibilities for the theoretical modeling of various karst-forms, their origin and the explanation of their morphological properties.

The Model of the Karstification of Uncovered Limestone Surfaces

A q_V volume of rainfall falls on the limestone surface shown on *Fig. 1.* q_V determines the direction of the rainfall and the volume of water falling at right angle at a unit surface at unit time. As a result water will flow on the rock surface with good approximation along the slope lines of the surface. (Only an approximation because if the horizontal projection of the slope line is a curve, the centrifugal force will drive the water particles from the slope lines, they go astray in the bends.) The volume of water flowing on the surface is not originated solely in the rain, but it is boosted by volumes coming from other parts of the surface outside of the studied area.

As the atmosphere contains 0.03% of carbon dioxide, rainwater becomes slightly acidic and dissolves limestone. While the rainwater flows on the rock surface its aggressive nature decreases due to the solution of limestone and also increases because of the addition of new rainwater still rich in carbonic acid content. As a result the aggressivity of the water-film will be different at the various points of the rock surface. For the denudation (corrosion) is the faster if the water is the more aggressive, the shape of the rock surface will be varied in space and time.

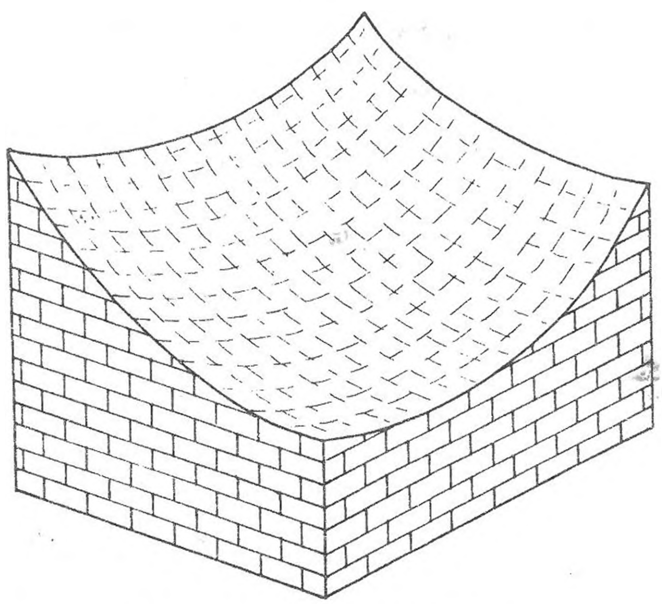

Figure 1. Detail of limestone surface exposed to solution

The Determination of the Differential Equation of the Function that Describes the Shape of the Rock Surface

At the modeling of the exposed limestone surface *the listed actions will be taken to consideration:*

1) The volume of calcium carbonate departing from the limestone in a time unit (the rate of dissolution) will be directly proportional with the aggressivity of the water flowing above it, that is: with the difference of the de facto calcium carbonate concentration and that of the saturated solution.

2) The calcium carbonate concentration of the water-film flowing on the surface will be increased by the dissolution of limestone but it is decreased by the increase of the solvent (rainfall on the surface).

3) The shift per time unit of an arbitrary point of the limestone surface (denudation) is directly proportional with the volume of rock that departs from that point in per time unit. With other words: where corrosion is quicker, quicker is the surface denudation.

4) The direction of the flow velocity of the liquid-film (at the definite point) is determined by the slope direction of the surface, its magnitude by the thickness and discharge of the liquid-film.

5) The thickness of the liquid-film (as for the laws of flow of free-surface viscous liquids) is basically determined by the volume of discharge and the gradient of the water tracks.

In the computation the listed quantities will be taken as well defined quantities

— the velocity of the flow from neighboring areas at the fringe of the studied area;

— the direction and volume of the rainfall;

— parameters defining the velocity of limestone dissolution;

— the saturation concentration of calcium carbonate of the water;

— elemental hydraulic and petrologic parameters.

In the computation the listed quantities will be taken as undefined quantities

— the formula that defines the limestone surface;

— the direction and measure of the velocity of water flow at an arbitrary point of the limestone surface;

— the concentration of calcium carbonate dissolved in water at any point of the limestone surface;

— the thickness of the fluid-film along the surface;

— the direction and degree of the limestone slope (related to space and time).

All undefined quantities shall be regarded as functions of the three spatial coordinates and time.

The Means of Mathematical Definition of the Limestone Surface

The formula that defines the limestone surface — to avoid the ruining of generality — will be sought in a coordinate-free form (that is: invariable regarding the types and position of coordinate systems) to enable the use of the most applicable coordinate system for the solution of the specific task. *(SZUNYOGH, G. 1994)* The vector pointing to an arbitrary point of the surface will be **r** and the equation to determine the surface is

$$t = F(\mathbf{r}) \tag{1}$$

where t is time and $F(\mathbf{r})$ is to be understood as a vectorial-scalar function. E.g. in the case of Descartian coordinates

$$t = F(x, y, z). \tag{2}$$

The (1) explicitly determines the time when the surface "passes" the point marked by the **r** vector. Implicitly it shows that at the t time what x, y, z coordinates are on the surface. If the $F(x,y,z)$ becomes known (as the solution of its differential equation) than figuring z from (2) z can be expressed explicitly as a function of the x and y spatial coordinates and t time.

$$z = G(x, y, t). \tag{3}$$

The expression of the limestone surface is better as in (1) than in (3) because it does not emphasize either spatial coordinate "suppressing" the others as does (3) with z when it may happen that in certain cases x or y would be the variants more fitting to the solution.

(1) is suitable to the mathematical description in the

$$t = F(r, \varphi, z) \tag{4}$$

form using cylindrical or

$$t = F(R, \varphi, \vartheta) \tag{5}$$

form using spherical coordinates.

The Velocity of the Shift of the Limestone Surface

Let's regard the position of a t point and it's position in a commencing $t+\Delta t$ time *(Fig. 2)*

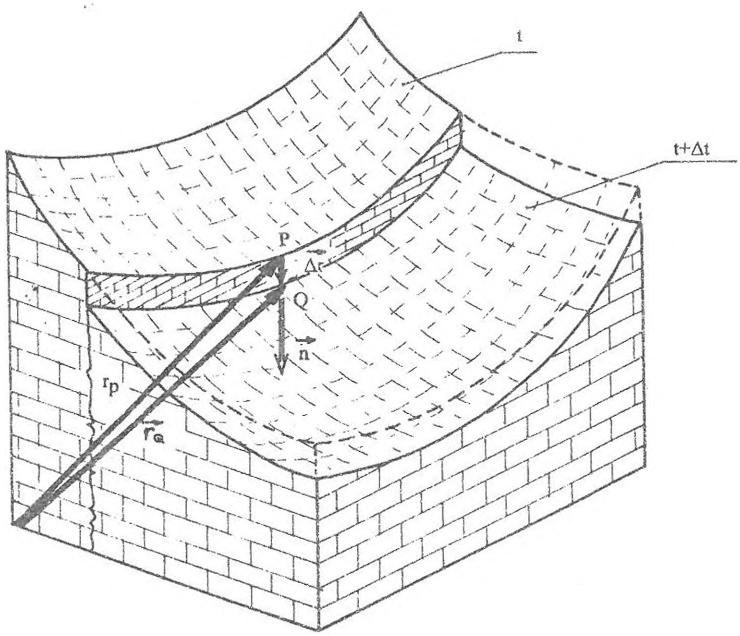

Figure 2. The shifting of the points of the rock surface during its dissolution

A P point will be selected on the surface belonging to t time and a Q pint belonging to the $t+\Delta t$ time doing it in a way that the PQ section shall be at right angle to the tangent plane of the $\Delta\mathbf{r} = \Delta r \cdot \mathbf{n}$ surface at P (or the PQ section shall be identical with the normal of the surface). It should point at the $\mathbf{r}_P$ P, the $\mathbf{r}_Q$ Q point. The $\Delta\mathbf{r}$ vector pointing from P to Q

$$\Delta\mathbf{r} = \mathbf{r}_Q - \mathbf{r}_P . \tag{6}$$

Consequently:

$$\Delta\mathbf{r} = \Delta r \cdot \mathbf{n}, \tag{7}$$

where Δr stands for the absolute value of the $\Delta\mathbf{r}$ vector. The velocity of the shifting of the surface will be:

$$\mathbf{w} = \lim_{\Delta t \to 0} \frac{\Delta\mathbf{r}}{\Delta t}. \tag{8}$$

The $\mathbf{w}$ shall be expressed with its $F(\mathbf{r})$ gradient. To achieve this (8) shall be reordered as follows:

$$\mathbf{w} = \lim_{\Delta t \to 0} \frac{\Delta r}{\Delta t} \cdot \mathbf{n} = \lim_{\Delta t \to 0} \frac{1}{\frac{\Delta t}{\Delta r}} \mathbf{n}. \tag{9}$$

As Δt converges zero point Q converges P beyond limits, so the $\Delta \mathbf{r} = \mathbf{r}_Q - \mathbf{r}_P$ vector converges zero itself. So it can be expressed:

$$\mathbf{w} = \lim_{\Delta r \to 0} \frac{1}{\frac{\Delta t}{\Delta r}} \mathbf{n}. \tag{10}$$

According to the rules of limit determination:

$$\lim_{\Delta r \to 0} \frac{1}{\frac{\Delta t}{\Delta r}} = \frac{1}{\lim\limits_{\Delta r \to 0} \frac{\Delta t}{\Delta r}}, \tag{11}$$

(unless the denominator of the right side is not zero) thus:

$$\mathbf{w} = \frac{1}{\lim\limits_{\Delta r \to 0} \frac{\Delta t}{\Delta r}} \mathbf{n}. \tag{12}$$

Δt can be expressed with the help $F(\mathbf{r})$ formula. As point P is situated on the surface belonging to t time:

$$F(\mathbf{r}_P) = t, \tag{13}$$

point Q is situated on the surface described by t+Dt, thus

$$F(\mathbf{r}_Q) = t + \Delta t. \tag{14}$$

The difference of (14) and (13)

$$\Delta t = F(\mathbf{r}_Q) - F(\mathbf{r}_P). \tag{15}$$

Using the equations (6) and (7)

$$\Delta t = F(\mathbf{r}_P + \Delta r \cdot \mathbf{n}) - F(\mathbf{r}_P). \tag{16}$$

Inserting Δt to the denominator of (12)

$$\mathbf{w} = \frac{1}{\lim\limits_{\Delta r \to 0} \frac{F(\mathbf{r}_P + \Delta r \cdot \mathbf{n}) - F(\mathbf{r}_P)}{\Delta r}} \mathbf{n} \tag{17}$$

is resulted. It can be recognized that the expression in the denominator of (12) is nothing else but the derivative of $F(\mathbf{r})$ in the $\mathbf{n}$ direction

$$\lim_{\Delta r \to 0} \frac{F(\mathbf{r}_P + \Delta r \cdot \mathbf{n}) - F(\mathbf{r}_P)}{\Delta r} = \frac{\partial F}{\partial n}. \tag{18}$$

It is well known that directional derivatives can be expressed by the gradients of the function to be derivated, so

$$\frac{\partial F}{\partial n} = \mathbf{n} \cdot \operatorname{grad} F. \tag{19}$$

As the $\mathbf{n}$ normal of the surface is identical with the direction of the gradient:

$$\mathbf{n} = \frac{\operatorname{grad} F}{|\operatorname{grad} F|}. \tag{20}$$

Consequently

$$\frac{\partial F}{\partial n} = \operatorname{grad} F \cdot \frac{\operatorname{grad} F}{|\operatorname{grad} F|} = \frac{\operatorname{grad} F \cdot \operatorname{grad} F}{|\operatorname{grad} F|} = \frac{(\operatorname{grad} F)^2}{|\operatorname{grad} F|}. \tag{21}$$

Substituting (21) to (17)

$$\mathbf{w} = \frac{|\operatorname{grad} F|}{(\operatorname{grad} F)^2} \mathbf{n}. \tag{22}$$

substituting (20) to the place of $\mathbf{n}$ and reducing it the next formula can be achieved for the $\mathbf{w}$ velocity of the shift of the rock surface.

$$\mathbf{w} = \frac{\operatorname{grad} F}{(\operatorname{grad} F)^2} \tag{23}$$

The Density of the Material Flux of Limestone into the Solution

The density of the material flux of limestone is the quantity of limestone removed from a unit area of the limestone surface in unit time

$$q_K = \lim_{\Delta t \to 0,\, \Delta A \to 0} \frac{\Delta m_K}{\Delta t \cdot \Delta A}, \tag{24}$$

where Δm_K is the quantity of calcium carbonate dissolved in some Δt time from a ΔA surface area.

For the determination of Δm_K a minor ΔA size area of the continuously denudating rock surface at t time shall be chosen.

As the surface of the rock is dissolved at a — according to the earlier coding — **w** velocity, the denudation will be in a Δt time interval:

$$\Delta r = \mathbf{w} \cdot \mathbf{n} \cdot \Delta t \tag{25}$$

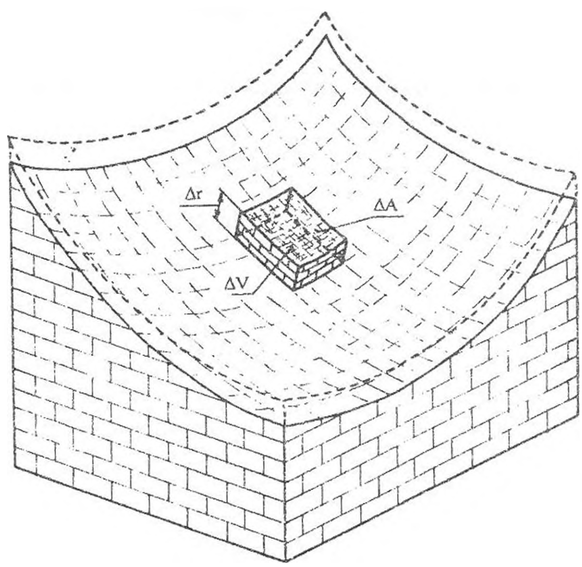

Figure 3. The presentation of the volume originally occupied by limestone dissolved from the ΔA surface element during Δt time

If ΔA is minute enough (that is $\Delta A \to 0$), than the surface of the rock can be approximated by a plane within ΔA-n and the value of **w** can be considered constant. Consequently the original volume of the limestone removed in the Δt time interval (see *Fig. 3*):

$$\Delta V = \Delta A \cdot \Delta r, \tag{26}$$

or the mass of the removed rock:

$$\Delta m_K = \rho_K \cdot \Delta V, \tag{27}$$

where ρ_K is the density of the limestone.

Considering (24), (25) and (26)

$$\Delta m_K = \rho_K \cdot \Delta A \cdot \mathbf{w} \cdot \mathbf{n} \cdot \Delta t, \tag{28}$$

this written into (24) the density of the material flux of calcium carbonate removed from the limestone during solution is received

$$q_K = \lim_{\Delta t \to 0,\, \Delta A \to 0} \frac{\rho_K \cdot \Delta A \cdot \mathbf{w} \cdot \mathbf{n} \cdot \Delta t}{\Delta t \cdot \Delta A}. \tag{29}$$

Formula (29) after some reduction and limit determination can be given in this form:

$$q_K = \mathbf{w} \cdot \mathbf{n} \tag{30}$$

Considering the form of w determined by (22) the scalar product indicated in (30) will be put into the form:

$$\mathbf{w} \cdot \mathbf{n} = \frac{|\mathrm{grad}\, F|}{(\mathrm{grad}\, F)^2} \mathbf{n} \cdot \mathbf{n} \tag{31}$$

Using that $\mathbf{n} \cdot \mathbf{n} = 1$, the density of the material flux of limestone will be:

$$q_K = \frac{\rho_K}{|\mathrm{grad}\, F|} \tag{32}$$

The Calcium Carbonate Concentration of the Water Flowing on the Rock Surface

The calcium carbonate concentration of the fluid-film should be determined by such a function that depends only on two coordinates (e.g. x and y) as the flow itself varies on a two dimensional surface. For example in a "normally positioned" Descartian coordinate system the general form of this function would be

$$c = c(x, y, t), \tag{33}$$

that expresses that on a point of x, y coordinates on the surface of the limestone body in question the calcium carbonate concentration is exactly $c(x,y,t)$.

It is proposed to deviate however from this type of writing using the fact that there is an unambiguous relation between the z elevation and t time according to (3), so (avoiding the ruining of generality) it can be determined in the function of the three spatial coordinates $c(x,y,z)$. The physical explanation of this would be that $c(x,y,z)$ determines the calcium carbonate concentration in a time when the rock surface that is continually in motion traverses the spatial point determined by the x,y,z coordinates. Naturally this time can be determined as written in (2). The sought for function shall be than

$$c = c(x, y, z), \qquad \text{while} \quad t = F(x, y, z). \tag{34}$$

The benefit of (34) is that it contains only coordinates and no time (at least not explicitly) offering a possibility to determine the calcium carbonate concentration of the solution similarly to (1) independently of the position or type of the coordinate system, that is: in invariant form:

$$c = c(\mathbf{r}), \qquad \text{while} \quad t = F(\mathbf{r}). \tag{35}$$

Differing from (31), (35) is not a two- but a three spatial dimensional function. Its explanation: $c(\mathbf{r})$ determines the concentration in the moment when the rock-surface traverses the point determined by the **r** vector. It will be revealed in the followings that this type of writing enables the creation of much more general equations than its creation observing concentration like in (33).

Relations between the concentration of calcium carbonate in the solution, the volume of rainfall and the density of the material flux of limestone shall be sought. The fact (according to observations) that the shifting of the limestone surface is slower by magnitudes than the velocity of the flow on it. (The rock dissolves 1-2 millimeters annually while the water make that distance in seconds.)

It shall be studied, how the concentration of the water varies at various points of the rock surface. To this purpose an infinitesimally small material volume of A base area and h height shall be pointed out. (*Fig. 4*)

The concentration of the solution (as concentration is defined):

$$c = \frac{m_K}{V}, \tag{36}$$

where m_K is the mass of calcium carbonate in the pointed out V volume. When this volume is shifting along the surface, its concentration changes because on the one hand the mass of the dissolved calcium carbonate in it changes on the other hand it is diluted by the rainfall recharge. Because the material volume shifts along with the water particles, its shift in Δt time is

$$\Delta\mathbf{r} = \mathbf{v} \cdot \Delta t. \tag{37}$$

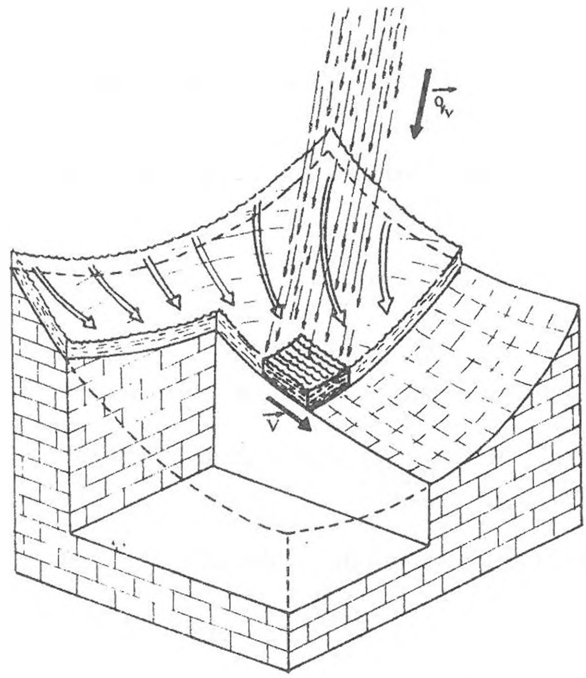

Figure 4. The position of the material volume cut from the water flowing on the rock surface

If the material volume was in the vicinity of the point determined by the **r** position vector in the t moment then it will obviously be at the point $\mathbf{r} + \Delta\mathbf{r}$ after the passing of Δt time. According to (35) the concentration of the solution is different in the $\mathbf{r} + \Delta\mathbf{r}$ point as it was in point **r**, its value will change by

$$\Delta c = c(\mathbf{r} + \Delta\mathbf{r}) - c(\mathbf{r}) \tag{38}$$

Δc compared with the elapsed time Δt (knowing that according to (37) is $\Delta\mathbf{r} = \mathbf{v} \cdot \Delta t$) the velocity of the change of the concentration is resulted:

$$\frac{\Delta c}{\Delta t} = \frac{c(\mathbf{r} + \mathbf{v} \cdot \Delta t) - c(\mathbf{r})}{\Delta t} . \tag{39}$$

The value of v shall be the product of its absolute value and the $\mathbf{e}_V$ direction of the flow:

$$\mathbf{v} = v \cdot \mathbf{e}_V , \tag{40}$$

thus

$$\frac{\Delta c}{\Delta t} = \frac{c(\mathbf{r} + v \cdot \Delta t \cdot \mathbf{e}_V) - c(\mathbf{r})}{\Delta t} . \tag{41}$$

The numerator and denominator of (41) multiplied by v, thus:

$$\frac{\Delta c}{\Delta t}=v\cdot\frac{c(\mathbf{r}+v\cdot\Delta t\cdot\mathbf{e}_V)-c(\mathbf{r})}{v\cdot\Delta t}. \tag{42}$$

Obviously $v\cdot\Delta t=\Delta r$, where Δr is the absolute value of $\Delta\mathbf{r}$. As a consequence

$$\frac{\Delta c}{\Delta t}=v\cdot\frac{c(\mathbf{r}+\Delta r\cdot\mathbf{e}_V)-c(\mathbf{r})}{\Delta r} \quad . \tag{43}$$

If $\Delta t\to 0$, than Δr converges to zero too, so the (43) formula is nothing else but the deviate of c in the $\mathbf{e}_V$ direction

$$\lim_{\Delta t\to 0}\frac{\Delta c}{\Delta t}=\lim_{\Delta r\to 0}\left\{v\cdot\frac{c(\mathbf{r}+\Delta r\cdot\mathbf{e}_V)-c(\mathbf{r})}{\Delta r}\right\}=\mathrm{v}\cdot\frac{\partial\,\mathrm{c}}{\partial\,\mathbf{e}_V} \tag{44}$$

The directional derivative can be produced as the gradient of c

$$\frac{\partial\,c}{\partial\,\mathbf{e}_V}=\mathbf{e}_V\cdot\operatorname{grad}\mathrm{c}, \tag{45}$$

or

$$\frac{\Delta c}{\Delta t}=\mathrm{v}\cdot\mathbf{e}_V\cdot\operatorname{grad}\mathrm{c}. \tag{46}$$

On the other hand according to (40) $\mathrm{v}\cdot\mathbf{e}_V=\mathbf{v}$, so finally the function:

$$\frac{dc}{dt}=\mathbf{v}\cdot\operatorname{grad}\mathrm{c} \tag{47}$$

has been achieved for the change of the concentration.

The derivative written in (47) indicates the so called material derivative, because it has been supposed that the material volume in question shifts together with the liquid.

The change of the dissolved calcium carbonate concentration in the liquid-film can be produced from (36) as well:

$$\frac{dc}{dt}=\frac{d}{dt}\left\{\frac{m_K}{V}\right\}. \tag{48}$$

The derivation of the quotient on the right side executed:

$$\frac{d}{dt}\left\{\frac{m_K}{V}\right\}=\frac{1}{V}\cdot\frac{dm_K}{dt}-\frac{m_K}{V^2}\cdot\frac{dV}{dt}, \tag{49}$$

After reduction and insertion to (48) comes to this form

$$\frac{dc}{dt}=\frac{1}{V}\cdot\frac{dm_K}{dt}-\frac{c}{V}\cdot\frac{dV}{dt} \tag{50}$$

The individual factors in (50) shall be determined.
Obviously

$$V = A\cdot h. \tag{51}$$

The time derivative of m_K is equal to the change per unit time of the volume of calcium carbonate in the material volume, that change can be originated only in the dissolution of the limestone surface.

As from the limestone surface a q_K quantity of rock material gets into the solution in a unit time, from an A surface A time that much in unit time, that is:

$$\frac{dm_K}{dt}=A\cdot q_K \tag{52}$$

quantity will be dissolved.

The time derivative of V in accordance with the concept of the derivative is the change of the volume of the water in unit time, that is, equal with the rainfall on A area in unit time. If the density of the volume flux is indicated with $\mathbf{q}_V$ and the density of water with ρ_V, then the derivative of V will be

$$\frac{dV}{dt}=\frac{|\mathbf{q}_V|}{\rho_V}\cdot A\cdot\cos\alpha \tag{53}$$

Where $\cos\alpha$ expresses that from the point of view of the new water supply only the projection of A surface to the direction of the rainfall shall be considered, because the rain does not fall on the surface at right angle but at an α angle.

Indicating the direction of the rainfall with $\mathbf{n}_V$, $\cos\alpha$ can be written as a scalar product:

$$\cos\alpha=\mathbf{n}\cdot\mathbf{n}_V, \tag{54}$$

where $\mathbf{n}$ is the normal of the rock surface. Inserting (54) to (53):

$$\frac{dV}{dt}=\frac{|\mathbf{q}_V|}{\rho_V}\cdot A\cdot\mathbf{n}\cdot\mathbf{n}_V. \tag{55}$$

Naturally $|\mathbf{q}_V|\mathbf{n}_V=\mathbf{q}_V$, thus

$$\frac{dV}{dt} = \frac{A}{\rho_V} \cdot \mathbf{q}_V \cdot \mathbf{n}. \tag{56}$$

Inserting the (52) and (56) equations to (50):

$$\frac{dc}{dt} = \frac{1}{V} \cdot A \cdot q_K - \frac{c}{V} \cdot \frac{A}{\rho_V} \cdot \mathbf{q}_V \cdot \mathbf{n}. \tag{57}$$

Writing V from (51) to (57) and executing the possible reductions:

$$\frac{dc}{dt} = \frac{q_K}{h} - \frac{c}{\rho_V \cdot h} \cdot \mathbf{q}_V \cdot \mathbf{n}. \tag{58}$$

Finally inserting (58) to the left side of (47) the below differential equation is resulted determining the calcium carbonate concentration dissolved in the water:

$$\mathbf{v} \cdot \operatorname{grad} c = \frac{q_K}{h} - \frac{c}{\rho_V \cdot h} \cdot \mathbf{q}_V \cdot \mathbf{n}. \tag{59}$$

From (59) we can eliminate **n** with respect of (20):

$$\mathbf{v} \cdot \operatorname{grad} c = \frac{q_K}{h} - \frac{c}{\rho_V \cdot h} \cdot \mathbf{q}_V \cdot \frac{\operatorname{grad} F}{|\operatorname{grad} F|}. \tag{60}$$

The Chemical Equation of Dissolution

According to the most simple model of solution the dissolution is the quicker if the difference between the saturation c_e and de facto c concentration is the bigger (*DREYBROT, W.* 1988). As a consequence the more calcium carbonate gets into the material volume showed in *Figure 4* the aggressivity of the solution is the bigger (that is: $c_e - c$ difference is the bigger), or the dissolution happens on a bigger A surface. In a formula:

$$\frac{dm_K}{dt} = k \cdot (c_e - c) \cdot A, \tag{61}$$

where k is a constant characteristic to the velocity of dissolution. Calculating with equation (36) the

$$A \cdot q_K = k \cdot (c_e - c) \cdot A \tag{62}$$

equation is resulted. Using this one the

$$q_K = k \cdot (c_e - c) \tag{63}$$

equation is gained for the relation of the concentration of the solution and the velocity of dissolution.

This equation along with the consideration of (32) creates a direct relation between the concentration and the shape of the surface:

$$\frac{\rho_K}{|\text{grad}\, F|} = k \cdot (c_e - c). \tag{64}$$

This paper does not describe the ways of the measurement of the c_e and k values, this has been worked out in other speleological studies in relatively good details. It has to be emphasized anyway that the k constant helps to involve the role of the mixing corrosion, the atmospheric temperature and carbon dioxide content, the increase of the partial pressure of carbon dioxide under extended snow covering.

The Flow Velocity of Water in the Fluid-Film

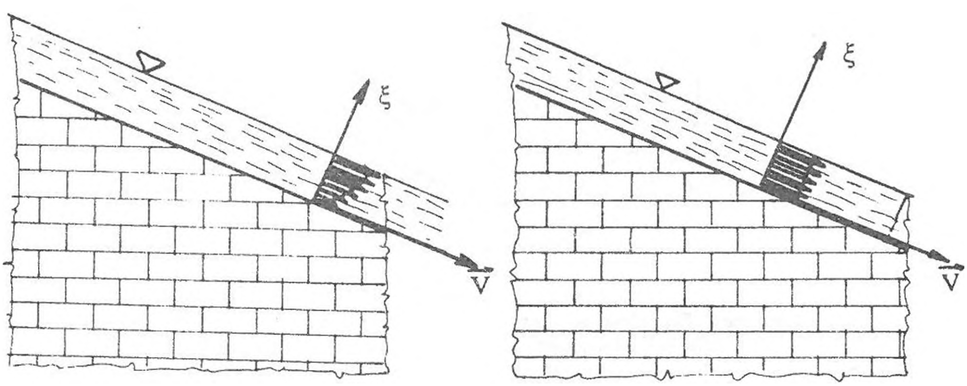

Figure 5. The actual and the equalized velocity profile of the liquid film

As the thin layer of water flowing on the rock surface behaves as a fluid with friction, its flow velocity gradually increases with the distance from the rock surface. The velocity of the flow is however meaningless concerning the material-transport. The real flow can be substituted with a fictive flow with uniform velocity-profile (*Fig. 5*) and with a discharge identical with the real flow.

It is known from the theory of frictional fluids that the discharge of a *B* wide *h* deep, *B* slope canal is

$$Q = \frac{\rho_V \cdot g \cdot h^3 \cdot B \cdot \sin\beta}{3 \cdot \eta}, \tag{65}$$

where ρ_V is the density of water, η is the coefficient of dynamic viscosity (*SZUNYOGH, G.* 1995). The linear velocity profile shall produce the same discharge, thus:

$$Q = v \cdot h \cdot B. \tag{66}$$

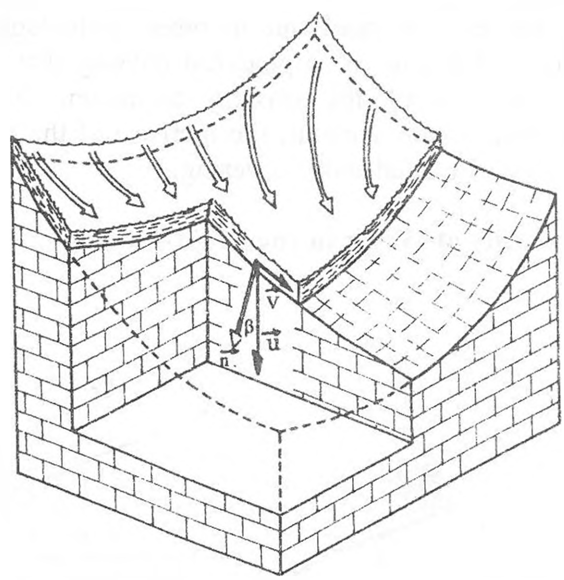

Figure 6. The relative position of the flow velocity of the liquid, the normal of the rock surface and the vectors of gravitational acceleration

Equalizing the (65) and (66) equations for the average flow velocity the following formula is resulted:

$$v = \frac{\rho_V \cdot g \cdot h^2 \cdot \sin\beta}{3 \cdot \eta} \tag{67}$$

The sin*B* coefficient occurring in (67) hints that *v* can be taken as the surface-dip oriented component of some vertical **u** vector (see *Figures 6* and *7*).

This particular **u** can be created by the help of **g** gravitational acceleration (g obviously vertical):

$$\mathbf{u} = \frac{\rho_V \cdot h^2}{3 \cdot \eta} \cdot \mathbf{g}. \tag{68}$$

According to the conditions stated at the beginning of this paper the direction of the flow is determined by the slope direction of the surface. The gradient lines are drawn up by the plane defined by the normal of the rock surface and the gravitational acceleration and curve of intersection of this plane with the rock surface. Figure 7 shows the section of the surface of the limestone body along the above defined plane.

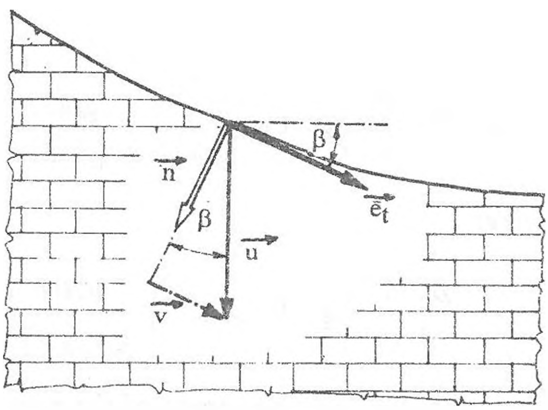

Figure 7. The section of the limestone formation along the plane determined by the normal of the rock surface and the vector of the gravitational acceleration

It can be seen on *Figure 7* that v is linear a combination of the **u** and **n** vectors

$$\mathbf{v} = \mathbf{u} - (\mathbf{u} \cdot \mathbf{n}) \cdot \mathbf{n}, \tag{69}$$

that has an absolute value (after *Fig. 7)*:

$$|\mathbf{v}| = |\mathbf{u}| \cdot \sin\beta = \left| \frac{\rho_V \cdot h^2}{3 \cdot \eta} \cdot \mathbf{g} \right| \cdot \sin\beta = \frac{\rho_V \cdot h^2}{3 \cdot \eta} \cdot g \cdot \sin\beta \quad . \tag{70}$$

It shows that the right side of (70) is really identical with the right side of (67), thus the guess has been proved that v can really be expressed with the help of a vertical **u** vector.

Inserting the expression of **u** in (68) to (69) it is resulted that

$$\mathbf{v} = \frac{\rho_V \cdot h^2}{3 \cdot \eta} \cdot \mathbf{g} - \left(\frac{\rho_V \cdot h^2}{3 \cdot \eta} \mathbf{g} \cdot \mathbf{n} \right) \cdot \mathbf{n}. \tag{71}$$

Reducing for the scalars:

$$\mathbf{v} = \frac{\rho_V \cdot h^2}{3 \cdot \eta} \cdot [\mathbf{g} - (\mathbf{g} \cdot \mathbf{n}) \cdot \mathbf{n}]. \tag{72}$$

It shall be taken into account that

$$\mathbf{n} = \frac{\operatorname{grad} F}{|\operatorname{grad} F|}, \tag{73}$$

thus

$$\mathbf{v} = \frac{\rho_V \cdot h^2}{3 \cdot \eta} \cdot \left[\mathbf{g} - \left(\mathbf{g} \cdot \frac{\operatorname{grad} F}{|\operatorname{grad} F|} \right) \cdot \frac{\operatorname{grad} F}{|\operatorname{grad} F|} \right]. \tag{74}$$

By further reducing:

$$\mathbf{v} = \frac{\rho_V \cdot h^2}{3 \cdot \eta} \cdot \left[\mathbf{g} - (\mathbf{g} \cdot \operatorname{grad} F) \cdot \frac{\operatorname{grad} F}{(\operatorname{grad} F)^2} \right]. \tag{75}$$

It can be seen that the last component of the rights side (according to (23) is identical shift velocity of the surface:

$$\mathbf{w} = \frac{\operatorname{grad} F}{(\operatorname{grad} F)^2}, \tag{76}$$

So finally the equation developed for the flow velocity of the fluid-film is:

$$\mathbf{v} = \frac{\rho_V \cdot h^2}{3 \cdot \eta} \cdot [\mathbf{g} - (\mathbf{g} \cdot \operatorname{grad} F) \cdot \mathbf{w}]. \tag{77}$$

The Thickness of the Fluid-Film

The thickness of the fluid film flowing on the rock surface can be determined using the law of conservation of mass. For this purpose a section of conduit, relatively narrow compared to its length will be pointed out.

According to the law of conservation of mass the mass of water flowing into and out of the conduit within unit time will be identical. Let (see *Fig. 8*) the width of the conduit b, its length s and its height (that is obviously the same as the height of the fluid film) h_1 at the point of entry and h_2 at the point of exit. The flow velocity shall be v_1 and v_2 The $\mathbf{r}_1$ position vector shall point at the entry point, $\mathbf{r}_2$ vector to the exit point. If the conduit is short enough the curvature of the flow line is negligible and the conduit can be approached by a straight line, thus

$$\mathbf{r}_2 \cong \mathbf{r}_1 + \mathbf{s}, \tag{78}$$

where s is a minute vector that is parallel with the flow lines and that has an absolute value that is the same as the length of the conduit. The water balance of this conduit shall be examined, that is that the entering and exiting of volumes of water shall be studied.

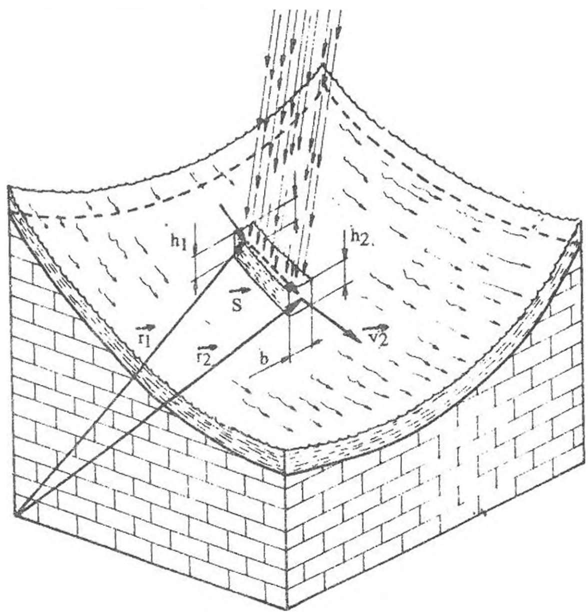

Figure 8. The position of the conduit necessary for the application of the law of mass conservation

There is gain originated from the recharge at one end of the conduit and on the top of it from the rainfall. Thus the mass of recharge water is:

$$Q_{BE} = \rho_V \cdot v_1 \cdot h_1 \cdot b + \mathbf{q}_V \cdot \mathbf{n} \cdot s \cdot \quad . \tag{79}$$

Discharge at the other end is responsible for the loss at the other end of the conduit. The mass of the discharge:

$$Q_{KI} = \rho_V \cdot v_2 \cdot h_2 \cdot b\,. \tag{80}$$

According to the law of conservation of mass

$$Q_{BE} = Q_{KI}, \tag{81}$$

that after equalizing (79) and (80) results

$$\frac{v_2 \cdot h_2 - v_1 \cdot h_1}{s} \cong \frac{\mathbf{q}_V \cdot \mathbf{n}}{\rho_V} \tag{82}$$

Approximation is the more accurate s is the more short, because the flow lines can the better substituted by straight lines.

v_1, v_2, h_1 and h_2 can be produced as the values of the $v(\mathbf{r})$ and $h(\mathbf{r})$ functions at $\mathbf{r}_1$ and $\mathbf{r}_2$

$$v_1 = v(\mathbf{r}_1), \tag{83}$$

$$v_2 = v(\mathbf{r}_2), \tag{84}$$

$$h_1 = h(\mathbf{r}_1), \tag{85}$$

$$h_2 = h(\mathbf{r}_2). \tag{86}$$

Inserting these expressions to (82) and observing that

$$\mathbf{r}_2 \cong \mathbf{r}_1 + \mathbf{r} \tag{87}$$

it follows that

$$\frac{v_2 \cdot h_2 - v_1 \cdot h_1}{s} \cong \frac{v(\mathbf{r}_1 + \mathbf{s}) \cdot h(\mathbf{r}_1 + \mathbf{l}) - v(\mathbf{r}_1) \cdot h(\mathbf{r}_1)}{s}. \tag{88}$$

It can be noted that on the right sight of (88) (in case $s \to 0$) the s-direction derivative of product $v(\mathbf{r}) \cdot h(\mathbf{r})$ appears, thus

$$\lim_{s \to 0} \frac{v_2 \cdot h_2 - v_1 \cdot h_1}{s} = \frac{\partial}{\partial s}\{v(\mathbf{r}) \cdot h(\mathbf{r})\}. \tag{89}$$

The directional derivative in question can be produced as the gradient of the $v(\mathbf{r}) \cdot h(\mathbf{r})$ product:

$$\frac{\partial}{\partial s}\{v(\mathbf{r})\cdot h(\mathbf{r})\} = \mathbf{e}_S \cdot \mathrm{grad}(v\cdot h), \tag{90}$$

where $\mathbf{e}_s$ stands for the s direction unit vector. According to the above described the direction of $\mathbf{e}_s$ is identical v direction of the flow.

The $\mathrm{grad}(v\cdot h)$ expression shall be developed by the rules of gradient making (*FRANK, Ph.— MIESES, R.* 1967):

$$\mathbf{e}_S \cdot \mathrm{grad}\,(v\cdot h) = \mathbf{e}_S \cdot v \cdot \mathrm{grad}\,h + \mathbf{e}_S \cdot h \cdot \mathrm{grad}\,v\,. \tag{91}$$

The first coefficient of the first term can be pooled like this:

$$\mathbf{e}_S \cdot v = \mathbf{v}\,, \tag{92}$$

as $\mathbf{e}_s$ is the unit vector pointing in the direction of v. The second term can be shaped like this:

$$\mathbf{e}_S \cdot h \cdot \mathrm{grad}\,v = \mathbf{e}_S \cdot h \cdot \mathrm{grad}\sqrt{\mathbf{v}^2} = \frac{\mathbf{e}_S \cdot h}{2\sqrt{\mathbf{v}^2}} \cdot \mathrm{grad}\,(\mathbf{v}\cdot\mathbf{v}) =$$

$$= \frac{\mathbf{e}_S \cdot h}{2\cdot \mathrm{v}} \cdot (\mathbf{v}\cdot \mathrm{div}\,\mathbf{v} + \mathbf{v}\cdot \mathrm{div}\,\mathbf{v}) = \frac{\mathbf{e}_S \cdot h}{\mathrm{v}} \cdot \mathbf{v}\cdot \mathrm{div}\,v\,. \tag{93}$$

As the water is an incompressible fluid, the divergence of its velocity field is zero, thus

$$\mathrm{div}\,\mathbf{v} = 0, \tag{94}$$

consequently

$$\mathbf{e}_S \cdot \mathrm{grad}(v\cdot h) = \mathbf{e}_S \cdot v \cdot \mathrm{grad}\,h\,. \tag{95}$$

Inserting (95) to (90) and that to (89) the following differential equation is produced for the thickness of the water-film.

$$\mathbf{v}\cdot \mathrm{grad}\,h = \frac{\mathbf{q}_V \cdot \mathbf{n}}{\rho_V} \tag{96}$$

It can be red in (96) that if rain falls on the rock, that is $\mathbf{q}_V \neq 0$, then the thickness of the fluid-film increases in the direction of the slope lines because $\mathbf{v}\cdot \mathrm{grad}\,h \geq 0$. The change of the fluid-film thickness can occur in the case of $\mathbf{q}_V = 0$ too because the flow lines of the flowing water can contract or spread out.

It can be deducted from (96) that if the direction of the rainfall and the normal of the rock surface are at a small angle than the $\mathbf{q}_V \cdot \mathbf{n}$ scalar product is small and the pace of thickening of the fluid film is smaller.

Summary

The equation system of the dissolution of limestone surface uncovered by soil (free) is composed of the following equations:

1. Relation between the normal of the rock surface and the function describing the shape of the surface:

$$\mathbf{n} = \frac{\operatorname{grad} F}{|\operatorname{grad} F|}; \tag{97}$$

2. Relation between the sinking velocity of the rock surface and the function describing the shape of the surface:

$$\mathbf{w} = \frac{\operatorname{grad} F}{(\operatorname{grad} F)^2}; \tag{98}$$

3. Relation between the density of the material flux of the dissolved limestone and the sinking velocity of the rock surface:

$$q_K = \mathbf{w} \cdot \mathbf{n} \cdot \rho_K; \tag{99}$$

4. Relation between the calcium carbonate concentration of the solution flowing on the surface, the density of the material flux of the dissolve limestone, the thickness of the fluid-film and rainfall:

$$\mathbf{v} \cdot \operatorname{grad} c = \frac{q_K}{h} - \frac{c}{\rho_V \cdot h} \cdot \mathbf{q}_V \cdot \mathbf{n}; \tag{100}$$

5. Relation between the calcium carbonate concentration of the solution flowing on the surface and the density of the material flux of the dissolved limestone:

$$q_K = k \cdot (c_e - c); \tag{101}$$

6. Relation between the flow velocity, the thickness of the fluid-film and the spatial position of the rock surface (its normal):

$$\mathbf{v} = \frac{\rho_V \cdot h^2}{3 \cdot \eta} \cdot [\mathbf{g} - (\mathbf{g} \cdot \mathbf{n}) \cdot \mathbf{n}]; \tag{102}$$

7. Relation between the thickness of the fluid-film, the flow velocity, the rainfall and the spatial position of the rock surface:

$$\mathrm{div}(h\mathbf{v}) = -\frac{\mathbf{q}_V \cdot \mathbf{n}}{\rho_V}. \tag{103}$$

Unknown quantities in the equations:

1. The $t=F(x,y,z)$ function describing the rock surface;
2. The normal of the rock surface (**n**);
3. The sinking velocity of the rock surface (**w**);
4. The mass of rock dissolved from a unit surface of limestone in unit time (that is: the density of the material flux of the dissolved limestone) (q_K);
5. The calcium carbonate concentration of the solution flowing on the surface (c);
6. The flow velocity of water in the fluid-film (v);
7. The thickness of the fluid-film (h)

The number of unknown quantities and equations. The (97)-(103) equation system consists of 3 vectorial and 4 scalar equations. 3 vectorial and 4 scalar values are sought for thus the number of equations and unknown quantities are equal.

Boundary conditions. The thickness of the fluid-film shall be known at the boundary of the studied area where the water enters it and also the concentration of the entering water shall be known. The rest of the boundary conditions can be derived in this course.

References

DREYBROT, W. (1988): Processes in Karst Systems. Springer-Verlag. 283.p. Berlin, 1988

DUBLJANSZKIJ, J. V. (1989): A víztükör alatti gömbfülke-képződés elméleti vizsgálata—*Karszt és Barlang* I-II. p.29-31

FRANK, Ph.—MIESES, R. (1967): A mechanika és fizika differenciál- és integrálegyenletei. Műszaki könyvkiadó, Budapest, 1967

JAKUCS, L. (1971): A karsztok morfogenetikája. Akadémiai kiadó, Budapest, 1971

SZUNYOGH, G. (1994): Szabad, talajjal nem borított mészkőfelszín karsztosodásának általános egyenletrendszere—*Karsztfejlődés I. (Totes Gebirge karrjai)*. Pauz kiadó, Celldömölk. p. 145-164

SZUNYOGH, G. (1995): A matematikai modellezés helye és szerepe a karsztosodással járó folyamatok leírásában — *Karszt és Barlangkutatás.* X. évf. 1981-95. p. 251-269
SZUNYOGH, G. (1995): Karrcsatornák vízszállító képességének elméleti meghatározása — *IV. Karsztológiai Szeminárium.* Szombathely, 1995
SZUNYOGH, G. (1995): Mészkőfelszíni alakzatok kialakulásának fizikája — *Studia Physica Savariesia. III.* Szombathely, 1995. p. 9.1-9.11
VERESS, M.—PÉNTEK, K. (1990): Kísérlet a karsztos felszínek denudációjának kvantitatív leírására—*Karszt és Barlang* I. p. 19-28
VERESS, M.—PÉNTEK, K. (1992): Felszíni karsztos formák vizsgálata matematikai módszerekkel—*Oktatási intézmények karszt és barlangkutató tevékenységének II. országos konferenciája*, Szombathely. p.21-29